



NTNU – Trondheim
Norwegian University of
Science and Technology

Analysis of Bivariate Extreme Values

Chris Egeland Busuttil

Master of Science in Physics and Mathematics

Submission date: February 2015

Supervisor: Arvid Næss, MATH

Norwegian University of Science and Technology
Department of Mathematical Sciences

Preface

The objective of this Master thesis is to compare the functional representation of the empirically estimated bivariate ACER surface to the bivariate extreme value copula approach. Specifically, we shall look at the Gumbel-logistic, Asymmetric logistic, Negative logistic and Asymmetric negative logistic dependence models combined with the univariate ACER functions and Gumbel distributions as marginals. Furthermore, we wish to determine which of the two marginal approaches yields the most accurate return values for the least amount of data.

This Master thesis is the culmination of the course TMA4905 - Master's thesis in Statistics taken at the Norwegian University of Science and Technology. The thesis was completed during the autumn semester of 2014 under the guidance of Arvid Næss, and counts for 30 credits.

I would like to express my sincere gratitude to my supervisor Arvid Næss for his support and valuable feedback throughout the completion of this thesis. He has provided me with constructive discussions and valuable feedback which has helped me to improve my thesis. I would also like to thank Oleh Karpa for his helpfulness and patience in coping with a MATLAB novice.

Furthermore, I am also indebted to Kristin Solbakken for proofreading this report.

Finally I wish to thank my grandmother for her unconditional support in a wannabe statistician.

Abstract

The aim of this thesis is to investigate how well the bivariate ACER function compares to the traditional copula approach using univariate ACER and Gumbel marginals. Using time series of different lengths, we intend to answer: Which one of the two marginals yields the highest accuracy with the least amount of data?

Results show that there is high agreement between the distribution of the bivariate ACER functions and the distribution of the copula models with ACER marginals for all time series. The distribution of the copula models with Gumbel marginals display great discrepancies to the distribution of the bivariate ACER functions. These disagreements are greatest for short time series, and decrease as the time series become longer.

In loving memory of Anne Dorteia Egeland

Contents

1	Introduction	1
2	The ACER distribution	3
2.1	The Univariate ACER Distribution	3
	Cascade of Conditioning Approximations	3
	Confidence Intervals for Return Levels	7
	Return Levels	7
2.2	The Bivariate ACER Distribution	8
	Cascade of Conditioning Approximations	8
	Empirical Estimation of the ACER Function	10
	Confidence Intervals for Return Levels	11
	Return Levels	11
3	Classical Extreme Value Theory	13
3.1	The Univariate Generalized Extreme Value Distribution	13
	Empirical Estimation of the GEV distribution	14
	Return Levels	15
3.2	Multivariate Extremes	15
3.3	Copulas	17
3.4	Calculation of Pickands Result	19
	Gumbel Marginals	19
	ACER Marginals	20
3.5	Optimizing Parameters	21
4	The Data	23
4.1	Synthetic Time Series	23
4.2	Wind Levels	25
5	Analysis	28
5.1	Synthetic Data	28
	10 years	28
	25 years	38
	50 years	46
	100 years	54

5.2	Wind Levels	62
6	Conclusion	69
	Bibliography	71
A	Appendix	73
A.1	Generation of Synthetic Time Series	73
	Theory	73
	R Code	74
A.2	MATLAB Code	75

Introduction

Man can believe the impossible,
but man can never believe the
improbable.

- Oscar Wilde, 1891.

Extreme value theory is a branch of statistics dealing with the extremes of a distribution, both minimum or maximum, relative to the expected value of its distribution. The main idea behind this theory is to model and calculate the probability of events that occur rarely from a large data set. Important applications of extreme value theory is e.g. portfolio adjustment in the insurance industry, risk assessment in the financial markets, and for structural design in the case of extreme weather conditions.

When studying the extremes of two or more processes, each individual process can be modeled using well developed univariate techniques, but there are strong arguments for also studying the extreme value inter-relationship. First, this may be because the combination of the processes themselves are of greater interest than each individual process; second, there is potential for data from one variable to inform inferences on each of the others. Examples of this may include the relationship between different stock values or wave heights and wind speeds.

Many have tried to model and estimate a function describing the dependence structures between extreme values of multiple processes. However, there are no estimation tools that grant us the possibility to decide on the joint distribution of the multivariate extremes from a given data set, with high accuracy.

For this reason, copula theory have been proposed. But even in the case of bivariate extreme value copulas, there is, due to the features of the dependence function, an infinite number of models. Furthermore, the copula approach is fairly ad hoc, meaning there is no theoretical justification for choosing one particular copula over the other.

As a result of this, it is of considerable interest to see how the concept of *average conditional exceedance rate* (ACER), developed during the last few years at the Norwegian University of Science and Technology, can be extended to several dimensions, in our case, to two. By the ACER function, we obtain a method for nonparametric statistical estimation of the exact bivariate extreme value distribution given by a bivariate time series.

The objective of this thesis is to investigate how the empirically estimated bivariate ACER surface holds up to the standard bivariate extreme value copula approach. Specifically, we will look at how the bivariate ACER function compares to the copula approach using the Gumbel-logistic, Asymmetric logistic, Negative logistic and Asymmetric negative logistic dependence models in a Pickands copula representation. Applying these results, we adopt asymptotically consistent extreme value marginals based on the univariate ACER functions and fitted Gumbel distributions.

The two approaches will be tested on both synthetic and real world data. The synthetic data sets have been created to gain further insight into the described methods, as the amount of data in real world data sets usually are limited. Therefore a total of four data sets consisting of 10, 25, 50 and 100 years of data have been produced from the same distribution. By comparing the sub-asymptotic distribution of the time series and the fitted copulas, we may conclude which of the two marginal approaches yield the best accuracy when observations are scarce.

In the two following chapters, an introduction to the theory that is considered relevant for the method presented in this project is given. The focus of [Chapter 2](#) is directed towards the construction of the univariate and bivariate ACER method through a cascade of conditioning approximations. Furthermore, we develop expressions for the confidence interval of the ACER function and return level, i.e. the levels expected to be exceeded during a given time period. In [Chapter 3](#) we evaluate the well developed classical asymptotic theory for multivariate extremes, and introduce copula representation by Sklar's Theorem. Based on the relationship between copulas and extreme value copulas, stated by Pickands, we introduce the four dependence functions that are used in the analysis and calculate their functional form using univariate ACER and Gumbel marginals.

[Chapter 4](#) gives an introduction to the five data sets that are being analyzed with the given methods. The data sets are summarized by both tables and figures.

Motivated by the previous chapters, we apply both the bivariate ACER and copula methods to the data. By doing this, we are able to answer which one of the copula approaches fit the sub-asymptotic distribution of the evaluated time series the best, and hence which copula approach is the preferred extreme value procedure to limited time series. This is done in [Chapter 5](#).

The project is rounded off with some concluding remarks in [Chapter 6](#).

As part of the work of this project, the synthetic data sets were created in R while the copula models were implemented by modification of the MATLAB code developed by Oleh Karpa. The R code and the modifications done to the MATLAB code can be found in the Appendix. To reduce the length of this report and increase readability, all MATLAB code and data sets can be found in a Dropbox folder by following the link in the [Appendix](#).

The ACER distribution

It's impossible that the
improbable will never happen.
- Emil J. Gumbel, 1958.

In this chapter, we first construct a sequence of nonparametric distribution functions that converge to the exact extreme value distribution for a given time series. We then extend this method for prediction of extreme value statistics to the bivariate case.

To fully comprehend this and the next chapter, the reader should have a basic understanding of extreme value theory. This is beautifully explained in [1].

2.1 The Univariate ACER Distribution

The ACER-method, or Average Conditional Exceedance Rates, is a novel method for estimation of extreme values in time series. The difference between this and the original GEV-method, is that the ACER is of no need of independent data points, but is rather conditioned on a sufficient amount of preceding points in use. The sufficient amount of data points needed in the condition varies from data set to data set.

Cascade of Conditioning Approximations

Consider a stochastic process $Z(t)$ that have been observed over a time period $(0, T)$. We assume the values X_1, \dots, X_N , derived from the process, are allocated to the discrete times t_1, \dots, t_N in the time interval $(0, T)$. Our objective is to find the distribution of the extreme value $M_N = \max_N \{X_j; j \in \{1, \dots, N\} \subset \mathbb{N}\}$, and then estimate $P(\eta) = \text{Prob}(M_N \leq \eta)$ for large values of η . An underlying assumption is to consider exceedances of the individual random variables X_j above a given treshold, just as in classical extreme value theory.

By the definition of $P(\eta)$ it follows that

$$\begin{aligned} P(\eta) &= \text{Prob}(X_N \leq \eta, \dots, X_1 \leq \eta) \\ &= \text{Prob}(X_N \leq \eta | X_{N-1} \leq \eta, \dots, X_1 \leq \eta) \cdot \text{Prob}(X_{N-1} \leq \eta, \dots, X_1 \leq \eta) \\ &= \text{Prob}(X_1 \leq \eta) \prod_{j=2}^N \text{Prob}(X_j \leq \eta | X_{j-1} \leq \eta, \dots, X_1 \leq \eta). \end{aligned} \quad (2.1)$$

Instead of assuming independence between the X_j 's, we can assume it to have a k -step memory, i.e. a dependence on the k previous data point(s). Using this, we may approximate Eq. (2.1):

$$\begin{aligned} P(\eta) &\approx P_k(\eta) \\ &:= \prod_{j=k}^N \text{Prob}(X_j \leq \eta | X_{j-1} \leq \eta, \dots, X_{j-k+1} \leq \eta) \\ &\quad \cdot \prod_{j=2}^{k-1} \text{Prob}(X_j \leq \eta | X_{j-1} \leq \eta, \dots, X_1 \leq \eta) \\ &\quad \cdot \text{Prob}(X_1 \leq \eta), \end{aligned} \quad (2.2)$$

where $P(\eta) = P_N(\eta)$. Note that a k -step memory approximation does not lead to a k -th order Markov chain, while a one-step approximation is not a Markov approximation.

If $k = 1$, we have that

$$\begin{aligned} P(\eta) &\approx P_1(\eta) := \prod_{j=1}^N \text{Prob}(X_j \leq \eta) \\ &= \prod_{j=1}^N (1 - \alpha_{1j}(\eta)), \end{aligned} \quad (2.3)$$

where $\alpha_{1j}(\eta) = \text{Prob}(X_j > \eta)$, $j = 1, \dots, N$. The approximation of Eq. (2.3), assuming independent data, can be written as

$$P(\eta) \approx F_1(\eta) := \exp \left\{ - \sum_{j=1}^N \alpha_{1j}(\eta) \right\}, \quad \eta \rightarrow \infty,$$

which expresses the approximation that the amount of exceedance events poses a non-stationary Poisson process.

Further, we may rewrite Eq. (2.2) using the same assumption, to be

$$P(\eta) \approx P_k(\eta) = \prod_{j=k}^N (1 - \alpha_{kj}(\eta)) \prod_{j=1}^{k-1} (1 - \alpha_{jj}(\eta)), \quad (2.4)$$

where $\alpha_{kj}(\eta) = \text{Prob}(X_j > \eta | X_{j-1} \leq \eta, \dots, X_{j-k+1} \leq \eta)$, for $j \geq k \geq 2$, denotes the probability of exceedance conditional on $k - 1$ previous nonexceedances. From Eq. (2.4), it is further obtained that

$$P(\eta) \approx F_k(\eta) := \exp \left\{ - \sum_{j=k}^N \alpha_{kj}(\eta) - \sum_{j=1}^{k-1} \alpha_{jj}(\eta) \right\}, \quad \eta \rightarrow \infty, \quad (2.5)$$

where $F_k(\eta) \rightarrow P(\eta)$ as $k \rightarrow N$ with $F_N(\eta) = P(\eta)$ for $\eta \rightarrow \infty$.

For the approximations $F_k(\eta)$ to have any practical use, it is assumed there is a cut-off value k_c satisfying $k_c \ll N$ such that $F_{k_c}(\eta) = F_N(\eta)$. We choose an arbitrary k -value of interest, $k \ll N$ such that $\sum_{j=1}^{k-1} \alpha_{jj}(\eta)$ is effectively negligible compared to $\sum_{j=k}^N \alpha_{kj}(\eta)$. Using this simplification we rewrite Eq. (2.5) as

$$F_k(\eta) = \exp \left\{ - \sum_{j=k}^N \alpha_{kj}(\eta) \right\}, \quad k \geq 1. \quad (2.6)$$

As discussed in [12], we can understand Eq. (2.6) by interpreting the expressions $\sum_{j=k}^N \alpha_{kj}(\eta)$ as the expected effective number of independent exceedance events provided by conditioning on $k - 1$ previous observations.

We introduce the univariate *average conditional exceedance rate* (ACER) of order k as:

$$\varepsilon_k(\eta) = \frac{1}{N - k + 1} \sum_{j=k}^N \alpha_{kj}(\eta), \quad k = 1, 2, \dots$$

For the underlying process $Z(t)$ there are typically two practical scenarios. Firstly, we may consider it to be a stationary process or rather an ergodic process, i.e. a process that will not change its statistical properties over time, and the properties may be found from a single, sufficiently long sample of the process. Secondly, we may view $Z(t)$ as a process depending on certain parameters whose variation in time can be modeled as an ergodic process. For each set of parameter values, the prerequisite is that $Z(t)$ can be modeled as an ergodic process. As discussed in [9], it is this scenario that opens for modeling of long-term statistics.

We continue by presenting some details concerning the numerical estimation of $\varepsilon_k(\eta)$ for $k \geq 2$:

$$A_{kj} = 1\{X_j > \eta, X_{j-1} \leq \eta, \dots, X_{j-k+1} \leq \eta\}, \quad j = k, \dots, N, \quad k = 2, 3, \dots,$$

and

$$B_{kj} = 1\{X_{j-1} \leq \eta, \dots, X_{j-k+1} \leq \eta\}, \quad j = k, \dots, N, \quad k = 2, 3, \dots, \quad (2.7)$$

where $1\{\vartheta\}$ is the indicator function of some event ϑ . This yield

$$\alpha_{kj} = \frac{\mathbb{E}[A_{kj}(\eta)]}{\mathbb{E}[B_{kj}(\eta)]}, \quad j = k, \dots, N, \quad k = 2, 3, \dots,$$

where $\mathbb{E}[\cdot]$ is the expectation operator. Assuming an ergodic process, we may write $\varepsilon_k(\eta)$ in terms of $a_{kj}(\eta)$ and $b_{kj}(\eta)$, these being realized values of $A_{kj}(\eta)$ and $B_{kj}(\eta)$. We obtain

$$\varepsilon_k(\eta) = \lim_{N \rightarrow \infty} \frac{\sum_{j=k}^N a_{kj}(\eta)}{\sum_{j=k}^N b_{kj}(\eta)}.$$

From Eq. (2.7), we clearly see that the limiting value as η increases, is equal to 1. This results in

$$\lim_{\eta \rightarrow \infty} \frac{\tilde{\varepsilon}_k(\eta)}{\varepsilon_k(\eta)} = 1,$$

where

$$\tilde{\varepsilon}_k(\eta) = \frac{\sum_{j=k}^N \mathbb{E}[A_{kj}(\eta)]}{N - k + 1}. \quad (2.8)$$

Using $\tilde{\varepsilon}_k(\eta)$ yield correct estimates for the function when η is at extreme levels, which is our main goal.

As a side note, Eq. (2.8) is also relevant for non-stationary time series. This can be shown by

$$\begin{aligned} P(\eta) &\approx \exp \left\{ - \sum_{j=k}^N \alpha_{kj}(\eta) \right\} \\ &= \exp \left\{ - \sum_{j=k}^N \frac{\mathbb{E}[A_{kj}(\eta)]}{\mathbb{E}[B_{kj}(\eta)]} \right\} \\ &\underset{\eta \rightarrow \infty}{\approx} \exp \left\{ - \sum_{j=k}^N \mathbb{E}[A_{kj}(\eta)] \right\}. \end{aligned}$$

If the time series of interest can be split into K blocks containing C_i indices for block no. i , where $i = 1, \dots, K$, such that $\mathbb{E}[A_{kj}(\eta)]$ remains roughly constant in each block and $\sum_{j \in C_i} \mathbb{E}[A_{kj}(\eta)] \approx \sum_{j \in C_i} a_{kj}(\eta)$ for a sufficient amount of η values, then $\sum_{j=k}^N \mathbb{E}[A_{kj}(\eta)] \approx \sum_{j=k}^N a_{kj}(\eta)$. It follows that

$$P(\eta) \approx \exp \{ -(N - k + 1) \hat{\varepsilon}_k(\eta) \},$$

where

$$\hat{\varepsilon}_k(\eta) = \frac{1}{N - k + 1} \sum_{j=k}^N a_{kj}(\eta).$$

We may interpret $\varepsilon_k(\eta)(N - k + 1)$ as the average number of clusters exceeding η separated by at least $k - 1$ nonexceedances, where a cluster is defined as a maximum number of consecutive exceedances above η .

For a wide range of systems, it is legitimate, [11], to assume the tail of the ACER function to be modeled as

$$\tilde{\varepsilon}_k(\eta) \approx q_k(\eta) \exp \{ -a_k(\eta - b_k)^{c_k} \}, \quad \eta > \eta_1, \quad (2.9)$$

for constants a_k, b_k and c_k with a slowly varying function $q_k(\eta)$ compared to the exponential function it is multiplied with, and η_1 is the *tail marker*. In general the function $q_k(\eta)$ is not a constant, but its variation in the tail region is often sufficiently slow to allow for its replacement by a constant, called q_k . As this assumption fails in the lower values, we need to specify a tail marker, η_1 , for

where the assumption may hold. This value may be found by visual inspection of the ACER plot, from where the function starts behaving on the form of Eq. (2.9). Another option is to apply the algorithm used in the univariate ACER program, [8]. As the form of Eq. (2.9) should hold above a chosen η_1 , choosing a higher tail marker should not affect the estimates to a large extent, but variance is increased as there is a decrease in points. Choosing a lower tail marker would, on the other hand, put too much emphasis on lower levels.

Confidence Intervals for Return Levels

It is of interest to estimate a confidence interval for the ACER function, $\varepsilon_k(\eta)$. Assuming a stationary time series, the sample standard deviation $\hat{s}_k(\eta)$ can be estimated by the formula

$$\hat{s}_k(\eta)^2 = \frac{1}{R-1} \sum_{r=1}^R \left(\hat{\varepsilon}_k^{(r)}(\eta) - \hat{\varepsilon}_k(\eta) \right)^2,$$

where R is the sample size, $\hat{\varepsilon}_k^{(r)}(\eta)$ is the ACER function estimate from realization no. r and $\hat{\varepsilon}_k(\eta) = \sum_{r=1}^R \hat{\varepsilon}_k^{(r)}(\eta)/R$.

Now, assuming independent samples and R large enough ($R \geq 20$), the 95% confidence interval for $\varepsilon_k(\eta)$ can be computed as

$$\text{CI}^\pm(\eta) = \hat{\varepsilon}_k(\eta) \pm \frac{1.96 \hat{s}_k(\eta)}{\sqrt{R}}.$$

For non-stationary time series we may use a different approach. We assume that the amount of conditional exceedances over the threshold η constitute a Poisson process, therefore the variance of the estimator $\hat{E}_k(\eta)$ of $\tilde{\varepsilon}_k(\eta)$, where

$$\hat{E}_k(\eta) = \frac{\sum_{j=k}^N A_{kj}(\eta)}{N - k + 1},$$

is

$$\text{Var}[\hat{E}_k(\eta)] = \tilde{\varepsilon}_k(\eta).$$

Again, the 95% confidence interval for $\tilde{\varepsilon}_k(\eta)$, as well as for $\varepsilon_k(\eta)$, can be computed as

$$\text{CI}^\pm(\eta) = \hat{\varepsilon}_k(\eta) \left(1 \pm \frac{1.96}{\sqrt{(N - k + 1)\hat{\varepsilon}_k(\eta)}} \right).$$

Return Levels

To estimate return levels, it is first necessary to find an expression for the return level η_p . The return level η_p satisfies the relation $P(\eta_p) = 1 - p$, where $P(\cdot)$ denotes the distribution of the yearly maximum, which correspond to a return period $T = (1/p)$. This probability approximates to

$$\begin{aligned} P(\eta_p) &= 1 - p \approx \exp \{-N\tilde{\varepsilon}_k(\eta_p)\} \\ &= \exp \{-Nq_k \exp \{-a_k(\eta_p - b_k)^{c_k}\}\}, \end{aligned}$$

where $q_k(\eta)$ is assumed constant, and N is the total number of data from 1 year. The parameters a_k, b_k, c_k and q_k are estimated using data of one year block sizes, i.e. all observations during a year is viewed as a realization of the same process.

To simplify notation we replace the approximation symbol with the equality sign, define $d = \ln(q_k)$ and drop subscripts on parameters. The resulting simplification yield

$$1 - p = \exp \{ -N \exp \{ d - a(\eta_p - b)^c \} \},$$

while solving for η_p give

$$\eta_p = b + \left[\frac{d - \ln(-\ln(1-p)) + \ln(N)}{a} \right]^{\frac{1}{c}}.$$

2.2 The Bivariate ACER Distribution

We encounter several challenges when evaluating the extension from the univariate to the bivariate case of extreme value statistics. Primarily, there is no generalization of the univariate extreme value theorem, see [1], to the bivariate case. A solution to this have been to adopt a copula to represent the joint distribution. There is a range of different copulas available to use, but a common flaw is that they are rather ad hoc.

It is therefore interesting to note that the ACER concept can be extended to several dimensions, and in this case, the bivariate. This was originally derived in [10].

Cascade of Conditioning Approximations

We consider a bivariate stochastic process $Z(t) = (X(t), Y(t))$ with dependent component processes, that have been observed over a time interval $(0, T)$. Further we assume that the values $Z_1 = (X_1, Y_1), \dots, Z_N = (X_N, Y_N)$ are distributed on the discrete times t_1, \dots, t_N in $(0, T)$. The goal is to find the joint distribution function, i.e.

$$\hat{X}_N = \max_{j=1, \dots, N} \{X_j\} \quad \hat{Y}_N = \max_{j=1, \dots, N} \{Y_j\},$$

$$\hat{Z}_N = (\hat{X}_N, \hat{Y}_N).$$

Note that \hat{Z}_N does not need to be an observed vector from the original data set. As in the univariate case, we also wish to estimate $P(\xi, \eta) = \text{Prob}(\hat{X}_N < \xi, \hat{Y}_N < \eta)$ for large values of ξ and η .

To ease the notation, we use $\zeta := (\xi, \eta)$ with component wise ordering relationship for Z_i , i.e. $Z_i \leq \zeta$ means $(X_i \leq \xi, Y_i \leq \eta)$. In addition we

introduce the event $C_{kj}(\zeta) = \{Z_{j-1} \leq \zeta, \dots, Z_{j-k+1} \leq \zeta\}$ of $k-1$ consecutive component wise nonexceedances ($k \geq 2$). By the definition of $P(\xi, \eta)$ we have

$$\begin{aligned} P(\xi, \eta) &= P(\zeta) = \text{Prob}(C_{N+1, N+1}(\zeta)) \\ &= \text{Prob}(Z_N \leq \zeta | C_{NN}(\zeta)) \cdot \text{Prob}(C_{NN}(\zeta)) \\ &= \prod_{j=2}^N \text{Prob}(Z_j \leq \zeta | C_{jj}(\zeta)) \cdot \text{Prob}(C_{22}(\zeta)). \end{aligned} \quad (2.10)$$

We may simplify Eq. (2.10) by assuming that all observed data are independent. This implies that all conditionings can be neglected.

In general, the variables Z_j are statistical dependent in a componentwise sense. Therefore, Eq. (2.10) may be written, by only conditioning on more than $k-1$ previous data points and where $k = 1, \dots, N$ and $j \geq k$, as:

$$P(\xi, \eta) = \prod_{j=k}^N \text{Prob}(Z_j \leq \zeta | C_{kj}(\xi, \eta)) \cdot \text{Prob}(C_{kk}(\xi, \eta)). \quad (2.11)$$

Notice that both data set need to be conditioned on k values each.

Further, for $k \leq i \leq N$, we introduce the notation

$$\begin{aligned} \alpha_{kj}(\xi; \eta) &:= \text{Prob}(X_j > \xi | C_{kj}(\xi, \eta)), \\ \beta_{kj}(\eta; \xi) &:= \text{Prob}(Y_j > \eta | C_{kj}(\xi, \eta)), \\ \gamma_{kj}(\xi, \eta) &:= \text{Prob}(Z_j > \zeta | C_{kj}(\xi, \eta)). \end{aligned}$$

Using this notation, the approximation of the first term of Eq. (2.11) is found to be

$$\begin{aligned} \prod_{j=k}^N \text{Prob}(Z_j \leq \zeta | C_{kj}(\xi, \eta)) &\approx \\ \exp \left\{ - \sum_{j=k}^N (\alpha_{kj}(\xi; \eta) + \beta_{kj}(\eta; \xi) - \gamma_{kj}(\xi; \eta)) \right\}; &\quad \xi, \eta \rightarrow \infty, \end{aligned}$$

while the second term of the equation is found to be

$$\text{Prob}(C_{kk}(\xi, \eta)) \approx \exp \left\{ - \sum_{j=1}^{k-1} (\alpha_{jj}(\xi; \eta) + \beta_{jj}(\eta; \xi) - \gamma_{jj}(\xi; \eta)) \right\}; \quad \xi, \eta \rightarrow \infty.$$

Collecting the terms yield

$$\begin{aligned} P(\xi, \eta) &\approx P_k(\xi, \eta) \\ &= \exp \left\{ - \sum_{j=k}^N (\alpha_{kj}(\xi; \eta) + \beta_{kj}(\eta; \xi) - \gamma_{kj}(\xi; \eta)) \right. \\ &\quad \left. - \sum_{j=1}^{k-1} (\alpha_{jj}(\xi; \eta) + \beta_{jj}(\eta; \xi) - \gamma_{jj}(\xi; \eta)) \right\}; \quad \xi, \eta \rightarrow \infty. \end{aligned} \quad (2.12)$$

Based on the definition of $P(\xi, \eta)$ and the properties of the conditional probability, the set $\{P_k(\xi, \eta)\}_{k=1}^N$ converges to the target distribution $P(\xi, \eta)$ of the extreme value M_N as k increases.

For practical and application purposes we make the assumption that there is an effective k_e satisfying $k_e \ll N$ such that $P(\xi, \eta) = P_{k_e}(\xi, \eta)$. Further, we assume that $\sum_{j=1}^{k-1} (\alpha_{jj}(\xi; \eta) + \beta_{jj}(\eta; \xi) - \gamma_{jj}(\xi; \eta))$ is negligible compared to $\sum_{j=k}^N (\alpha_{kj}(\xi; \eta) + \beta_{kj}(\eta; \xi) - \gamma_{kj}(\xi; \eta))$. This lead to the approximation of Eq. (2.12)

$$P(\xi, \eta) \approx P_k(\xi, \eta) \approx \exp \left\{ - \sum_{j=k}^N (\alpha_{kj}(\xi; \eta) + \beta_{kj}(\eta; \xi) - \gamma_{kj}(\xi; \eta)) \right\}; \quad \xi, \eta \rightarrow \infty, \quad (2.13)$$

resulting in the conclusion that it is sufficient, for the estimation of the bivariate extreme value distribution, to calculate $\{\alpha_{kj}(\xi; \eta) + \beta_{kj}(\eta; \xi) - \gamma_{kj}(\xi; \eta)\}_{j=k}^N$.

Empirical Estimation of the ACER Function

It is now appropriate to introduce the concept of k 'th order bivariate ACER function as follows

$$\mathcal{E}_k(\xi, \eta) = \frac{\sum_{j=k}^N (\alpha_{kj}(\xi; \eta) + \beta_{kj}(\eta; \xi) - \gamma_{kj}(\xi, \eta))}{N - k + 1}, \quad k = 1, 2, \dots$$

For $N \gg k$, we may write Eq. (2.13) as

$$P(\xi, \eta) \approx \exp \{ -(N - k + 1) \mathcal{E}_k(\xi, \eta) \}; \quad \xi, \eta \rightarrow \infty. \quad (2.14)$$

Further details on the numerical estimation of the ACER function are appropriate. We introduce a set of random functions. For $k = 2, \dots, N$ and $k \leq j \leq N$, let

$$\begin{aligned} A_{kj}(\xi; \eta) &= 1 \{ X_j > \xi \cap C_{kj}(\xi, \eta) \}, \\ B_{kj}(\eta; \xi) &= 1 \{ Y_j > \eta \cap C_{kj}(\xi, \eta) \}, \\ G_{kj}(\xi, \eta) &= 1 \{ Z_j > \zeta \cap C_{kj}(\xi, \eta) \}, \\ C_{kj}(\xi, \eta) &= 1 \{ C_{kj}(\xi, \eta) \}, \end{aligned}$$

where $1\{\vartheta\}$ is the indicator function of some event ϑ .

From the definitions stated above, we may see that

$$\alpha_{kj}(\xi; \eta) = \frac{\mathbb{E}[A_{kj}(\xi; \eta)]}{\mathbb{E}[C_{kj}(\xi, \eta)]}, \quad \beta_{kj}(\eta; \xi) = \frac{\mathbb{E}[B_{kj}(\eta; \xi)]}{\mathbb{E}[C_{kj}(\xi, \eta)]}, \quad \gamma_{kj}(\xi; \eta) = \frac{\mathbb{E}[G_{kj}(\xi; \eta)]}{\mathbb{E}[C_{kj}(\xi, \eta)]},$$

where $\mathbb{E}[\cdot]$ denotes the expectation operator.

Assuming ergodicity of the process $Z(t) = (X(t), Y(t))$, then $\mathcal{E}_k(\xi, \eta) = (\alpha_{kk}(\xi; \eta) + \beta_{kk}(\eta; \xi) - \gamma_{kk}(\xi, \eta)) = \dots = (\alpha_{kN}(\xi; \eta) + \beta_{kN}(\eta; \xi) - \gamma_{kN}(\xi, \eta))$, and it may be assumed that

$$\mathcal{E}_k(\xi, \eta) = \lim_{N \rightarrow \infty} \frac{\sum_{j=k}^N (a_{kj}(\xi; \eta) + b_{kj}(\eta; \xi) - g_{kj}(\xi, \eta))}{\sum_{j=k}^N c_{kj}(\xi, \eta)}, \quad (2.15)$$

where $a_{kj}(\xi; \eta)$, $b_{kj}(\eta; \xi)$, $g_{kj}(\xi; \eta)$ and $c_{kj}(\xi; \eta)$ are realizations of $A_{kj}(\xi; \eta)$, $B_{kj}(\eta; \xi)$, $\gamma_{kj}(\xi; \eta)$ and $C_{kj}(\xi; \eta)$, respectively.

Obviously, $\lim_{\xi, \eta \rightarrow \infty} \mathbb{E}[C_{kj}(\xi, \eta)] = 1$. Therefore,

$$\lim_{\xi, \eta \rightarrow \infty} \frac{\tilde{\mathcal{E}}_k(\xi, \eta)}{\mathcal{E}_k(\xi, \eta)} = 1,$$

where

$$\tilde{\mathcal{E}}_k(\xi, \eta) = \lim_{N \rightarrow \infty} \frac{\sum_{j=k}^N (\mathbb{E}[A_{kj}] + \mathbb{E}[B_{kj}] - \mathbb{E}[G_{kj}])}{N - k + 1}. \quad (2.16)$$

Using the modified bivariate ACER function $\tilde{\mathcal{E}}_k(\xi, \eta)$ for $k \geq 2$, some advantages are achieved. The modified function is easier to use for non-stationary or long-term statistics than $\mathcal{E}_k(\xi, \eta)$, and since we are only interested in the values of the ACER functions at the extreme levels, we may use any function providing correct predictions of the ACER function at these extreme levels.

Confidence Intervals for Return Levels

Provided multiple realizations of the time series $Z(t)$, or a time series that can be appropriately sectioned into several records, e.g. several annual, the sample estimate of $\mathcal{E}_k(\xi, \eta)$ would be

$$\hat{\mathcal{E}}_k(\xi, \eta) = \frac{1}{R} \sum_{r=1}^R \hat{\mathcal{E}}_k^{(r)}(\xi, \eta),$$

where R is the amount of realizations, the index (r) refers to realization number r , and $\hat{\mathcal{E}}_k^{(r)}(\xi, \eta)$ is the estimate of the stationary time series using Eq. (2.15) or of the non-stationary time series using Eq. (2.16). The standard deviation of the sample $\hat{s}_k(\xi; \eta)$ can then be estimated using the formula

$$\hat{s}_k(\xi; \eta)^2 = \frac{1}{R-1} \sum_{r=1}^R \left(\hat{\mathcal{E}}_k^{(r)}(\xi, \eta) - \hat{\mathcal{E}}_k(\xi, \eta) \right)^2. \quad (2.17)$$

Assuming independent realizations, Eq. (2.17) can be used to create a 95% confidence interval

$$\text{CI}^{\pm}(\xi, \eta) = \hat{\mathcal{E}}_k(\xi, \eta) \pm \tau \cdot \frac{\hat{s}_k(\xi, \eta)}{\sqrt{R}}$$

where $\tau = t^{-1}((1 - 0.95)/2, R - 1)$ is the corresponding quantile in the Student's t-distribution with $R - 1$ degrees of freedom.

Return Levels

From the definition of $\mathcal{E}_k(\xi, \eta)$, the product $\mathcal{E}_k(\xi, \eta) \cdot (N - k + 1)$ represents the expected number of the bivariate observations $Z_j = (X_j, Y_j)$ where their

components exceed the corresponding levels ξ and η , and follow after at least $k - 1$ previous simultaneous nonexceedances. As a result of this, the product captures the spatial and temporal dependence structure of the bivariate time series. Thus, high quantiles of the bivariate extreme value distribution should potentially be obtained.

The joint T -year return period contour related to the event that either \widehat{X}_N or \widehat{Y}_N or both are exceeded is presented by

$$1 - F^{1yr}(\xi^T, \eta^T) = \frac{1}{T}, \quad (2.18)$$

where $F^{1yr}(\xi, \eta)$ is the joint distribution function of the annual maxima. Assuming the observations of the bivariate process are collected over a period n_y ,

$$F^{1yr}(\xi, \eta) = \exp \left\{ -\frac{N - k + 1}{n_y} \mathcal{E}_k(\xi, \eta) \right\}. \quad (2.19)$$

Combining Eq. (2.18) and (2.19) yield the T -year return levels (ξ^T, η^T) as a solution of

$$\mathcal{E}_k(\xi^T, \eta^T) = -\log \left(1 - \frac{1}{T} \right) \frac{n_y}{N - k + 1}. \quad (2.20)$$

By Eq. (2.20), it is clear that the empirically estimated k -th order bivariate ACER function does not contain enough information for estimation of quantiles outside its observed period, i.e. if the observation period is 10 years, the function will only contain enough information to make an estimate of the 10 year return values, with high uncertainty. In addition, the behavior of the bivariate ACER function as a continuous function with two variables can not be decided using the data. As a result of this, a sub-asymptotic functional form of the bivariate ACER surface can perhaps be achieved using a copula representation of a bivariate extreme value distribution.

Classical Extreme Value Theory

It seems that the rivers know the theory. It only remains to convince the engineers of the validity of this analysis.

- Emil J. Gumbel, 1958.

In this chapter we give an introduction to classical extreme value theory for both the univariate and the multivariate cases relevant for the analysis. Furthermore, a brief introduction to copula theory is given followed by a step-by-step calculation of the copula models used in the analysis.

For the multivariate state, we focus on the bivariate case. This enables us to illustrate the key concepts while keeping notation simple.

3.1 The Univariate Generalized Extreme Value Distribution

Again our objective is to find the distribution of the extreme value $M_N = \max_N\{X_j; j \in \{1, \dots, N\} \subset \mathbb{N}\}$, where we consider the X_1, \dots, X_N to be a sequence of independent random variables collected from a common distribution function F . In application, the X_i usually represent values measured on a general time scale, e.g. hourly wind levels. M_N then represent the maximum value of the process over N observations. If N is the total amount of observations in a year, M_N corresponds to the annual maxima.

Estimating $P(z) = \text{Prob}(M_N \leq z)$ for large values of z may be derived exactly for all values of N ,

$$\begin{aligned} P(z) &= \text{Prob}(X_1 \leq z, \dots, X_N \leq z) \\ &= \text{Prob}(X_1 \leq z) \cdot \text{Prob}(X_2 \leq z) \cdot \dots \cdot \text{Prob}(X_N \leq z) \\ &= (F(z))^N. \end{aligned}$$

In practice, we might not have the distribution function F , but the *Extreme Value Theorem*, also known as the *Fisher-Tippett-Gnedenko Theorem* provides an asymptotic result.

Theorem 1 ([1, page. 46]). *If there exist a sequence of constants $\{a_N > 0\}$ and $\{b_N\}$ such that*

$$\text{Prob}\{M_N^* \leq z\} = \text{Prob}\left\{\frac{M_N - b_N}{a_N} \leq z\right\} \rightarrow G(z) \quad \text{as } N \rightarrow \infty,$$

where G is a non-degenerate distribution function, then G belongs to one of the following families:

$$\begin{aligned} \text{I: } G(z) &= \exp\left\{-\exp\left[-\left(\frac{z-b}{a}\right)\right]\right\}, & -\infty < z < \infty; \\ \text{II: } G(z) &= \begin{cases} 0, & z \leq b; \\ \exp\left\{-\left(\frac{z-b}{a}\right)^{-\alpha}\right\}, & z > b; \end{cases} & (3.1) \\ \text{III: } G(z) &= \begin{cases} \exp\left\{-\left[-\left(\frac{z-b}{a}\right)^\alpha\right]\right\}, & z < b; \\ 1, & z \geq b; \end{cases} \end{aligned}$$

for parameters $a > 0$, b and, in case of families II and III, $\alpha > 0$.

In words, Theorem 1 states that the rescaled sample maxima M_N^* converge in distribution to one of the three distributions otherwise known as the Gumbel, Fréchet and Weibull families. Each of them includes a location and scale parameter, b and a , respectively; while the Fréchet and Weibull also have a shape parameter, α .

By doing simple reformulations of these three distributions, it is possible to combine them into a single family of models known as the *Generalized Extreme Value distribution*, or GEV for short. The GEV distribution is written on the form

$$G(z) = \exp\left\{-\left[1 + \xi\left(\frac{z-\mu}{\sigma}\right)\right]^{-1/\xi}\right\}, \quad (3.2)$$

where $\{z : 1 + \xi(z - \mu)/\sigma > 0\}$, and the parameters satisfy $-\infty < \mu < \infty$, $\sigma > 0$ and $-\infty < \xi < \infty$. The three parameters corresponding to the location parameter, μ ; the scale parameter, σ ; and the shape parameter, ξ . The shape parameter decides which of the three extreme value distributions the GEV distribution correspond to. For $\xi > 0$ the GEV distribution become the Fréchet distribution, while for $\xi < 0$ the Weibull distribution is obtained. The subfamily of the GEV family for $\xi = 0$ is interpreted as $\xi \rightarrow 0$, which yield the Gumbel family.

Empirical Estimation of the GEV distribution

Modeling extremes of a time series are solved by dividing the observations into sequences of length n , for some large value n , generating a series of block maxima, $M_{n,1}, \dots, M_{n,m}$ where the assumption of independent observations may be assumed. Furthermore, the GEV distribution may then be fitted using

maximum likelihood estimation. When $\xi \neq 0$, the log-likelihood becomes

$$\begin{aligned} \ell(\mu, \sigma, \xi) = & -m \log \sigma - \left(1 + \frac{1}{\xi}\right) \sum_{i=1}^m \log \left[1 + \xi \left(\frac{z_i - \mu}{\sigma}\right)\right] \\ & - \sum_{i=1}^m \log \left[1 + \xi \left(\frac{z_i - \mu}{\sigma}\right)\right]^{-\frac{1}{\xi}} \end{aligned} \quad (3.3)$$

provided that

$$1 + \xi \left(\frac{z_i - \mu}{\sigma}\right) > 0, \quad i = 1, \dots, m.$$

In the Gumbel case, i.e. $\xi = 0$, the log-likelihood becomes

$$\ell(\mu, \sigma) = -m \log \sigma - \sum_{i=1}^m \left(\frac{z_i - \mu}{\sigma}\right) - \sum_{i=1}^m \exp \left\{ - \left(\frac{z_i - \mu}{\sigma}\right) \right\}. \quad (3.4)$$

Maximizing both Eq. (3.3) and (3.4) with respect to the (μ, σ, ξ) leads to the maximum likelihood estimate for the entire GEV distribution family.

Return Levels

The return level, z_p , which is exceeded by the annual maximum in any particular year with probability p , may be found by inverting Eq. (3.2). Estimates of extreme quantiles of the annual maximum distribution will then be calculated using

$$z_p = \begin{cases} \mu - \frac{\sigma}{\xi} \left[1 - \{-\log(1-p)\}^{-\xi}\right], & \text{for } \xi \neq 0, \\ \mu - \sigma \log \{-\log(1-p)\}, & \text{for } \xi = 0, \end{cases} \quad (3.5)$$

where $G(z_p) = 1 - p$. As quantiles enable probability models to be expressed on the scale of data, the relationship of the GEV model to its parameters are interpreted in terms of the quantile expressions of Eq. (3.5). Defining $y_p = -\log(1-p)$, such that

$$z_p = \begin{cases} \mu - \frac{\sigma}{\xi} \left[1 - y_p^{-\xi}\right], & \text{for } \xi \neq 0, \\ \mu - \sigma \log y_p, & \text{for } \xi = 0, \end{cases}$$

it follows that, if z_p is plotted against y_p on a logarithmic scale, the plot is linear if $\xi = 0$. If $\xi < 0$ the plot is convex, and if $\xi > 0$ the plot is concave.

3.2 Multivariate Extremes

Suppose $(X_1, Y_1), (X_2, Y_2), \dots$ is a sequence of vectors that are independent versions of a random vector having distribution function $F(x, y)$. We base the characterization of the extremal behavior of multivariate extremes on the limiting behavior of block maxima. Consider

$$M_{x,n} = \max_{i=1, \dots, n} \{X_i\}, \quad M_{y,n} = \max_{i=1, \dots, n} \{Y_i\},$$

$$\mathbf{M}_n = (M_{x,n}, M_{y,n}), \quad (3.6)$$

where \mathbf{M}_n is the vector of componentwise maxima. The index i , for which the maximum of the X_i sequence occurs, need not be the same as that of the Y_i sequence, i.e. \mathbf{M}_n does not have to be an observed vector from the original series.

The asymptotic theory of multivariate extremes begins with an analysis of \mathbf{M}_n in Eq. (3.6) as $n \rightarrow \infty$. We may simplify the problem by considering $\{X_i\}$ and $\{Y_i\}$ separately as sequences of independent, univariate random variables. Furthermore, we can therefore apply standard univariate extreme value results to both components. This means we may gain some simplicity by assuming the X_i and Y_i variables to have known marginal distributions. In case the assumed marginal distribution is wrong, marginal distributions whose extremal properties are determined by the univariate characterizations, can always be transformed into the standard form.

Representations are particularly easy if we assume both X_i and Y_i to have a standard Fréchet distribution, i.e.

$$F(z) = \exp\left\{-\frac{1}{z}\right\}, \quad z > 0.$$

To obtain standard univariate results for each margin, we should consider the re-scaled vector

$$\mathbf{M}_n^* = \left(\max_{i=1, \dots, n} \{X_i\}/n, \max_{i=1, \dots, n} \{Y_i\}/n \right). \quad (3.7)$$

This representation leads to the following theorem that gives a characterization of the limiting joint distribution of \mathbf{M}_n^* , as $n \rightarrow \infty$.

Theorem 2 ([1, page. 144]). *Let $\mathbf{M}_n^* = (M_{x,n}^*, M_{y,n}^*)$ be defined by Eq. (3.7), where the (X_i, Y_i) are independent vectors with standard Fréchet marginal distributions. Then if*

$$\text{Prob}\{M_{x,n}^* \leq x, M_{y,n}^* \leq y\} \xrightarrow{d} G(x, y), \quad (3.8)$$

where G is a non-degenerate distribution function, G has the form

$$G(x, y) = \exp\{-V(x, y)\}, \quad x > 0, y > 0, \quad (3.9)$$

where

$$V(x, y) = 2 \int_0^1 \max\left(\frac{w}{x}, \frac{1-w}{y}\right) dH(w), \quad (3.10)$$

and H is a distribution function on $[0, 1]$ satisfying the mean constraint

$$\int_0^1 w dH(w) = \frac{1}{2}. \quad (3.11)$$

The family of distributions that arise as limits in Eq. (3.8) is termed the class of *bivariate extreme value distributions*. [Theorem 2](#) implies that the class

of bivariate extreme value distributions is in one-to-one correspondence with the set of distribution functions H on $[0, 1]$ satisfying Eq. (3.11).

If H is differentiable with density h , Eq. (3.10) is simplified to be

$$V(x, y) = 2 \int_0^1 \max\left(\frac{w}{x}, \frac{1-w}{y}\right) h(w) dw.$$

However, H does not need to be a differentiable function. For example, if H is a measure that places mass 0.5 on $w = 0$ and $w = 1$, the constraint in Eq. (3.11) is trivially satisfied, and Eq. (3.10) becomes

$$V(x, y) = x^{-1} + y^{-1}.$$

The corresponding bivariate extreme value distribution turn into

$$G(x, y) = \exp\{-(x^{-1} + y^{-1})\}, \quad x > 0, y > 0.$$

By using this property in Eq. (3.9), we obtain

$$G^n(x, y) = G(n^{-1}x, n^{-1}y),$$

for $n = 2, 3, 4, \dots$. This implies that if (X, Y) have distribution G , then apart from the rescaling by n^{-1} , M_n also have distribution G . Therefore G possesses a multivariate version of the max-stability property.

Even though [Theorem 2](#) provides a complete characterization of bivariate limit distributions, the possible limit of classes are only constrained by Eq. (3.11). Basically, any distribution function H on $[0, 1]$ satisfying the mean constraint of Eq. (3.11), gives rise to a valid limit in Eq. (3.8). This leads to complications as the limit family has no finite parametrization. One possible solution is to use *Copulas*.

3.3 Copulas

Copulas are the most general, margin-free description of the dependence structure of a multivariate distribution. Let (U, V) be a pair of random variables, uniformly distributed on the interval $[0, 1]$. The joint distribution of (U, V) , found by

$$\mathbf{C}(u, v) = \text{Prob}(U \leq u, V \leq v),$$

where $u, v \in [0, 1]$, is called a *copula*. The link between bivariate copulas and bivariate distributions is provided by *Sklar's* theorem:

Theorem 3 (Sklar's Theorem (bivariate case) [2, page 134]). *Let F_{XY} be a joint distribution function with marginals F_X and F_Y . Then there exists a bivariate copula \mathbf{C} such that*

$$F_{XY}(\xi, \eta) = \mathbf{C}(F_X(\xi), F_Y(\eta)). \quad (3.12)$$

for all reals ξ and η . If F_X and F_Y are continuous, then \mathbf{C} is unique; otherwise, \mathbf{C} is uniquely defined on $\text{Range}(F_X) \times \text{Range}(F_Y)$. Conversely, if \mathbf{C} is a bivariate copula and F_X and F_Y are distribution functions, then the function F_{XY} given by Eq. (3.12) is a joint distribution with marginals F_X and F_Y .

Since copulas represent an important tool in describing the structure of multivariate distributions, it is helpful to show the connection between classical multivariate extreme value theory and copulas, as stated in [Definition 1](#).

Definition 1 (Extreme Value Copula [[2](#), page. 192]). *A bivariate copula \mathbf{C} satisfying the relationship*

$$\mathbf{C}^t(u, v) = \mathbf{C}(u^t, v^t),$$

for all $t > 0$, is called an *Extreme Value copula*.

The use of extreme-value bivariate copulas is highly facilitated by the representation introduced by Pickands, [[13](#)], stating: a copula \mathbf{C} is an extreme-value copula if, and only if, there exists a real-value function \mathcal{D} on the interval $[0,1]$ such that

$$\mathbf{C}(F_X(\xi), F_Y(\eta)) = \exp \left\{ \log(F_X(\xi)F_Y(\eta)) \mathcal{D} \left(\frac{\log(F_X(\xi))}{\log(F_X(\xi)F_Y(\eta))} \right) \right\}, \quad (3.13)$$

for $F_X(\xi)$ and $F_Y(\eta) \in [0, 1]$. The function \mathcal{D} is called *Pickands dependence function*. The properties of the dependence function include:

1. $\mathcal{D}(0) = \mathcal{D}(1) = 1$
2. $\max(t, 1 - t) \leq \mathcal{D}(t) \leq 1$ for all $0 \leq t \leq 1$
3. \mathcal{D} is convex.

The notation of Eq. [\(3.13\)](#) may be simplified to

$$\mathbf{C}(F_X(\xi), F_Y(\eta)) = \exp \left\{ -(x + y) \mathcal{D} \left(\frac{x}{x + y} \right) \right\}, \quad (3.14)$$

where $x = -\log(F_X(\xi))$ and $y = -\log(F_Y(\eta))$.

Depending on the choice of dependence function, different parametric differentiable and non-differentiable models may be considered. In this thesis we will consider four differentiable dependence functions: two of which have 1 parameter, and two with 3 parameters.

The logistic or Gumbel-logistic dependence model, derived by Gumbel [[4](#)], is written as

$$\mathcal{D} \left(\frac{x}{x + y} \right) = \frac{1}{x + y} [x^r + y^r]^{\frac{1}{r}}, \quad (3.15)$$

where $r \geq 1$. Independence is obtained when r approaches 1, while complete dependence is revealed if r tends to infinity.

The asymmetric version of the Gumbel-logistic dependence model known as the Asymmetric logistic model was developed by Tawn [[14](#)] and is given as

$$\mathcal{D} \left(\frac{x}{x + y} \right) = \frac{1}{x + y} \left([(\phi x)^r + (\theta y)^r]^{\frac{1}{r}} - \phi x - \theta y \right) + 1, \quad (3.16)$$

where $r > 1$ and $0 < \theta, \phi < 1$. When $\theta = \phi = 1$ the Asymmetric logistic model is equivalent to the Gumbel-logistic model. Independence is attained

when either $r = 1$, $\phi = 0$ or $\theta = 0$, while complete dependence is achieved when $\phi = \theta = 1$ and r tends to infinity.

The model obtained by Galambos, [3], is called the Negative logistic dependence function,

$$\mathcal{D}\left(\frac{x}{x+y}\right) = 1 - \frac{(x^{-r} + y^{-r})^{-\frac{1}{r}}}{x+y}, \quad (3.17)$$

with the only parameter constraint given as $r > 0$. Independence is obtained in the limit as r approaches zero, while complete dependence is obtained as r tends to infinity.

The last dependence model, named the Asymmetric negative logistic, is acquired from Joe, [7], and given as

$$\mathcal{D}\left(\frac{x}{x+y}\right) = 1 - \frac{((\phi x)^{-r} + (\theta y)^{-r})^{-\frac{1}{r}}}{x+y}, \quad (3.18)$$

where the parameter constraints are $r > 0$ and $0 < \theta, \phi < 1$. As the Asymmetric logistic dependence function, when $\theta = \phi = 1$ the Asymmetric negative logistic model is equivalent to the Negative logistic model. Independence is obtained in the limit as either r, θ or ϕ approaches zero. Complete dependence is obtained in the limit when $\phi = \theta = 1$ and r tends to infinity.

3.4 Calculation of Pickands Result

Gumbel Marginals

Consider the result of Pickands, as seen in Eq. (3.14), and the marginal extreme value distributions $F_X(\xi)$ and $F_Y(\eta)$ given by the univariate Gumbel distribution seen in Eq. (3.1) (Type I), i.e.

$$F_X(\xi) = \exp\left\{-\exp\left[-\left(\frac{\xi - \mu_\xi}{\sigma_\xi}\right)\right]\right\},$$

$$F_Y(\eta) = \exp\left\{-\exp\left[-\left(\frac{\eta - \mu_\eta}{\sigma_\eta}\right)\right]\right\}.$$

Evaluating each part of Eq. (3.14) yield:

$$x = -\log(F_X(\xi)) = \exp\left[-\left(\frac{\xi - \mu_\xi}{\sigma_\xi}\right)\right] = g(\xi)$$

and

$$\begin{aligned} x + y &= -\log(F_X(x)) - \log(F_Y(y)) \\ &= \exp\left[-\left(\frac{\xi - \mu_\xi}{\sigma_\xi}\right)\right] + \exp\left[-\left(\frac{\eta - \mu_\eta}{\sigma_\eta}\right)\right] \\ &= g(\xi) + g(\eta) \end{aligned}$$

resulting in

$$H_{xy}(\xi, \eta) = \exp\left\{-(g(\xi) + g(\eta)) \cdot \mathcal{D}\left(\frac{g(\xi)}{g(\xi) + g(\eta)}\right)\right\}. \quad (3.19)$$

Our goal now is to compare the copula approach to the bivariate extreme value distribution of the data. As we have seen from Eq. (2.14), this can be expressed through the bivariate ACER function.

As the ACER function measures the probability of non-exceedances given $k - 1$ previous non-exceedances over the time of the observations n_y , we need to use the annual form of the ACER function if we are to compare the bivariate ACER function to the Gumbel copula approach. This is given in Eq. (2.19), i.e.

$$F^{1yr}(\xi, \eta) = \exp \left\{ -\frac{N - k + 1}{n_y} \mathcal{E}_k(\xi, \eta) \right\}.$$

By doing so, the functional form of the bivariate ACER surface can be obtained by

$$F^{1yr}(\xi, \eta) = H_{XY}(\xi, \eta),$$

equivalent to

$$\mathcal{E}_k(\xi, \eta) = \left(\frac{n_y}{N - k + 1} \right) \cdot (g(\xi) + g(\eta)) \cdot \mathcal{D} \left(\frac{g(\xi)}{g(\xi) + g(\eta)} \right).$$

Inserting the [Gumbel-logistic dependence](#) function in the argument above, the functional form of the bivariate ACER surface becomes

$$\mathcal{E}_k(\xi, \eta) = \left(\frac{n_y}{N - k + 1} \right) \cdot [g(\xi)^r + g(\eta)^r]^{\frac{1}{r}}, \quad (3.20)$$

while inserting the [Asymmetric logistic dependence](#) function yield

$$\mathcal{E}_k(\xi, \eta) = \left(\frac{n_y}{N - k + 1} \right) \cdot \left([(\phi g(\xi))^r + (\theta g(\eta))^r]^{\frac{1}{r}} + (1 - \phi)g(\xi) + (1 - \theta)g(\eta) \right). \quad (3.21)$$

Using the [Negative logistic dependence](#) function, the functional form becomes

$$\mathcal{E}_k(\xi, \eta) = \left(\frac{n_y}{N - k + 1} \right) \cdot \left(g(\xi) + g(\eta) - [g^{-r}(\xi) + g^{-r}(\eta)]^{-\frac{1}{r}} \right), \quad (3.22)$$

and by applying the [Asymmetric negative logistic dependence](#) function, we get

$$\mathcal{E}_k(\xi, \eta) = \left(\frac{n_y}{N - k + 1} \right) \cdot \left(g(\xi) + g(\eta) - [(\phi g(\xi))^{-r} + (\theta g(\eta))^{-r}]^{-\frac{1}{r}} \right). \quad (3.23)$$

ACER Marginals

Staying true to classical extreme value theory, we continue using the annual adaptation of the ACER function in both the univariate and bivariate case. The annual univariate ACER marginals are then given by

$$\begin{aligned} F^{1yr}(\xi) &= \exp \left\{ -\frac{N - k + 1}{n_y} \varepsilon_k(\xi) \right\}, \\ F^{1yr}(\eta) &= \exp \left\{ -\frac{N - k + 1}{n_y} \varepsilon_k(\eta) \right\}, \end{aligned} \quad (3.24)$$

where the sub-asymptotic functional form of the univariate ACER function is defined to be $\varepsilon_k(\xi) = q_k \exp\{-a_k(\xi - b_k)^{c_k}\}$, with similar result for $\varepsilon_k(\eta)$.

Using the annual univariate ACER functions, each part of Eq. (3.14) becomes:

$$x = -\log(F_X(\xi)) = \frac{N - k + 1}{n_y} \varepsilon_k(\xi),$$

and

$$\begin{aligned} x + y &= -\log(F_X(x)) - \log(F_Y(y)) \\ &= \frac{N - k + 1}{n_y} \varepsilon_k(\xi) + \frac{N - k + 1}{n_y} \varepsilon_k(\eta) \\ &= \left(\frac{N - k + 1}{n_y} \right) (\varepsilon_k(\xi) + \varepsilon_k(\eta)), \end{aligned}$$

resulting in

$$H_{xy}(\xi, \eta) = \exp \left\{ - \left(\frac{N - k + 1}{n_y} \right) (\varepsilon_k(\xi) + \varepsilon_k(\eta)) \cdot \mathcal{D} \left(\frac{\varepsilon_k(\xi)}{\varepsilon_k(\xi) + \varepsilon_k(\eta)} \right) \right\}.$$

Using the annual form of the ACER function as given in Eq. (2.19), the functional form of the bivariate ACER surface can be obtained by

$$\mathcal{E}_k(\xi, \eta) = (\varepsilon_k(\xi) + \varepsilon_k(\eta)) \cdot \mathcal{D} \left(\frac{\varepsilon_k(\xi)}{\varepsilon_k(\xi) + \varepsilon_k(\eta)} \right). \quad (3.25)$$

By applying the [Gumbel-logistic dependence](#) function in the argument above, the functional form of the bivariate ACER surface emerge as

$$\mathcal{E}_k(\xi, \eta) = [\varepsilon_k^r(\xi) + \varepsilon_k^r(\eta)]^{\frac{1}{r}}, \quad (3.26)$$

while inserting the asymmetric version, namely the [Asymmetric logistic dependence](#) function, yield

$$\mathcal{E}_k(\xi, \eta) = [(\phi \varepsilon_k(\xi))^r + (\theta \varepsilon_k(\eta))^r]^{\frac{1}{r}} + (1 - \phi) \varepsilon_k(\xi) + (1 - \theta) \varepsilon_k(\eta). \quad (3.27)$$

By inserting the [Negative logistic dependence](#) function, we need to compare

$$\mathcal{E}_k(\xi, \eta) = \varepsilon_k(\xi) + \varepsilon_k(\eta) - [\varepsilon_k^{-r}(\xi) + \varepsilon_k^{-r}(\eta)]^{-\frac{1}{r}}, \quad (3.28)$$

and finally, by using the [Asymmetric negative logistic dependence](#) function, we get

$$\mathcal{E}_k(\xi, \eta) = \varepsilon_k(\xi) + \varepsilon_k(\eta) - [(\phi \varepsilon_k(\xi))^{-r} + (\theta \varepsilon_k(\eta))^{-r}]^{-\frac{1}{r}}. \quad (3.29)$$

3.5 Optimizing Parameters

The optimized parameters r^* , ϕ^* and θ^* are found by minimizing the mean square error function, which is simplest explained by considering the non-symmetric and asymmetric cases individually.

In the non-asymmetric case, r^* is found by minimizing:

$$F(r) = \sum_{j=1}^{N_\eta} \sum_{i=1}^{N_\xi} w'_{ij} \left(\log \left(\hat{\mathcal{E}}_k(\xi_i, \eta_j) \right) - \log \left(\mathcal{N}\mathcal{A}_k(\xi_i, \eta_j) \right) \right)^2, \quad (3.30)$$

where N_η, N_ξ are numbers of levels η and ξ , respectively, at which the ACER function have been empirically estimated, $\mathcal{N}\mathcal{A}$ is the functional form of the bivariate ACER surface in one of the non-asymmetric cases, and $w'_{ij} = w_{ij} / \sum \sum w_{ij}$ where

$$w_{ij} = \left(\log (CI^+(\xi_i, \eta_j)) - \log (CI^-(\xi_i, \eta_j)) \right)^{-2}, \quad (3.31)$$

are the normalized weight factors prioritizing the most reliable estimates. The optimization problem with the objective function defined in Eq. (3.30) is written as

$$\begin{cases} F(r) \rightarrow \min; \\ \{r\} \in \mathcal{S}, \end{cases} \quad (3.32)$$

with the constraint domain

$$\mathcal{S} = \left\{ \{r\} \in \mathbb{R} \mid r \in [1, +\infty) \right\}, \quad (3.33)$$

in the Gumbel-logistic case, and

$$\mathcal{S} = \left\{ \{r\} \in \mathbb{R} \mid r \in [0, +\infty) \right\}, \quad (3.34)$$

in the Negative logistic case.

Using one of the asymmetric dependence functions, the optimized parameters r^*, ϕ^* and θ^* are found by minimizing the mean square error function:

$$F(r, \phi, \theta) = \sum_{j=1}^{N_\eta} \sum_{i=1}^{N_\xi} w'_{ij} \left(\log \left(\hat{\mathcal{E}}_k(\xi_i, \eta_j) \right) - \log \left(\mathcal{A}_k(\xi_i, \eta_j) \right) \right)^2, \quad (3.35)$$

where \mathcal{A} is the functional form of the bivariate ACER surface in one of the asymmetric dependence function cases. The constrained optimization problem becomes

$$\begin{cases} F(r, \phi, \theta) \rightarrow \min; \\ \{r, \phi, \theta\} \in \mathcal{S}, \end{cases}$$

with the constraint domain

$$\mathcal{S} = \left\{ \{r, \phi, \theta\} \in \mathbb{R}^3 \mid \theta, \phi \in [0, 1]; r \in [1, +\infty) \right\}, \quad (3.36)$$

for the Asymmetric Logistic case, and

$$\mathcal{S} = \left\{ \{r, \phi, \theta\} \in \mathbb{R}^3 \mid \theta, \phi \in [0, 1]; r \in [0, +\infty) \right\}, \quad (3.37)$$

in the Asymmetric Negative Logistic case.

The Data

In the following chapter, the data sets being analyzed by the bivariate ACER function and copula methods are being presented. The data used in this project are a total of four synthetic time series and one real world data set. The synthetic data sets are Gaussian time series. The reason for choosing Gaussian time series is the relationship between the Gaussian and Gumbel distribution: The asymptotic limiting distribution of the rescaled maxima of the Gaussian distribution is Gumbel distributed. The fifth data set, the real world time series, consists of wind level measurements from two locations on the Norwegian coast.

These five data sets are used to test the empirically estimated bivariate ACER function and the represented copula models real world applicability.

In this thesis, Gaussian time series have been generated using the time series theory and R-code found in the Appendix, [section A](#), while the real world data set is obtained from www.eklima.no.

4.1 Synthetic Time Series

The generated Gaussian data sets are created with the α and β variables of Eq. (A.1) to be 0.6 and 0.7, and a Pearson correlation coefficient between a_{1t} and a_{2t} to 0.9. The amount of data have been generated to simulate hourly observations with mean 0 and standard deviation 1 over periods of 10, 25, 50 and 100 years. This results in a total of 87600, 219000, 438000 and 876000 data points, respectively, with the statistics seen in Table 4.1.

Figure 4.1 depicts four scatter plots of the synthetic data sets. These figures confirm high correlation for all the four pairs, and calculation of the Pearson correlation coefficient yields approximately 0.88 for all data sets, roughly as intended.

Table 4.1: The minimum, mean, maximum and standard deviation of the four Gaussian time series.

Type	X	Y
min	-5.25	-5.54
mean	0.00	0.00
max	5.17	6.10
sd	1.25	1.40

(a) 10 years

Type	X	Y
min	-5.38	-6.63
mean	0.00	0.00
max	5.70	6.58
sd	1.24	1.40

(b) 25 years

Type	X	Y
min	-5.64	-6.88
mean	0.00	0.00
max	6.10	6.42
sd	1.24	1.39

(c) 50 years

Type	X	Y
min	-7.70	-7.44
mean	0.00	0.00
max	6.29	7.13
sd	1.25	1.40

(d) 100 years

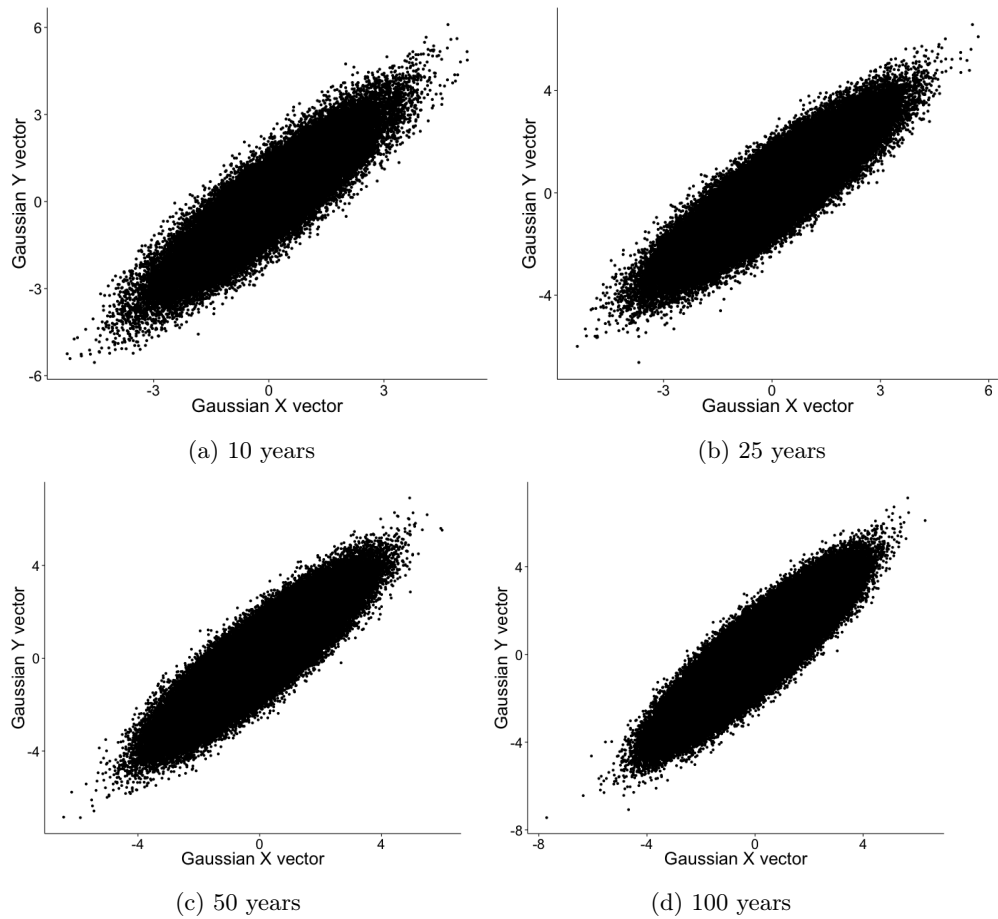


Figure 4.1: Plot of the Gaussian X time series vectors against the Gaussian Y time series vectors, for the four time series.

4.2 Wind Levels

The fifth data set for the methods used in this project are wind speed levels collected by the Norwegian Meteorological Institute, [5], over a time period of 29 years. These are being measured on two adjacent weather stations, namely Obrestad Fyr (station number 44080 and 47300, respectively), see Figure 4.2.

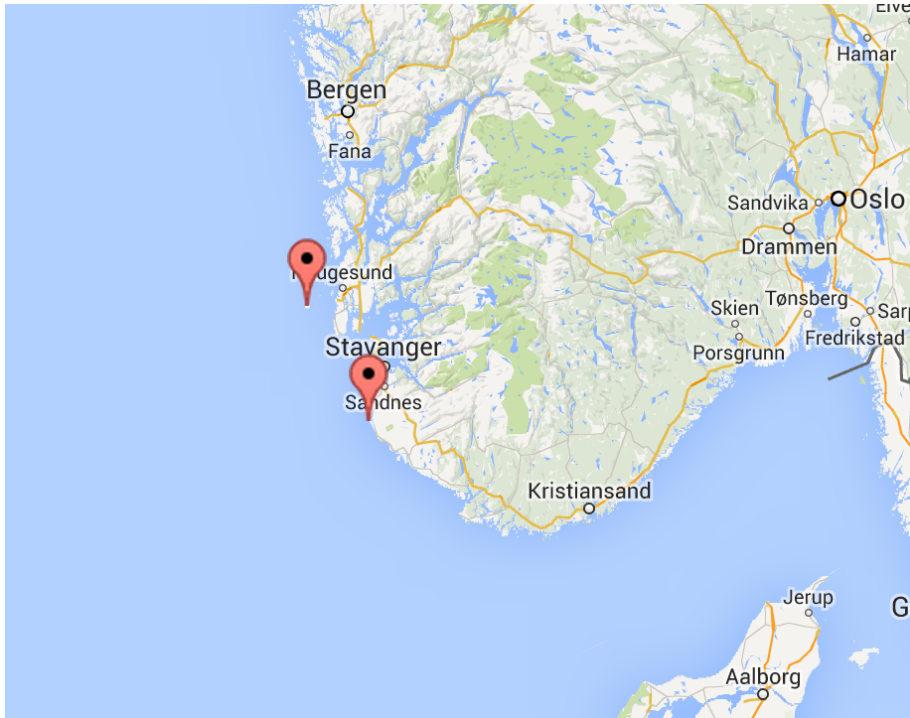


Figure 4.2: Map of the part of Norway indicating the locations from where data were collected. South: Obrestad Fyr, North: Utsira Fyr. Map obtained from www.google.no/maps.

The maximum wind gust was recorded 10 meters above the ground, four times a day, over a time period stretching from 01.01.1983 to 31.12.2013 - a total of 29 years. This has resulted in 1460 data points being registered per year, a total of 42340 data points from each station during the observation period. A brief statistical summary of the windspeed measurements from the two locations is given in Table 4.2.

Table 4.2: The minimum, mean, maximum and standard deviation of the wind-speed measurements from Obrestad and Utsira Fyr. All values in [m/s].

Type	Obrestad Fyr	Utsira Fyr
min	0	0
mean	6.99	8.32
max	32.58	30.58
sd	4.00	4.57

These values may be seen in context to their respective locations. The values obtained from Utsira Fyr are on average greater than those from Obrestad Fyr, which may be because Utsira Fyr is situated in the Norwegian Sea, while Obrestad Fyr is located on the Norwegian coast. In addition, it is worth noting that the wind gust levels are higher in the winter months as seen in Figure 4.3.

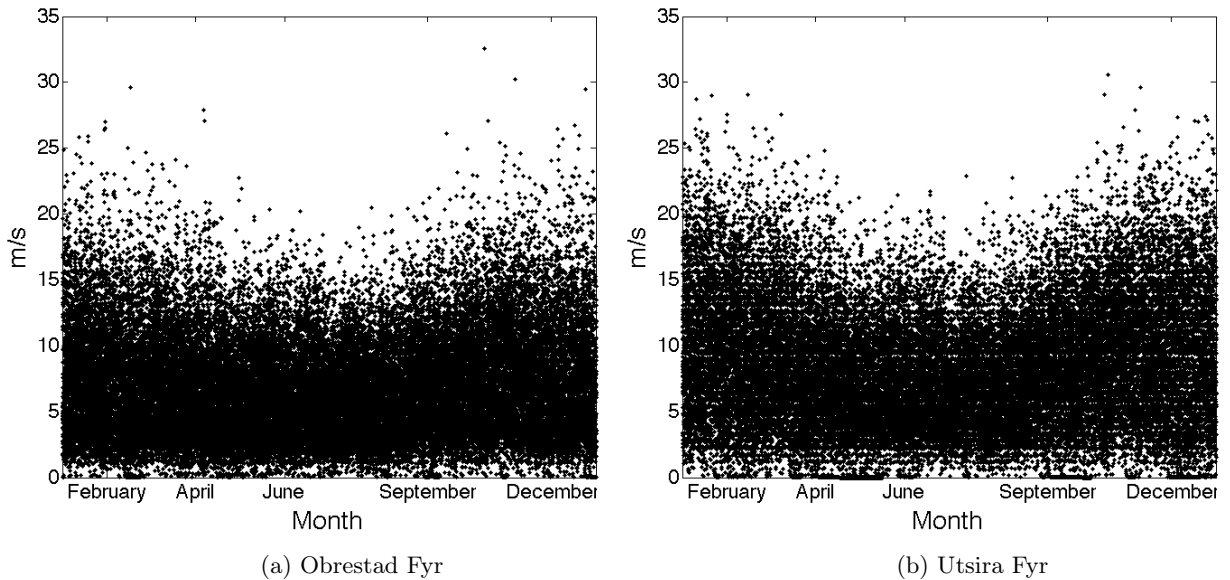


Figure 4.3: Scatterplots of the wind levels from both locations, showing the wind speed levels with respect to the months, over a period of 29 years.

Furthermore we check the correlation of the two data sets. Plotting the two data sets from each location against each other, we obtain Figure 4.4. The figure clearly shows a high correlation of the observed wind level data, and the Pearson correlation coefficient is calculated to be 0.74.

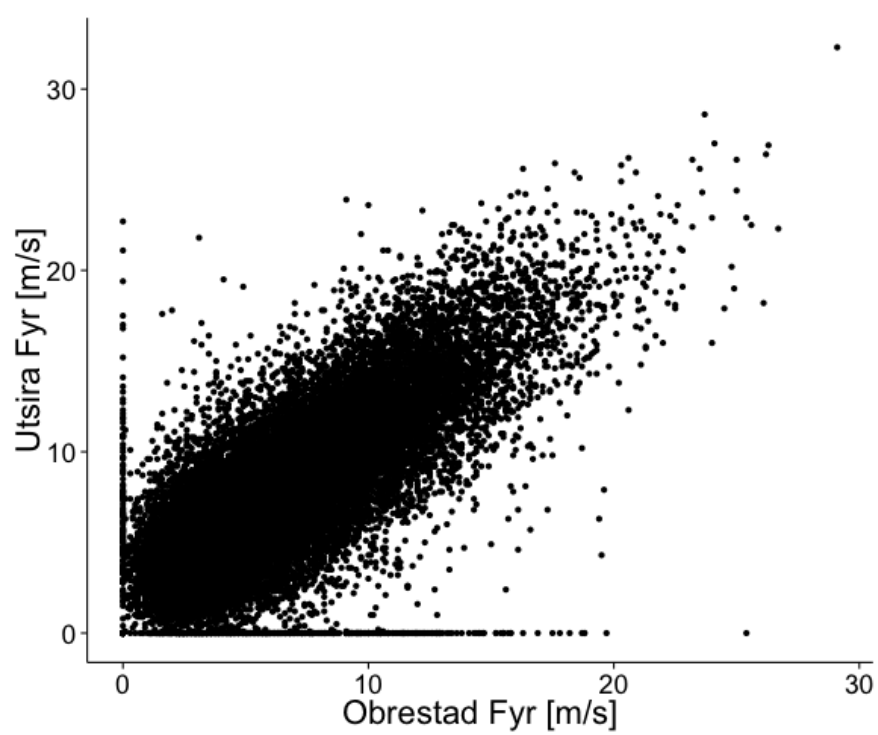


Figure 4.4: Coupled observations of Wind speed data observed at Obrestad and Utsira Fyr station, all in [m/s].

Analysis

Prediction is very difficult,
especially about the future.
- Niels Bohr.

In this chapter, the synthetic and real-world data sets that were introduced in [Chapter 4](#) are being analyzed. This is done using the empirically estimated bivariate ACER function and the presented copula functions with asymptotically consistent marginal extreme value distributions based on the univariate ACER function and fitted Gumbel distribution. We solve this task by using the MATLAB code found in the [Appendix](#). The four Gaussian time series with the same underlying distribution are the first data sets to be analyzed, followed by the real world data set obtained from the county of Rogaland.

It is worth noting that the logistic and Negative logistic copula approaches, in both the symmetric and asymmetric case, will yield the same result, i.e. the Gumbel-logistic and Asymmetric logistic model allows $r \leq 1$ as well. The proof may be found in [6]. As a result of this, the Negative logistic models will not be plotted in the countour plots of the surfaces.

5.1 Synthetic Data

10 years

Using the ACER method on the 10 year Gaussian data set, we first determine which ACER function, $\hat{\varepsilon}_k(\xi)$, that is appropriate. A way to do this is to plot the ACER function for an increasing number of k 's, and when $\hat{\varepsilon}_k(\xi) \approx \hat{\varepsilon}_{k+1}(\xi)$ in the tail, we have convergence, making the k 'th ACER function a good choice. We proceed with plotting the cascade of $\hat{\varepsilon}_1(\xi), \dots, \hat{\varepsilon}_{24}(\xi)$ and $\hat{\varepsilon}_1(\eta), \dots, \hat{\varepsilon}_{24}(\eta)$, as seen in [Figure 5.1](#) and [5.3](#), respectively. We regard $k = 24$ as the final converged result, as $\hat{\varepsilon}_{24}(\xi) \approx \hat{\varepsilon}_k(\xi)$ in the tail for all values of $k > 24$.

[Figure 5.1](#) and [5.3](#) show temporary dependence between consecutive data, but a complete convergence of all $\hat{\varepsilon}_k(\xi)$ and $\hat{\varepsilon}_k(\eta)$ in the tail. As we are dealing with stationary data we may plot the autocorrelation function of the time series to check the set of correlation coefficients between the series and lags of itself over time. The autocorrelation and partial autocorrelation plots may

be found in Figure 5.2 and 5.4. Figure 5.2a and 5.4a clearly show that the autocorrelations are significant for a large number of lags for both data sets, but as Figure 5.2b and 5.4b illustrate, the autocorrelations at lag 2 and above are merely due to the propagation of the autocorrelation at lag 1.

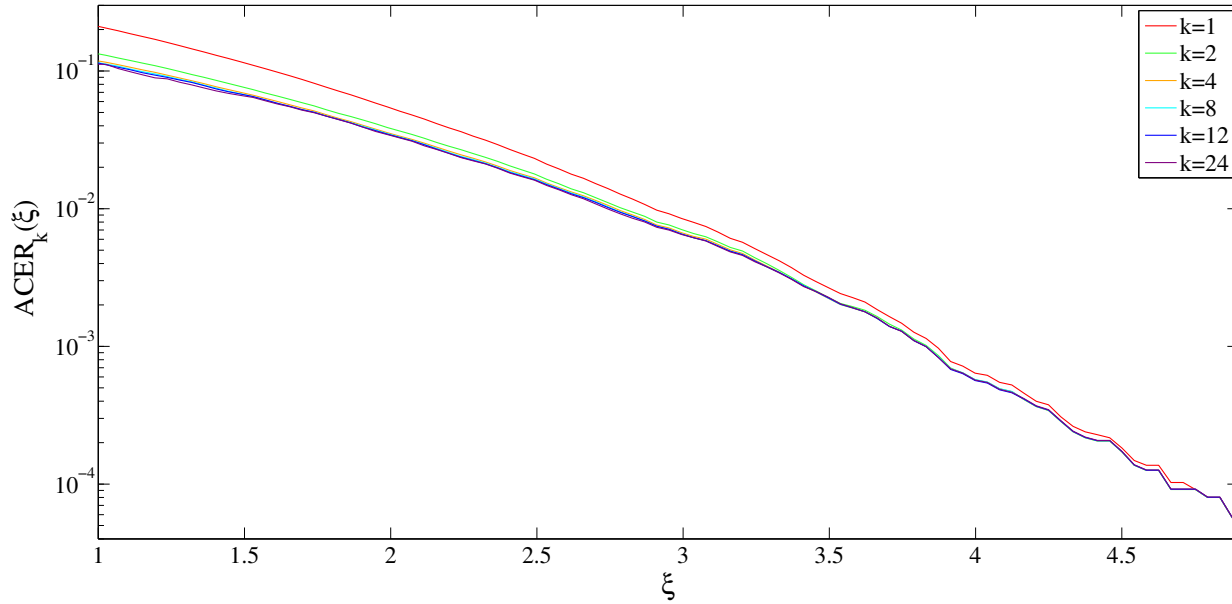


Figure 5.1: Comparison of the ACER estimates for $k = 1, 2, 4, 8, 12$ and 24 degrees of conditioning for the 10 year Gaussian X data set.

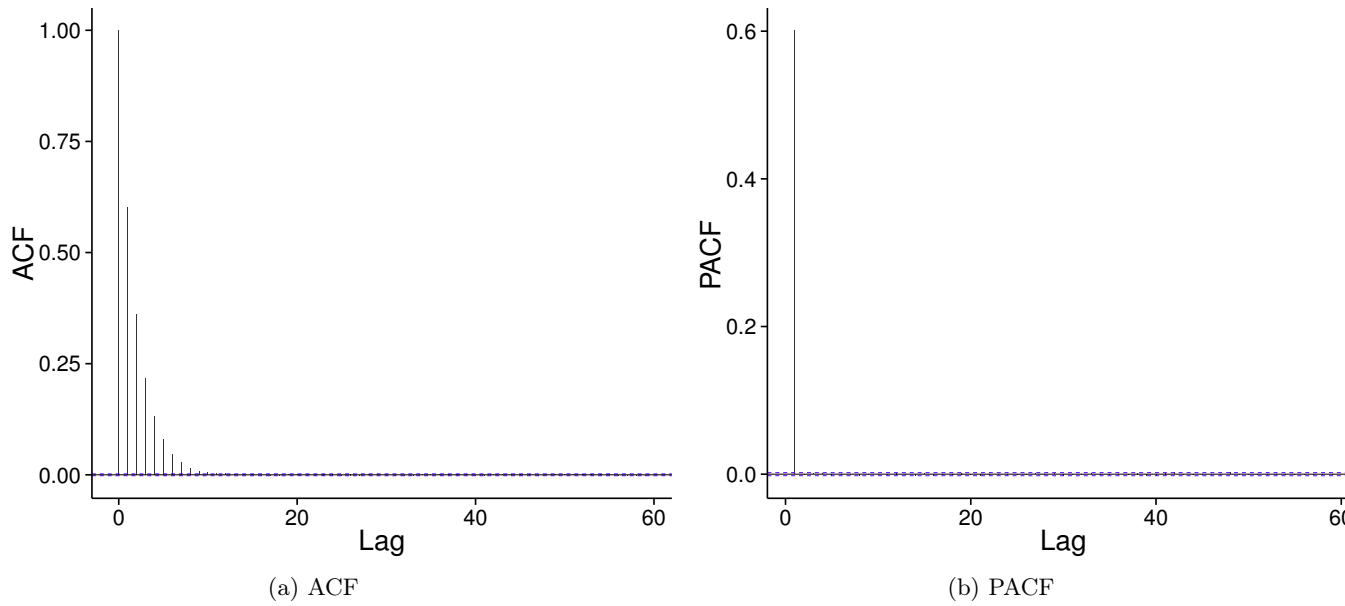


Figure 5.2: The ACF and PACF plot of the synthetic 10 year Gaussian X data set.

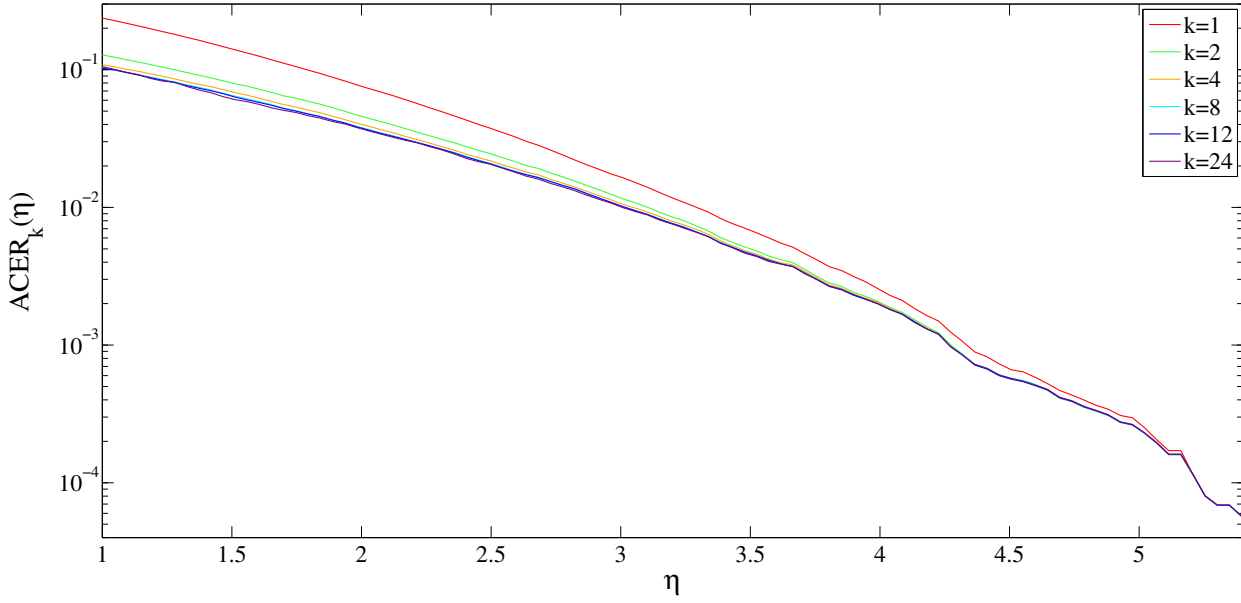


Figure 5.3: Comparison of the ACER estimates for $k = 1, 2, 4, 8, 12$ and 24 degrees of conditioning for the 10 year Gaussian Y data set.

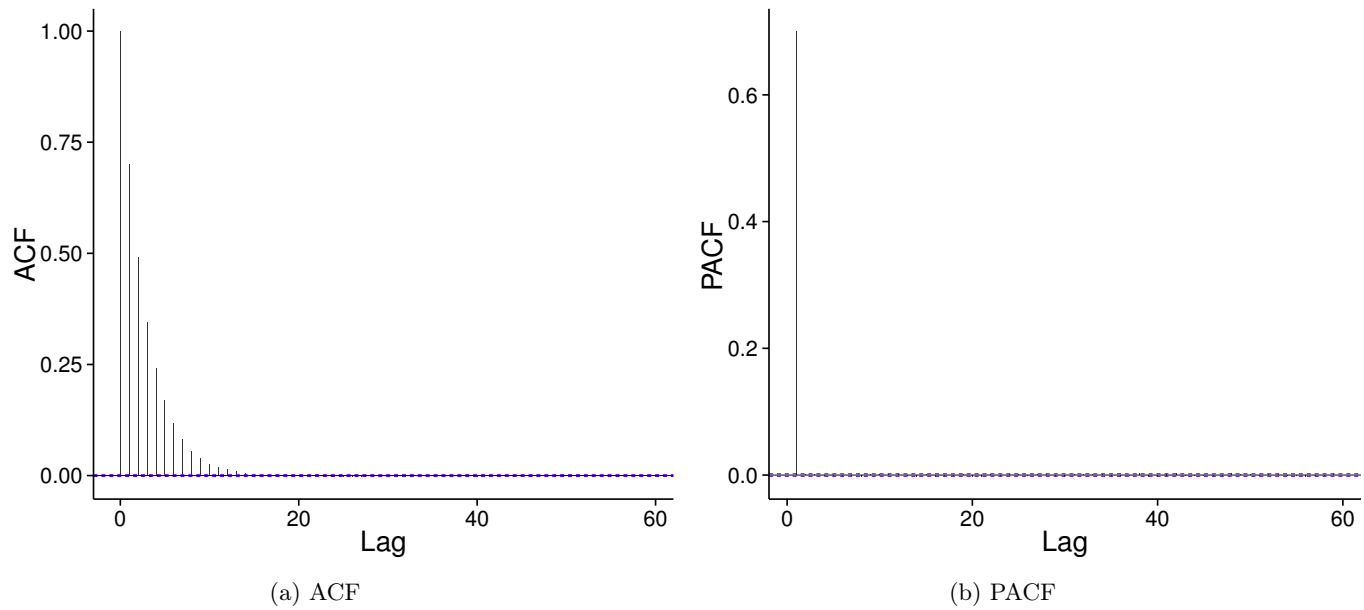


Figure 5.4: The ACF and PACF plot of the synthetic 10 year Gaussian Y data set.

The obvious choice, for both data sets, is to choose the first ACER function, i.e. $\hat{\varepsilon}_1(\xi)$ and $\hat{\varepsilon}_1(\eta)$. This will allow us to use all the data available, reducing the uncertainty of the estimations.

The resulting cascade of estimated bivariate ACER surfaces, $\hat{\mathcal{E}}_k(\xi, \eta)$, is seen in Figure 5.5. As all ACER functions converge, the upper most surface, i.e. that of $k = 1$, is partly overwritten by the subsequent surfaces corresponding to greater k -values in the area of convergence. This is seen in Figure 5.5 as a purple tail. This further strengthens our choice of k -value.

The figure also shows that the cross-section of the surfaces at the high values of ξ gives the univariate ACER estimates for the X data set whilst the cross section at a high value of η gives the univariate ACER function for the Y data set.

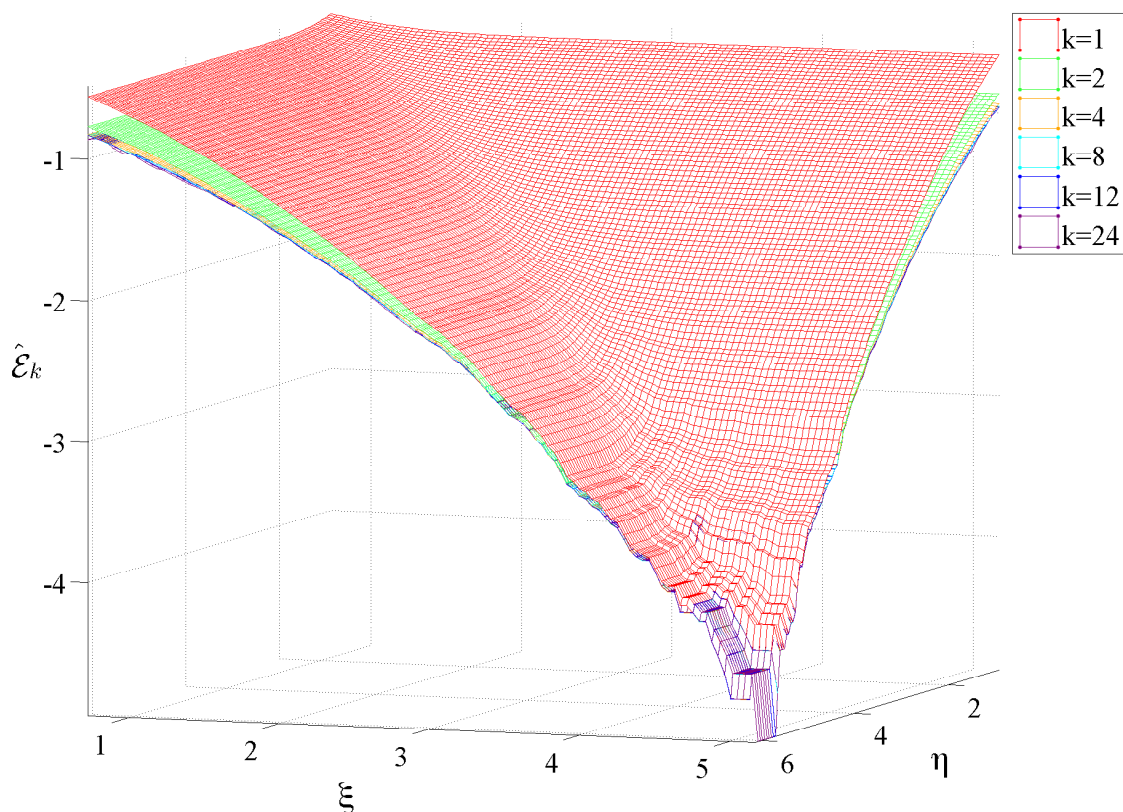


Figure 5.5: Comparison of the bivariate ACER surface estimates for $k = 1, 2, 4, 8, 12$ and 24 degrees of conditioning for the 10 year Gaussian X and Y data set, on a logarithmic scale.

We continue by fitting the univariate ACER and Gumbel distribution.

To fit the ACER function, we first calculate the empirical estimation of the ACER function and then fit the asymptotic ACER model seen in Eq. (2.9) to these values. This procedure is thoroughly described in [12].

The Gumbel marginals are fitted with maximum likelihood using the block maximum values. Each block consists of all the observations done in one year, culminating in 10 annual maxima.

To be able to compare the two marginal values we may set the annual univariate ACER distribution found in Eq. (3.24) equal to the Gumbel distri-

bution seen in Eq. (3.1) (Type I), i.e.

$$\exp \left\{ -\frac{N-k+1}{n_y} \varepsilon_k(\xi) \right\} = \exp \left\{ -\exp \left[-\left(\frac{\xi - \mu_\xi}{\sigma_\xi} \right) \right] \right\}.$$

Solving for $\varepsilon_k(\xi)$ yields

$$\varepsilon_k(\xi) = \frac{n_y}{N-k+1} \exp \left[-\left(\frac{\xi - \mu_\xi}{\sigma_\xi} \right) \right].$$

The same procedure is used to transform the cumulative distribution of the extreme values, i.e. $F(x_i) = \frac{i}{n+1}$. The calculations are as follows:

$$\begin{aligned} \exp \left\{ -\frac{N-k+1}{n_y} \varepsilon_k(\xi_i) \right\} &= \frac{i}{n+1} \\ \varepsilon_k(\xi_i) &= \frac{-n_y}{N-k+1} \log \left(\frac{i}{n+1} \right). \end{aligned}$$

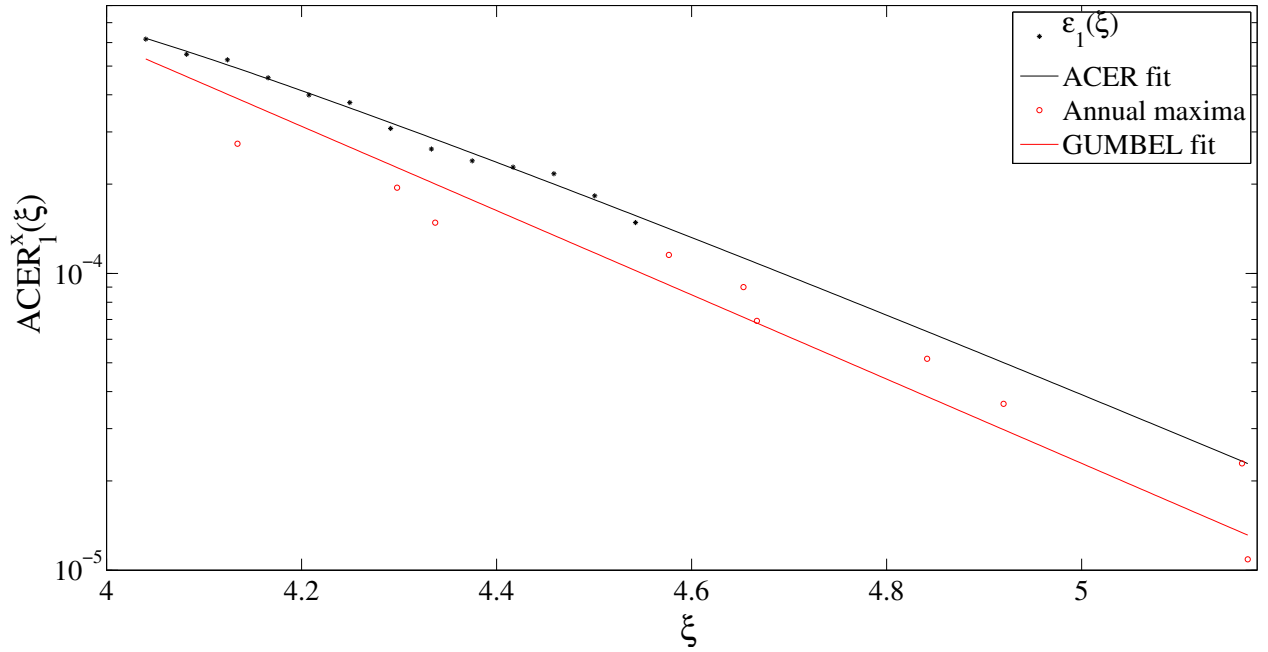
The result of this distribution fitting is seen in Figure 5.6. As we see, there is limited agreement between the adapted ACER function and the fitted Gumbel distribution using the 10 maximum values. This mismatch suggest that the approaches will yield different sub-asymptotic distributions. The inequality between the two lines are calculated to be $5.08 \cdot 10^{-5}$ and $1.03 \cdot 10^{-5}$ in the far end of the tail for the X and Y data set, respectfully. This indicates that the calculated return values will be very different from each other.

We extend the analysis by estimating parameters of optimal fit between the bivariate ACER model and the copula approaches using the Gumbel-logistic, Asymmetric logistic, Negative logistic and Asymmetric negative logistic dependence functions. The optimal estimates obtained are presented in Table 5.1.

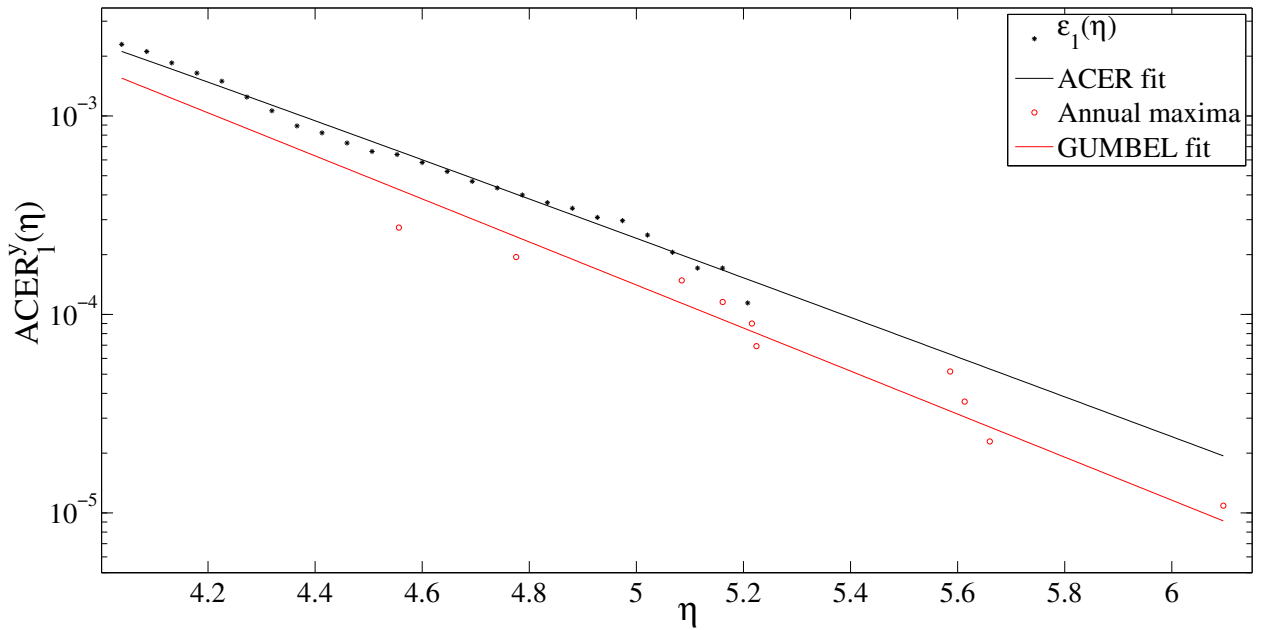
Table 5.1: Optimal parameters of the Gumbel-logistic (GL), Asymmetric logistic (AL), Negative logistic (NL) and Asymmetric negative logistic (ANL) fit with Gumbel and ACER marginals with their respective minimized mean square error (MSE) for the Gaussian 10 year data.

Marginal	Model	Parameters	MSE
Gumbel	GL	$r = 1$	0.0936
	AL	$r = 3.03, \phi = 0, \theta = 0.53$	0.0936
	NL	$r = 0.03$	0.0936
	ANL	$r = 0.03, \phi = 0.37, \theta = 0.43$	0.0936
ACER	GL	$r = 1.45$	0.0052
	AL	$r = 2.36, \phi = 0.58, \theta = 0.77$	0.0048
	NL	$r = 0.73$	0.0053
	ANL	$r = 1.64, \phi = 0.57, \theta = 0.78$	0.0048

The table shows, in the Gumbel case, that all copula models give the same minimized mean square error, implying that the asymmetric copula models should not yield a better fit than the non-asymmetric copulas. Furthermore, as $r = 1$ in the Gumbel-logistic, $\phi = 0$ in the Asymmetric logistic and $r \approx 0$ in the Negative logistic cases, the copula models using Gumbel marginals will imply independence.



(a) The X data set.



(b) The Y data set.

Figure 5.6: Plot of the empirically estimated ACER functions, the fitted univariate ACER function, the annual maximum and the fitted Gumbel distribution for the synthetic 10 year Gaussian data set.

For the copula models with ACER marginals, there is a slight decrease in the calculated minimized mean square error when using asymmetric copula models. These copulas also give a much smaller mean square error than the copula models using Gumbel marginals. The parameters of the Gumbel-logistic and Negative logistic models indicate, in contrast to the copulas using Gumbel marginals, a dependence between the data.

The contour plot of the bivariate extreme value copula models using the optimal estimated parameters and the bivariate ACER functions are found in Figure 5.7. Note that the Gumbel-logistic and the Asymmetric logistic copula models with Gumbel marginals return the same contour line, resulting in a purple line.

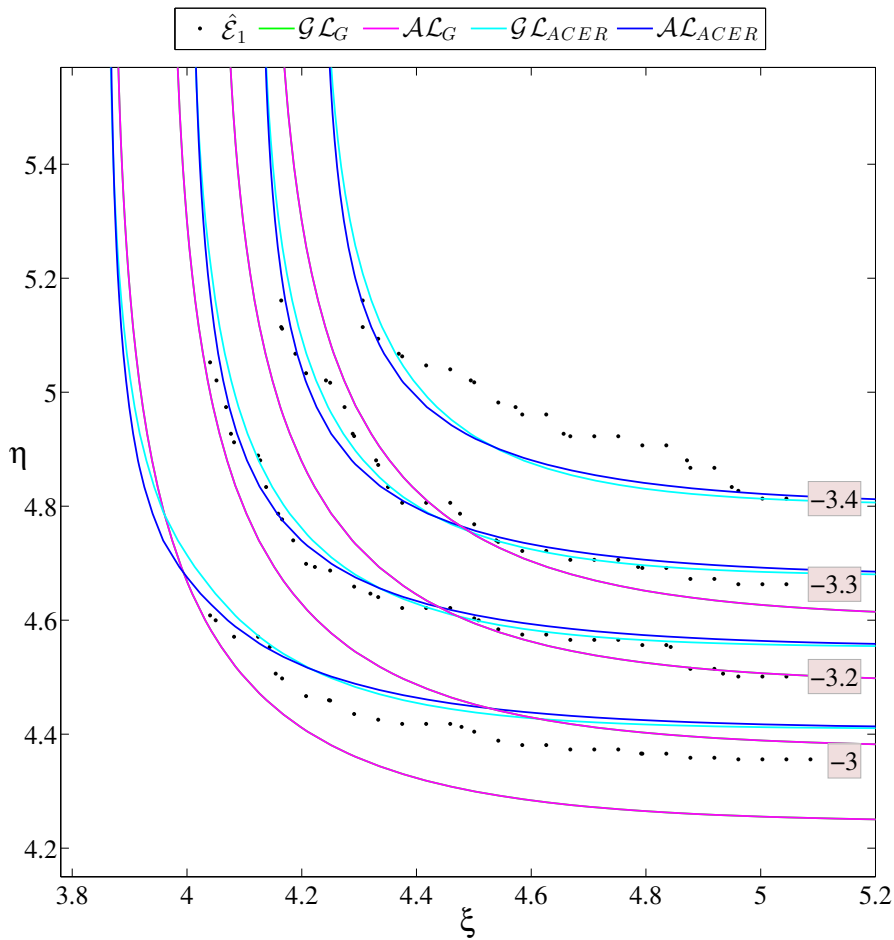


Figure 5.7: Contour plot of the empirically estimated bivariate ACER ($\hat{\xi}_1$) surface, optimized Gumbel-logistic (\mathcal{GL}) and optimized Asymmetric logistic (\mathcal{AL}) surfaces using Gumbel and ACER marginals for the 10 year Gaussian data set. The red boxes indicate levels on a logarithmic scale.

Figure 5.7 shows that the copula models with ACER marginals follow the empirically estimated bivariate ACER functions with high accuracy for the -3.3 level. For the levels -3, -3.2 and -3.4 however, the contour lines show a small misfit. Despite this, the overall fit of the ACER copula contour lines fit the empirically data very well, and also capture the dependence structure of the data.

For all levels, it is clear that the copula models with the fitted Gumbel marginals badly reflect the distribution of the data. In addition, the Gumbel copula approach does not capture the dependence structure of the empirically bivariate ACER functions. Furthermore, based on Figure 5.7, we see that the estimated return values from each marginal copula approach will yield completely different values.

Comparing the return values of \mathcal{GL}_G , \mathcal{GL}_{ACER} and \mathcal{AL}_{ACER} is done by looking at Figure 5.8. We discard the \mathcal{AL}_G model due to equality between the \mathcal{GL}_G and \mathcal{AL}_G .

The return values have been collected and combined into Table 5.2 to give a more accurate representation of the return values. In this table we have discarded the return values gotten from the \mathcal{AL}_{ACER} as they are the same as the \mathcal{GL}_{ACER} model.

Table 5.2: Estimated 10, 25, 50 and 100 year return values for the Gumbel-logistic copula models with ACER and Gumbel marginals fitted based on the Gaussian 10 year synthetic data.

Return period	\mathcal{GL}_{Gumbel}		\mathcal{GL}_{ACER}	
	X	Y	X	Y
10	5.19	5.98	5.37	6.30
25	5.48	6.36	5.66	6.71
50	5.70	6.64	5.88	7.01
100	5.91	6.92	6.09	7.31

Figure 5.8 and Table 5.2 shows the same tendency observed in Figure 5.7, i.e. the approaches using different marginal distribution clearly yield different return values.

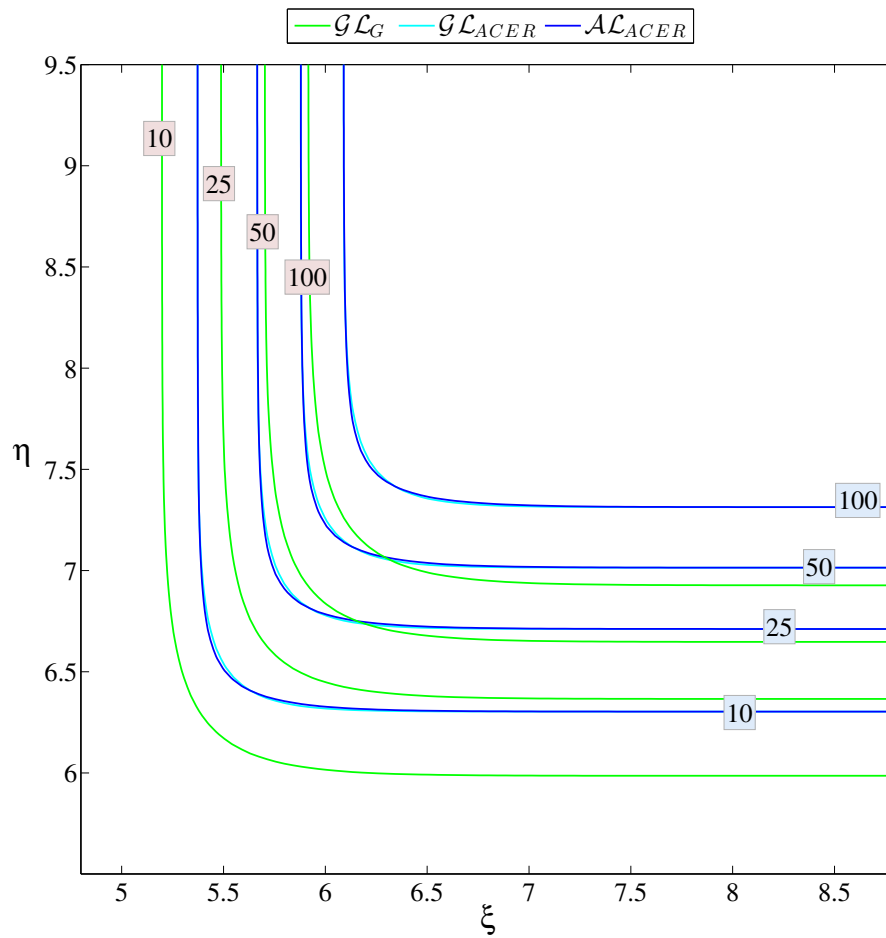


Figure 5.8: Contour plot of the return period levels for the optimized Gumbel-logistic (\mathcal{GL}) and Asymmetric logistic (\mathcal{AL}) surfaces with Gumbel and ACER marginals with respect to the 10 year Gaussian data. The red and blue boxes indicate return levels in years.

25 years

We continue with the analysis of the 25 year Gaussian data set, where we will follow the same procedure as in the previous subsection. The cascade of ACER functions, $\hat{\varepsilon}_1(\xi), \dots, \hat{\varepsilon}_{24}(\xi)$ and $\hat{\varepsilon}_1(\eta), \dots, \hat{\varepsilon}_{24}(\eta)$, are plotted and found in Figure 5.9 and 5.11.

Figure 5.9 and 5.11 show a marginal temporarily dependence between consecutive data. In both cases, convergence of $\hat{\varepsilon}_k(\xi)$ and $\hat{\varepsilon}_k(\eta)$, for all presented values of k , is achieved in the tail.

The corresponding autocorrelation and partial autocorrelation plots may be found in Figure 5.10 and 5.12. Figure 5.10a and 5.12a clearly show that there are significant autocorrelations for a large number of lags for both data sets, but as Figure 5.10b and 5.12b reveal, the autocorrelations at lag 2 and above are only due to the propagation of the autocorrelation at lag 1.

The clear choice, for both data sets, is to choose the first ACER function, i.e. $\hat{\varepsilon}_1(\xi)$ and $\hat{\varepsilon}_1(\eta)$. This will allow us to use all the data available, lowering the uncertainty of the estimations.

Figure 5.13 shows a cascade of estimated bivariate ACER surfaces, $\hat{\mathcal{E}}_k(\xi, \eta)$, for $k = 1, 2, 4, 8, 12$ and 24 degrees of conditioning. As all ACER functions converge, the upper most surface, i.e. that of $k = 1$, is partly overwritten by the subsequent surfaces corresponding to greater k -values in the area of convergence. This is seen in Figure 5.13 as a purple area.

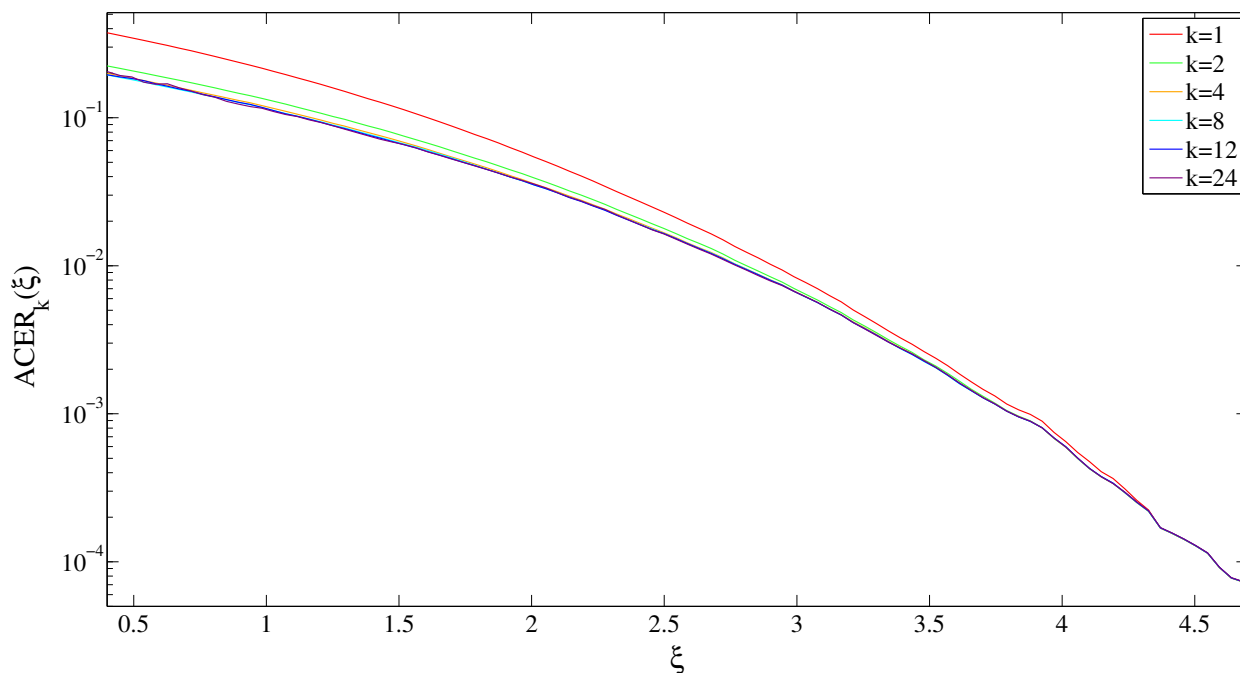


Figure 5.9: Comparison of the ACER estimates for $k = 1, 2, 4, 8, 12$ and 24 degrees of conditioning for the 25 year Gaussian X data set.

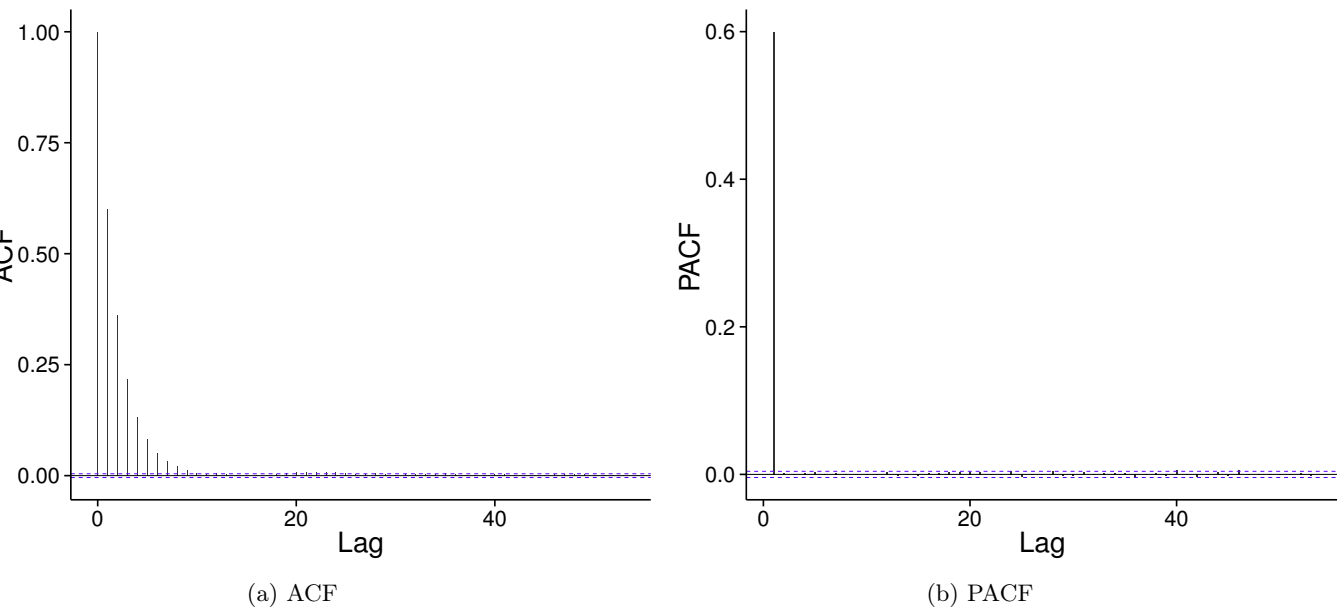


Figure 5.10: The ACF and PACF plot of the synthetic 25 year Gaussian X data set.

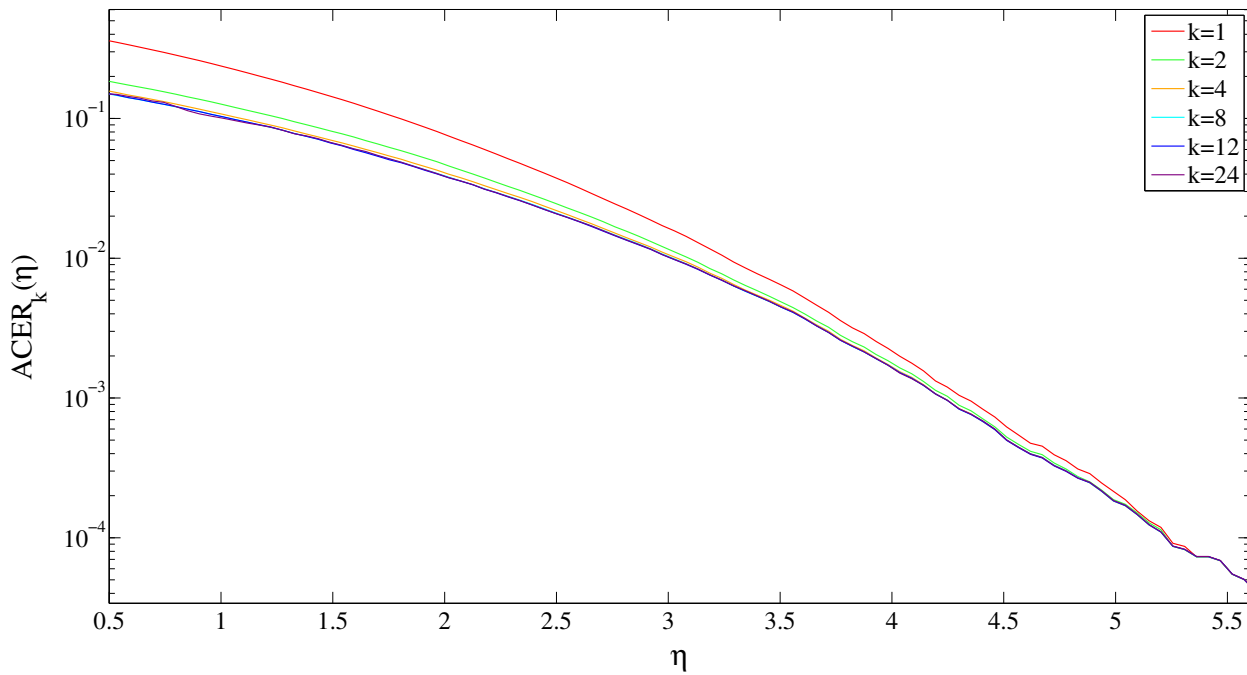


Figure 5.11: Comparison of the ACER estimates for $k = 1, 2, 4, 8, 12$ and 24 degrees of conditioning for the 25 year Gaussian Y data set.

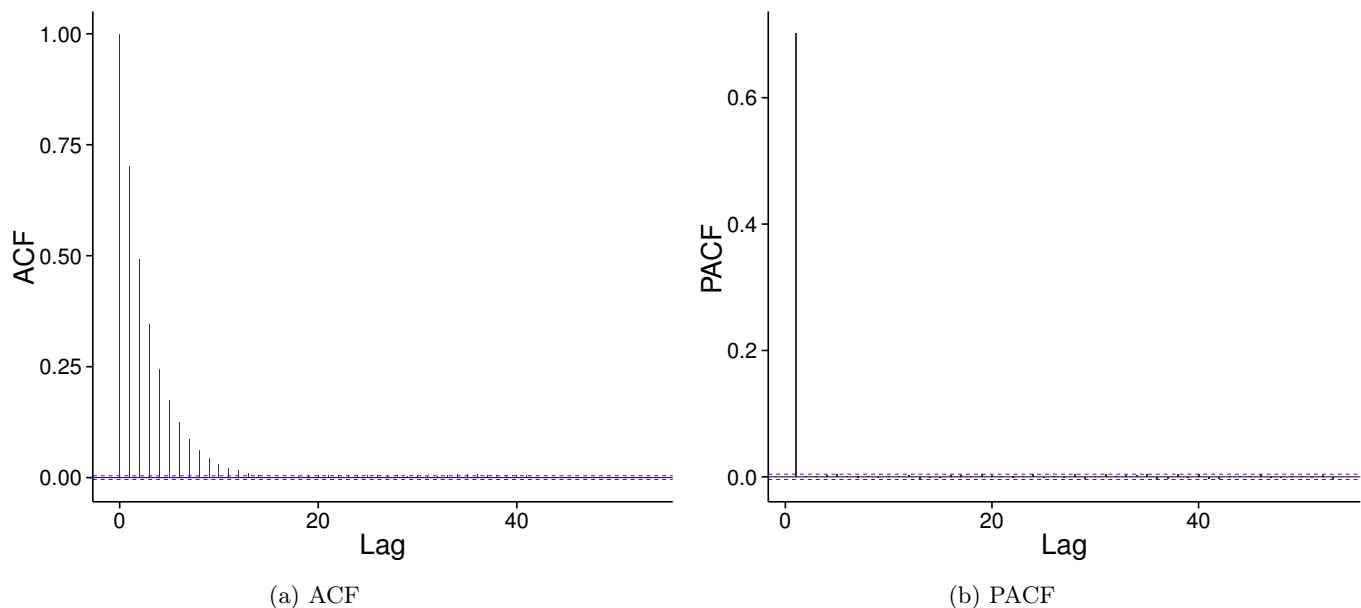


Figure 5.12: The ACF and PACF plot of the synthetic 25 year Gaussian Y data set.

Proceeding with the first ACER function, $\hat{\varepsilon}_1(\xi)$, we compare the fit of the univariate marginals to the data at hand. The result of the distribution fitting is seen in Figure 5.14. As we see, there is an overall good agreement between the adapted ACER function and the fitted Gumbel distribution using the 25 maximum values. Comparing the tails of the univariate lines, there is a high agreement in the Y case. For the lines in the X case, there is a difference of approximately $6 \cdot 10^{-7}$ between the two distribution lines. Despite being small, the differences between the two lines in both plots may result in different return values for the two methods for large return periods, e.g. for the 100 year return value. As the observed maximums in the 25 year data set is not comparable to the estimated 100 year return value, Figure 5.14 gives a bad representation of the differences in higher return levels.

We continue with estimating the parameters for optimal fit between the empirical bivariate ACER values and the four copula models. The estimates are given in Table 5.3.

The result of the parameter estimation shows, in the Gumbel marginal case, a slight decrease in the minimized mean square error when using an asymmetric copula model. In addition, the ϕ parameter is, in both asymmetric copula models, set to 0.15, while the θ parameter is set to 1. I.e. the asymmetric models have an optimal fit when we introduce asymmetry. Evaluating the copula models with ACER marginals, the table shows that there is a general consent between the four logistic models. They have approximately the same dependence parameter r , and the ϕ and θ parameters, in the asymmetric cases, seem to be close to 1. In addition, there is no reduction in the calculated mean square error for the asymmetric models. This indicate that the asymmetric copula models should be roughly equal to the non-asymmetric copulas when plotted in a countour plot.

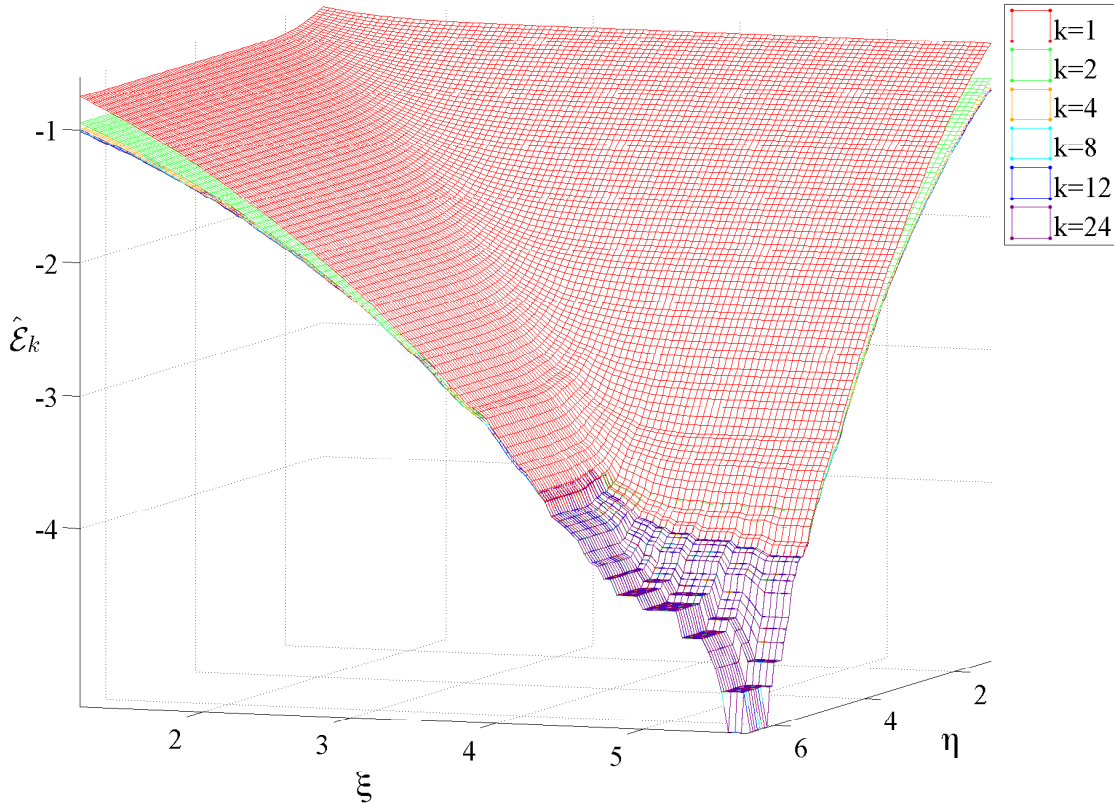
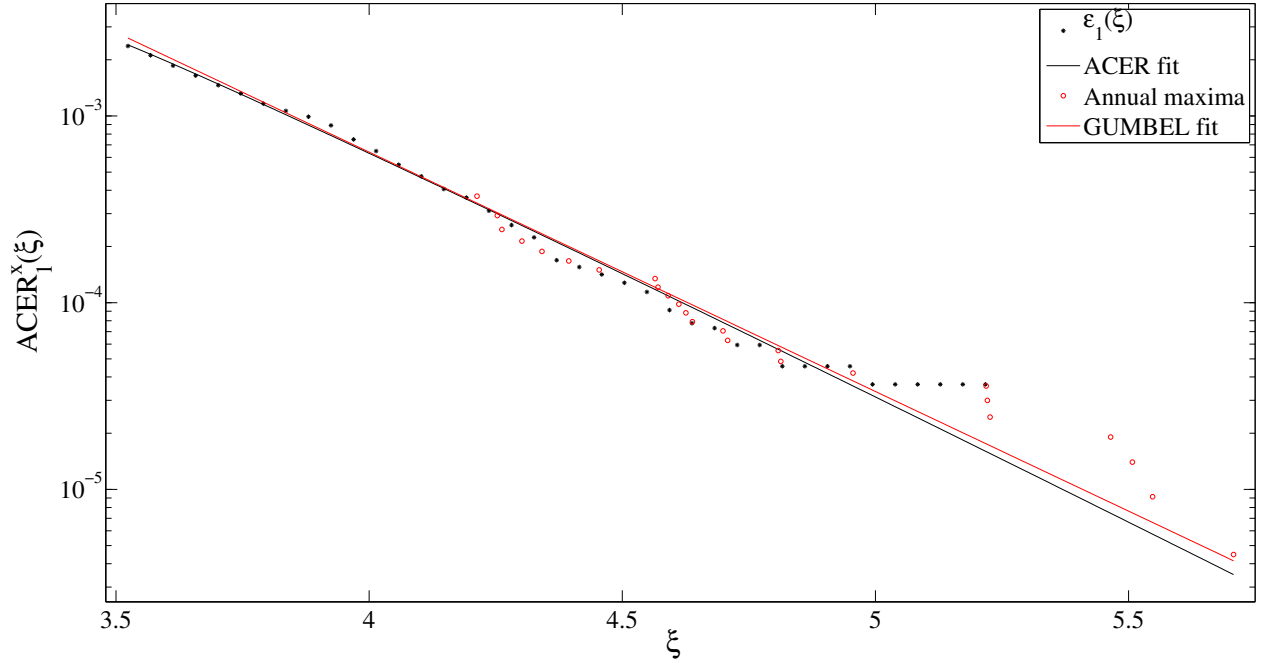


Figure 5.13: Comparison of the bivariate ACER surface estimates for $k = 1, 2, 4, 8, 12$ and 24 degrees of conditioning for the 25 year Gaussian X and Y data set, on a logarithmic scale.

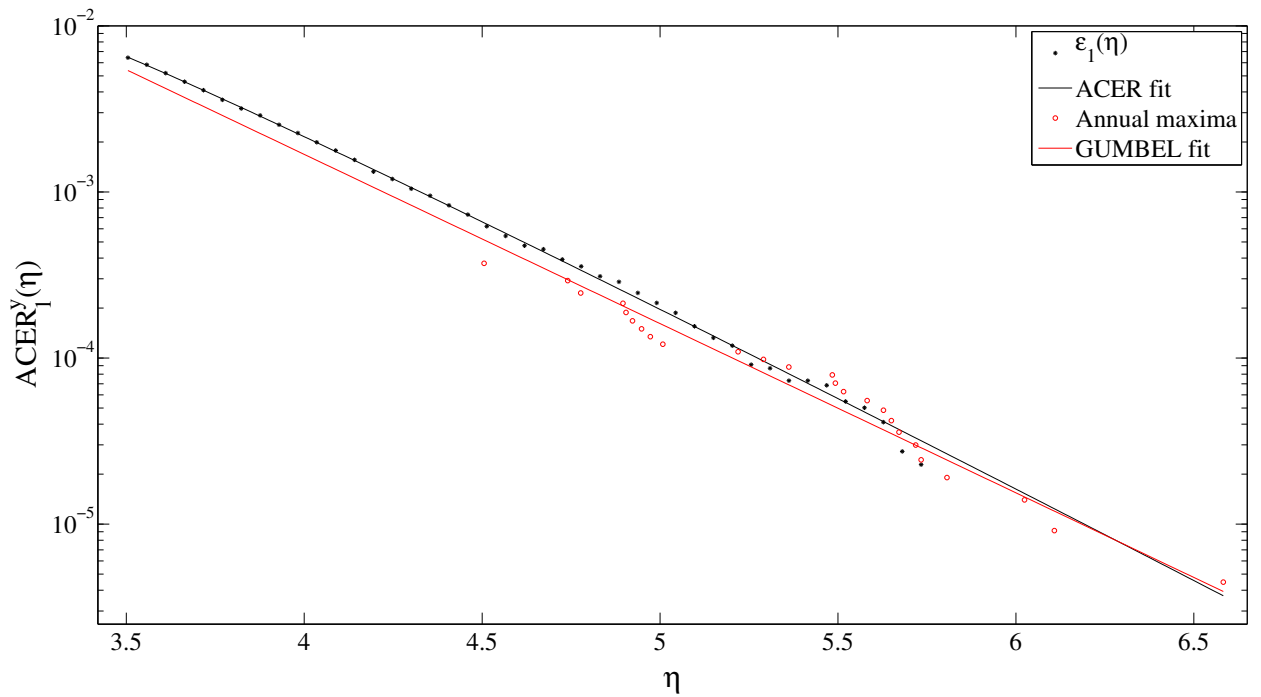
Table 5.3: Optimal parameters of the Gumbel-logistic (GL), Asymmetric logistic (AL), Negative logistic (NL) and Asymmetric negative logistic (ANL) fit with Gumbel and ACER marginals with their respective minimized mean square error(MSE) of the Gaussian 25 year data.

Marginal	Model	Parameters	MSE
Gumbel	GL	$r = 1.06$	0.0205
	AL	$r = 6.96, \phi = 0.15, \theta = 1$	0.0175
	NL	$r = 0.25$	0.0207
	ANL	$r = 6.71, \phi = 0.15, \theta = 1$	0.0175
ACER	GL	$r = 1.54$	0.0015
	AL	$r = 1.55, \phi = 1, \theta = 0.96$	0.0015
	NL	$r = 0.81$	0.0015
	ANL	$r = 0.82, \phi = 1, \theta = 0.97$	0.0015

The corresponding contour plot of these optimal fitted analytical bivariate extreme value models together with the empirically estimated bivariate ACER functions are found in Figure 5.15.



(a) The X data set.



(b) The Y data set.

Figure 5.14: Plot of the empirically estimated ACER functions, the fitted univariate ACER function, the annual maximum and the fitted Gumbel distribution for the synthetic 25 year Gaussian data set.

Figure 5.15 shows a high equality between the empirically estimated bivariate ACER functions and the copula models with ACER marginals. The prediction of roughly equal contour lines for the copula models with ACER marginals also seem to hold up. Moreover, there is an increase in compatibility between the asymmetric copula model with Gumbel marginals and the bivariate ACER functions due to an improved dependence structure. Despite this, all Gumbel marginal copulas yields contour lines that slightly differ in the Y dimension compared to the bivariate ACER functions.

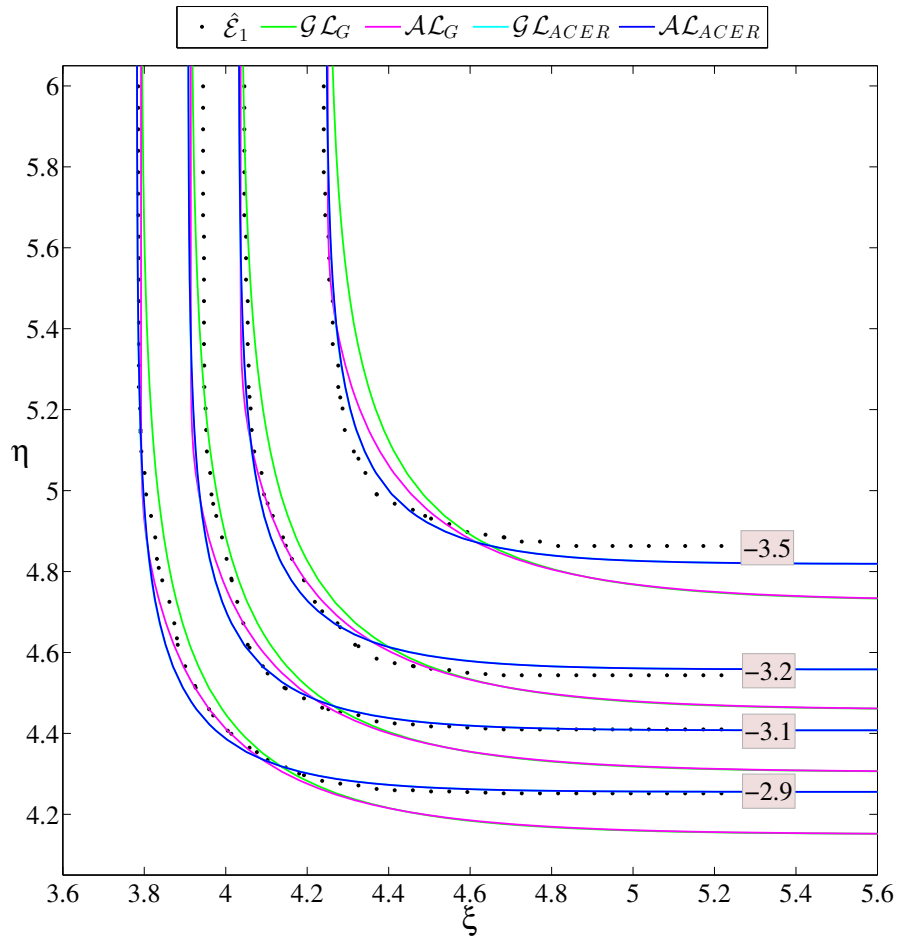


Figure 5.15: Contour plot of the empirically estimated bivariate ACER ($\hat{\mathcal{E}}_1$) surface, optimized Gumbel-logistic (\mathcal{GL}) and optimized Asymmetric logistic (\mathcal{AL}) surfaces using Gumbel and ACER marginals for the 25 year Gaussian data set. The red boxes indicate levels on a logarithmic scale.

We continue with plotting the return value plot as seen in Figure 5.16. In this figure we compare the return values of the copula models with different marginal distribution to each other. The models graphed in Figure 5.16 are chosen based on the similarities and differences between the countour lines observed in Figure 5.15.

The 10, 25, 50 and 100 year return values are obtained and arranged into Table 5.4. Due to similarities, the \mathcal{GL}_G and \mathcal{GL}_{ACER} are used.

Table 5.4: Estimated 10, 25, 50 and 100 year return values for the Gumbel-logistic copula models with ACER and Gumbel marginals fitted based on the Gaussian 25 year synthetic data set.

Return period	\mathcal{GL}_{Gumbel}		\mathcal{GL}_{ACER}	
	X	Y	X	Y
10	5.34	6.10	5.31	6.12
25	5.66	6.51	5.61	6.49
50	5.90	6.81	5.84	6.76
100	6.14	7.10	6.06	7.04

Figure 5.16 and Table 5.4 show that there is now a much greater agreement between the two copula approaches than previously observed. The differences between the return values are growing, but these values are utmost 0.08 and 0.06 for the X and Y case, respectfully.

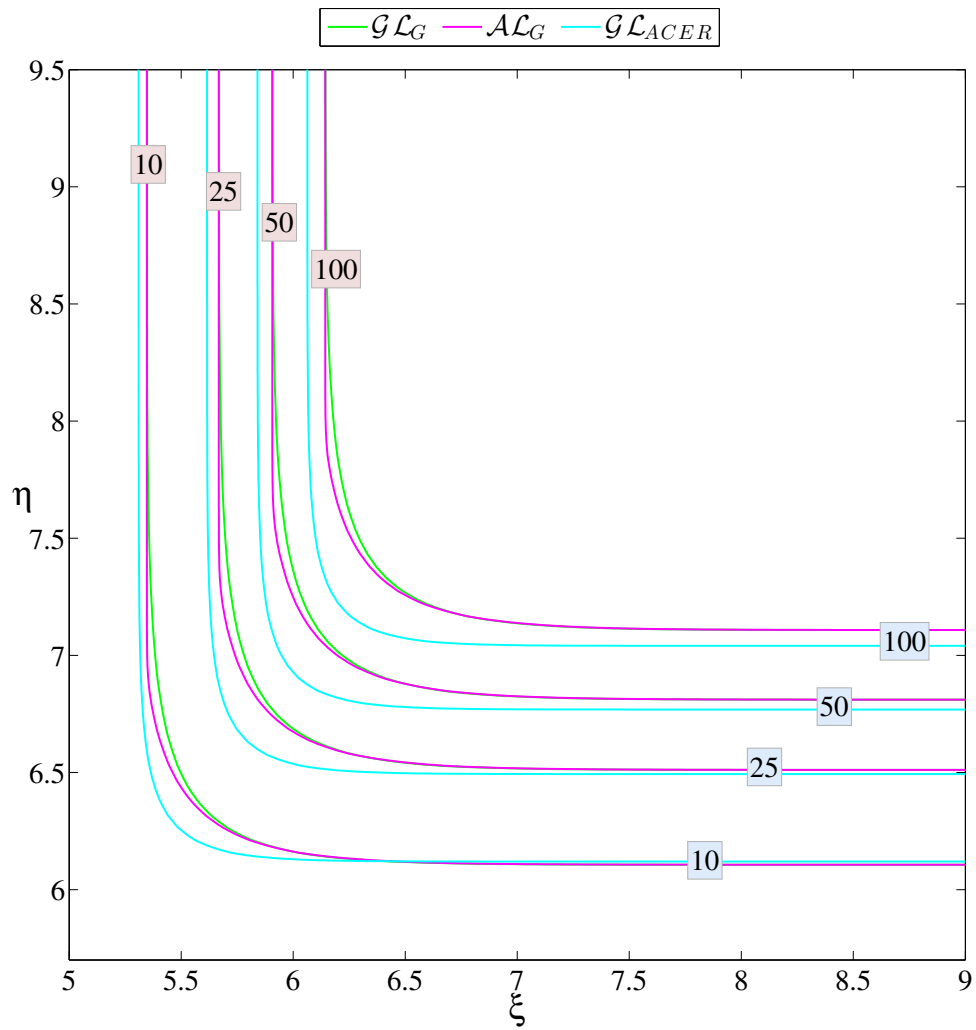


Figure 5.16: Contour plot of the return period levels for the optimized Gumbel-logistic (\mathcal{GL}) and Asymmetric logistic (\mathcal{AL}) surfaces with Gumbel and ACER marginals with respect to the 25 year Gaussian data set. The red and blue boxes indicate return levels in years.

50 years

We advance this analysis by looking at the 50 year Gaussian data set. The cascade of ACER functions, $\hat{\varepsilon}_1(\xi), \dots, \hat{\varepsilon}_{24}(\xi)$ and $\hat{\varepsilon}_1(\eta), \dots, \hat{\varepsilon}_{24}(\eta)$, are plotted and displayed in Figure 5.17 and 5.19.

Both Figure 5.17 and 5.19 show a marginal temporarily dependence between consecutive data, but a full convergence of $\hat{\varepsilon}_k(\xi)$ and $\hat{\varepsilon}_k(\eta)$, for all presented values of k , is achieved in the tail.

In addition, the autocorrelation and partial autocorrelation plots found in Figure 5.18a and 5.20a show that the autocorrelations are significant for a large number of lags for both data sets, but as Figure 5.2b and 5.4b illustrates, the autocorrelations at lag 2 and above are merely due to the propagation of the autocorrelation at lag 1.

For both data sets, we choose the first ACER functions, i.e. $\hat{\varepsilon}_1(\xi)$ and $\hat{\varepsilon}_1(\eta)$, with the added benefit of allowing us to use all available data, reducing the uncertainty of the estimations.

Figure 5.21 shows the cascade of empirically estimated bivariate ACER surfaces, $\hat{\mathcal{E}}_k(\xi, \eta)$. As all ACER functions converge, the upper most surface, i.e. that of $k = 1$, is partly overwritten by the subsequent surfaces corresponding to greater k -values in the area of convergence. This is seen in Figure 5.5 as a purple tail, and further strengthens our choice of k -value.

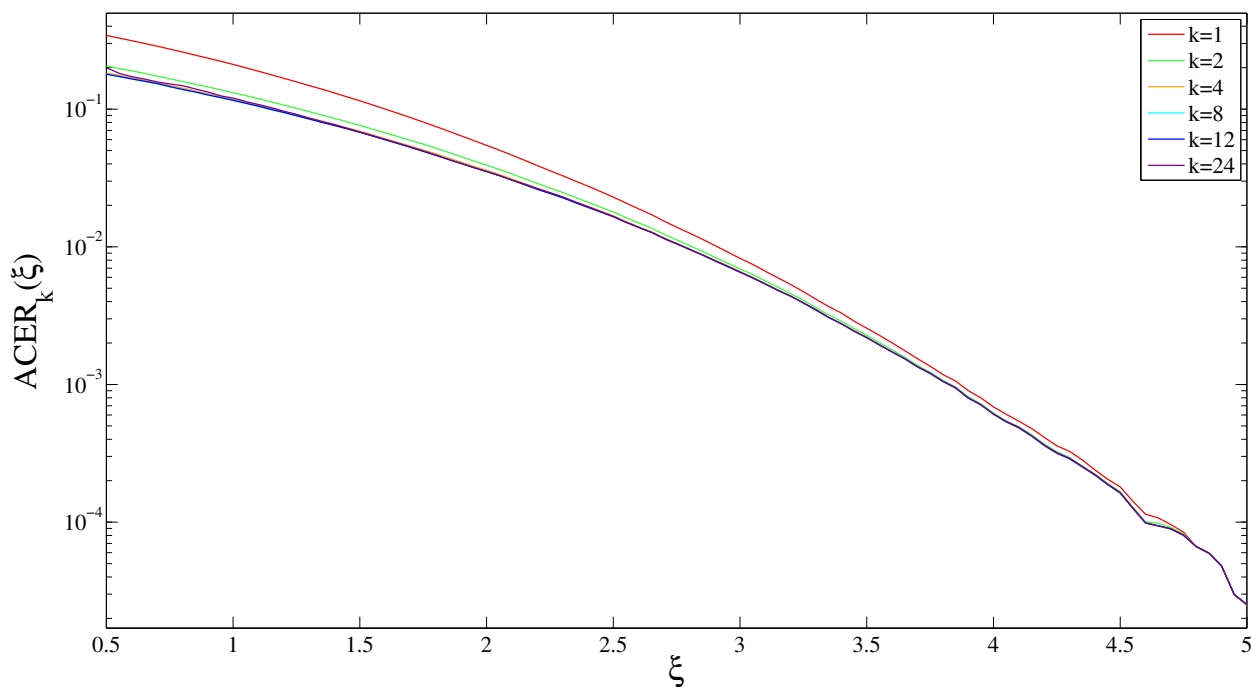


Figure 5.17: Comparison of the ACER estimates for $k = 1, 2, 4, 8, 12$ and 24 degrees of conditioning for the 50 year Gaussian X data set.

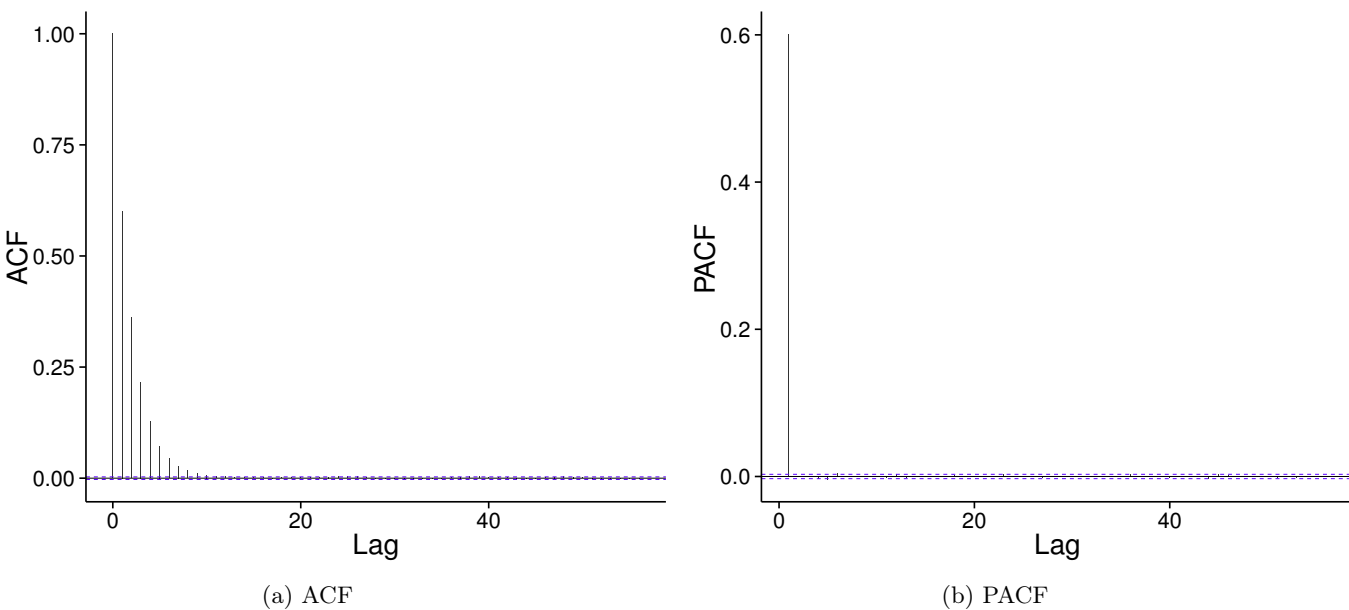


Figure 5.18: The ACF and PACF plot of the synthetic 50 year Gaussian X data set.

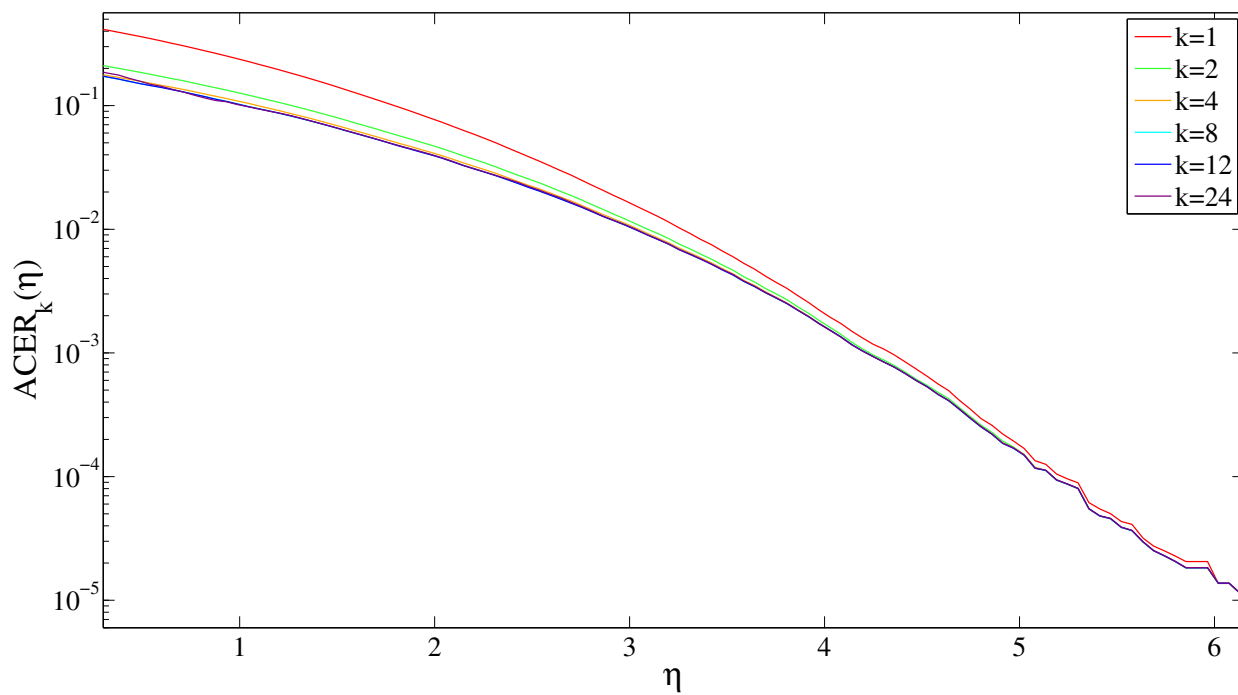


Figure 5.19: Comparison of the ACER estimates for $k = 1, 2, 4, 8, 12$ and 24 degrees of conditioning for the 50 year Gaussian Y data set.

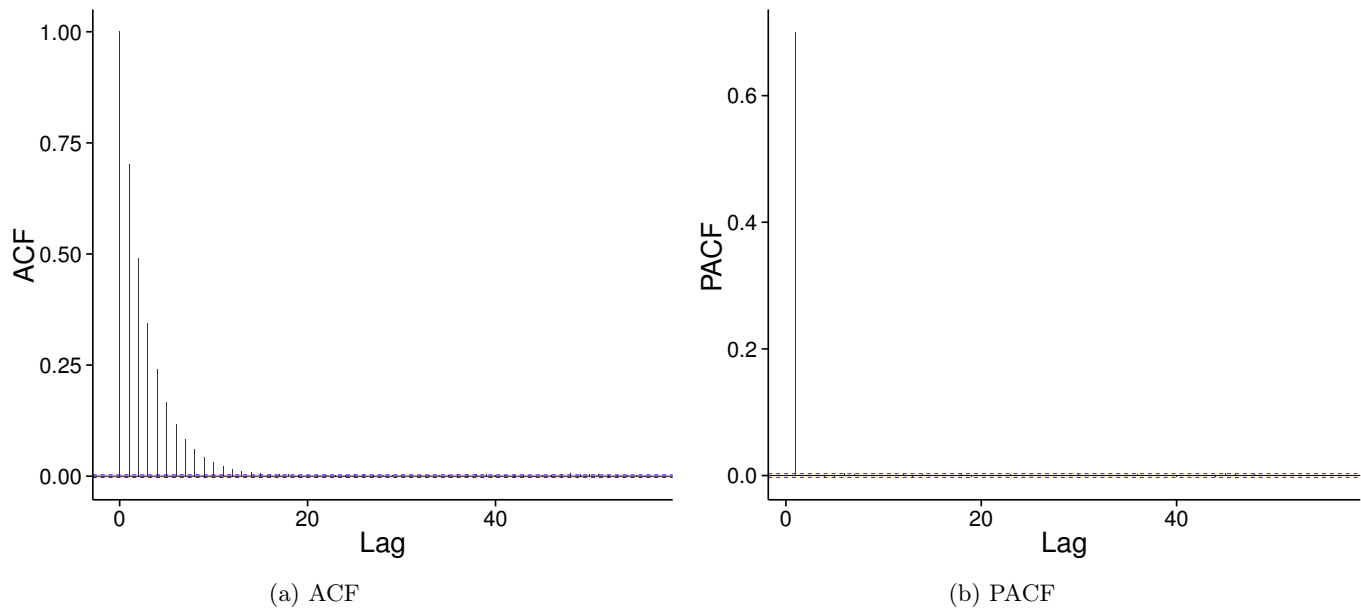


Figure 5.20: The ACF and PACF plot of the synthetic 50 year Gaussian Y data set.

We move ahead by plotting the univariate fitted marginals. These are seen in Figure 5.22. The lines clearly show a high agreement between the two distributions in both the X and Y data set. In this case, we see a misfit between the two methods in the beginning of the tail. This may indicate discrepancies between the distributions of the copula approaches and the sub-asymptotic distribution of the bivariate ACER values, for low return levels. Again we see a slight difference in the far end of the tail of the marginal fit for the Y data. This difference is found to be $1.5 \cdot 10^{-7}$. Although smaller than the differences for the 25 year data set, this difference might culminate in different return values for large return periods. In the X data case, the fit of both the ACER function and the Gumbel distribution fit does seem to match perfectly in the far end of the tail. This indicates a high agreement between the two marginals when estimating 50 year return values.

We further present the parameters for optimal fit between the empirically estimated bivariate ACER function and the four copula models in Table 5.5.

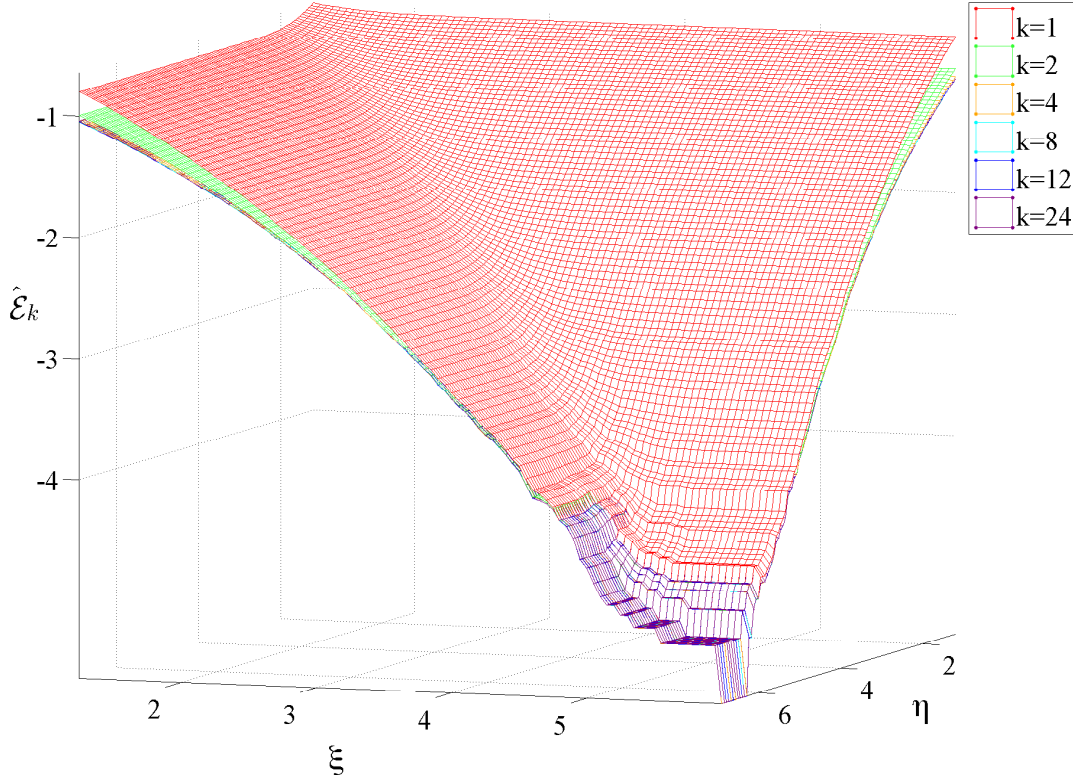
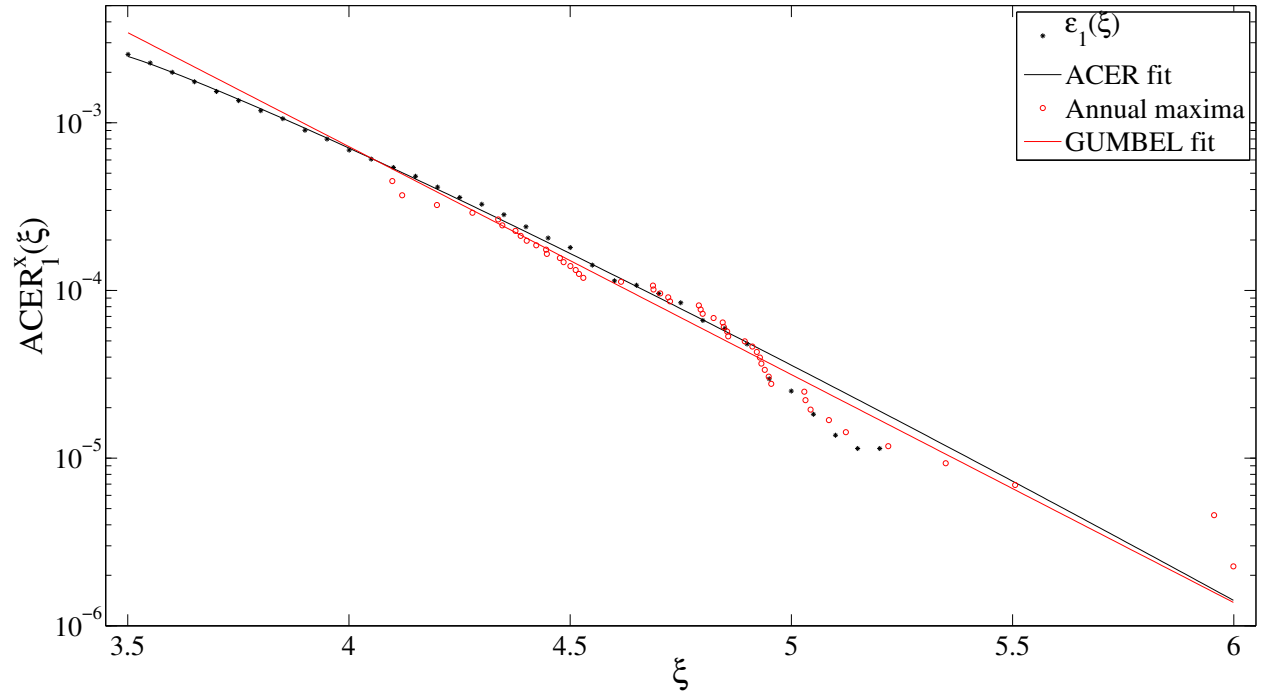


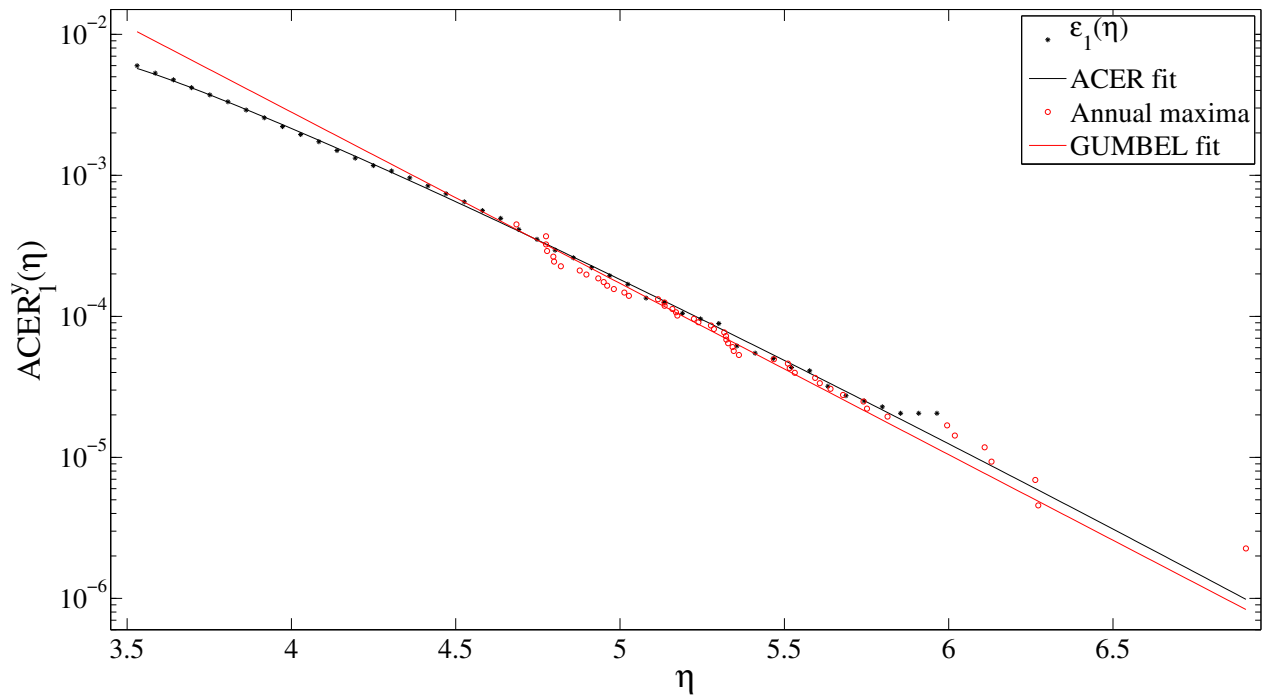
Figure 5.21: Comparison of the bivariate ACER surface estimates for $k = 1, 2, 4, 8, 12$ and 24 degrees of conditioning for the 50 year Gaussian X and Y data set, on a logarithmic scale.

Table 5.5: Optimal parameters of the Gumbel-logistic (GL), Asymmetric logistic (AL), Negative logistic (NL) and Asymmetric negative logistic (ANL) fit with Gumbel and ACER marginals with their respective minimized mean square error (MSE) for the Gaussian 50 year data set.

Marginal	Model	Parameters	MSE
Gumbel	GL	$r = 2.81$	0.1113
	AL	$r = 3.63, \phi = 1, \theta = 0.82$	0.1112
	NL	$r = 2.04$	0.1112
	ANL	$r = 2.70, \phi = 1, \theta = 0.85$	0.1111
ACER	GL	$r = 1.50$	0.0009
	AL	$r = 1.60, \phi = 0.95, \theta = 0.86$	0.0009
	NL	$r = 0.77$	0.0009
	ANL	$r = 0.95, \phi = 0.89, \theta = 0.81$	0.0009



(a) The X data set.



(b) The Y data set.

Figure 5.22: Plot of the empirically estimated ACER functions, the fitted univariate ACER function, the annual maximum and the fitted Gumbel distribution for the synthetic 50 year Gaussian data set.

Table 5.5 reveals that the asymmetric models yield an insignificant decrease in the minimized mean square error, in both marginal cases. In addition, the ϕ and θ parameters are close to 1 for all asymmetric copula models indicating a resemblance between the asymmetric and non-asymmetric copula models. Furthermore, the dependence parameters are significantly different from 1 and 0 for the logistic and negative logistic families, respectively.

The corresponding contour plot of these optimal fitted analytical bivariate extreme value models together with the empirically estimated bivariate ACER functions are found in Figure 5.23.

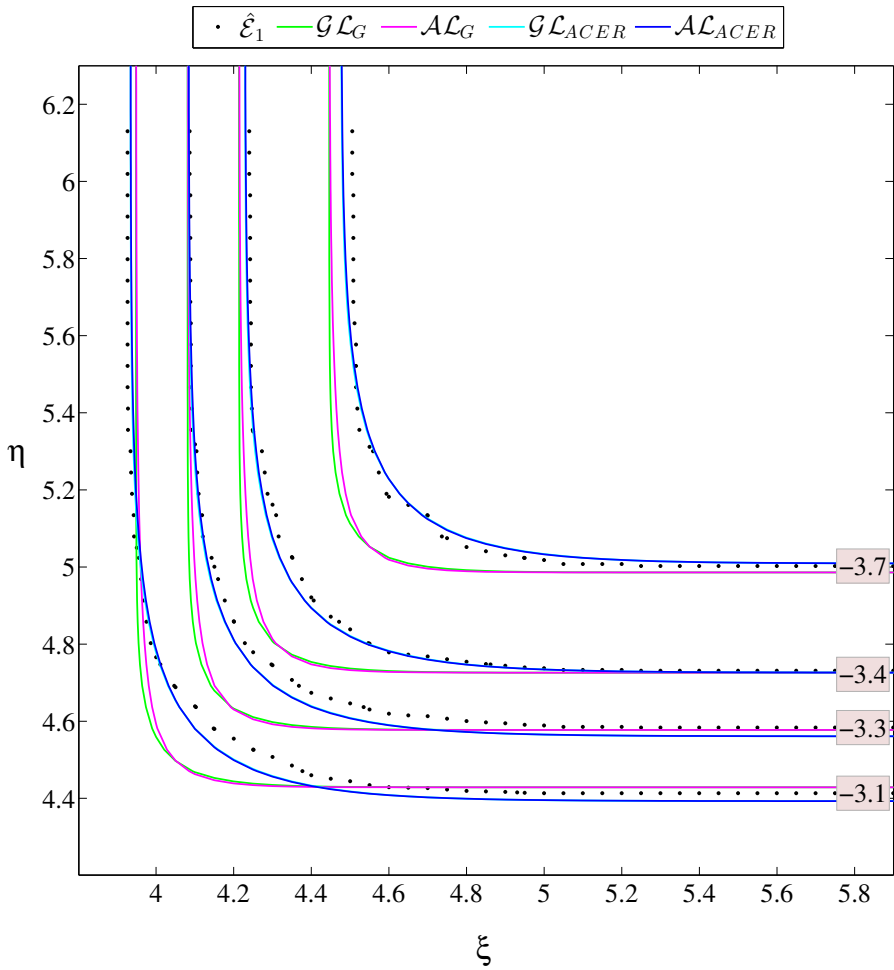


Figure 5.23: Contour plot of the empirically estimated bivariate ACER ($\hat{\mathcal{E}}_1$) surface, optimized Gumbel-logistic (\mathcal{GL}) and optimized Asymmetric logistic (\mathcal{AL}) surfaces using Gumbel and ACER marginals for the 50 year Gaussian data set. The red boxes indicate levels on a logarithmic scale.

Figure 5.23 shows high agreement between the empirically estimated bivariate ACER functions and the copula models with ACER marginals. It is obvious that the dependence structure of the Gumbel marginal copula models

are different than that of the data. This is due to the nature of our parameter optimization as the dependence structure is sacrificed to decrease mean square error. Despite this, there is a high consensus between the Gumbel marginal copula and the empirically estimated bivariate ACER approach in the tails.

Furthermore, we see that the difference between the distribution of the Gumbel marginal copula and the distribution of the observed time series in the Y dimension, are decreasing in the -3.1 to -3.4 levels, and then increasing in -3.7 level.

These differences are also noticeable in the return value plot found in Figure 5.24. In this figure we compare the return values of the three copula models \mathcal{GL}_G , \mathcal{AL}_G and \mathcal{GL}_{ACER} . We further collect the return values and combine them into Table 5.6.

Table 5.6: Estimated 10, 25, 50 and 100 year return values for the Gumbel-logistic copula models with ACER and Gumbel marginals fitted based on the Gaussian 50 year synthetic data set.

Return period	GL_{Gumbel}		GL_{ACER}	
	X	Y	X	Y
10	5.31	5.95	5.34	6.01
25	5.61	6.29	5.63	6.35
50	5.83	6.54	5.85	6.60
100	6.01	6.79	6.06	6.85

Comparing the estimated return values using the copula models with 50 years of hourly data shows that both copula approaches yield very similar return values for all return periods. In fact, the difference in the X case is at most 0.05, while the difference in the Y case is 0.06, consistently. In addition, these differences are even smaller than those observed between the estimated return values for the 25 year data set, indicating a higher agreement between the two methods.

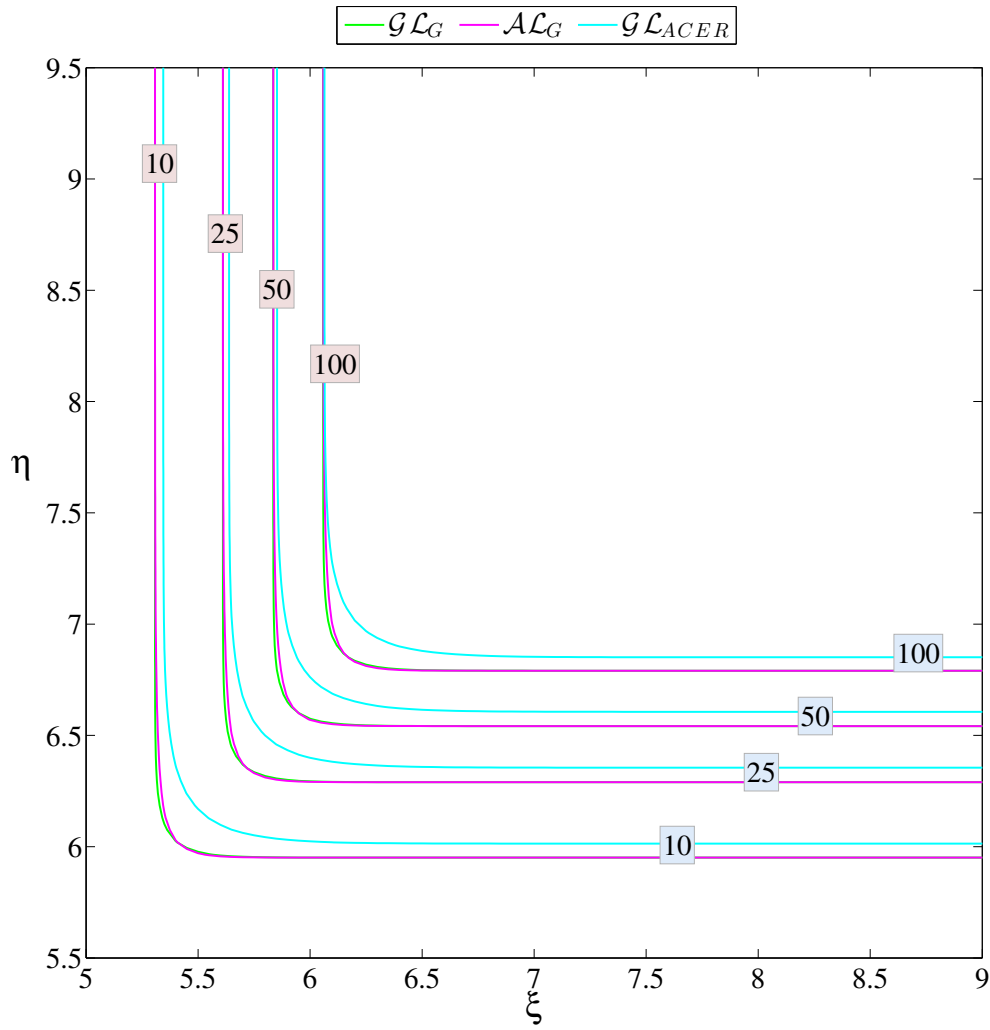


Figure 5.24: Contour plot of the return period levels for the optimized Gumbel-logistic (\mathcal{GL}) and Asymmetric logistic (\mathcal{AL}) surfaces with Gumbel and ACER marginals with respect to the 50 year Gaussian data. The red and blue boxes indicate return levels in years.

100 years

We complete the analysis of the synthetic data sets by considering the 100 year Gaussian time series. Following the same pattern as in the previous subsections, the cascade of ACER functions, $\hat{\varepsilon}_1(\xi), \dots, \hat{\varepsilon}_{24}(\xi)$ and $\hat{\varepsilon}_1(\eta), \dots, \hat{\varepsilon}_{24}(\eta)$, are plotted and found in Figure 5.25 and 5.27.

Both figures show a marginal temporarily dependence between consecutive data. In both cases, convergence of $\hat{\varepsilon}_k(\xi)$ and $\hat{\varepsilon}_k(\eta)$, for all presented values of k , is achieved in the tail.

The corresponding autocorrelation and partial autocorrelation plots are found in Figure 5.26 and 5.28. Figure 5.26a and 5.28a clearly show that there are significant autocorrelations for a large number of lags for both data sets, but as Figure 5.26b and 5.28b reveal, the autocorrelations at lag 2 and above are due to the propagation of the autocorrelation at lag 1. The self-evident choice, for both data sets, is to choose the first ACER function, i.e. $\hat{\varepsilon}_1(\xi)$ and $\hat{\varepsilon}_1(\eta)$.

Figure 5.29 shows the cascade of estimated bivariate ACER surfaces, $\hat{\mathcal{E}}_k(\xi, \eta)$, for $k = 1, 2, 4, 8, 12$ and 24 degrees of conditioning. This figure also suggests using the first ACER function.

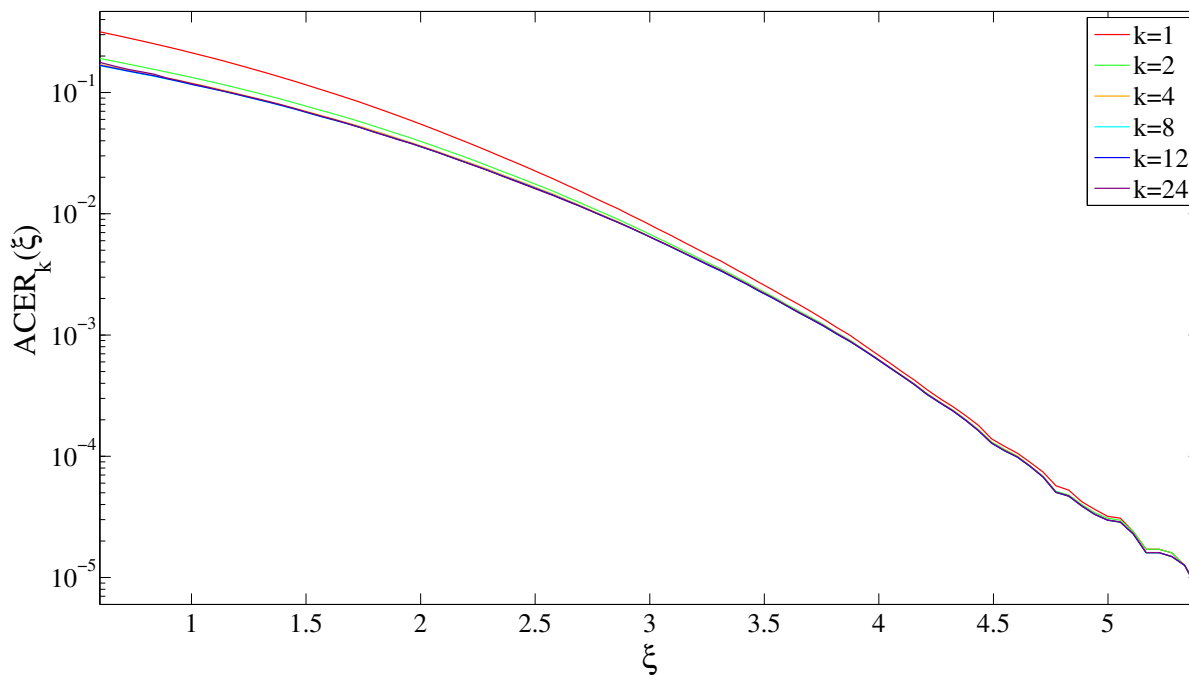


Figure 5.25: Comparison of the ACER estimates for $k = 1, 2, 4, 8, 12$ and 24 degrees of conditioning for the 100 year Gaussian X data set.

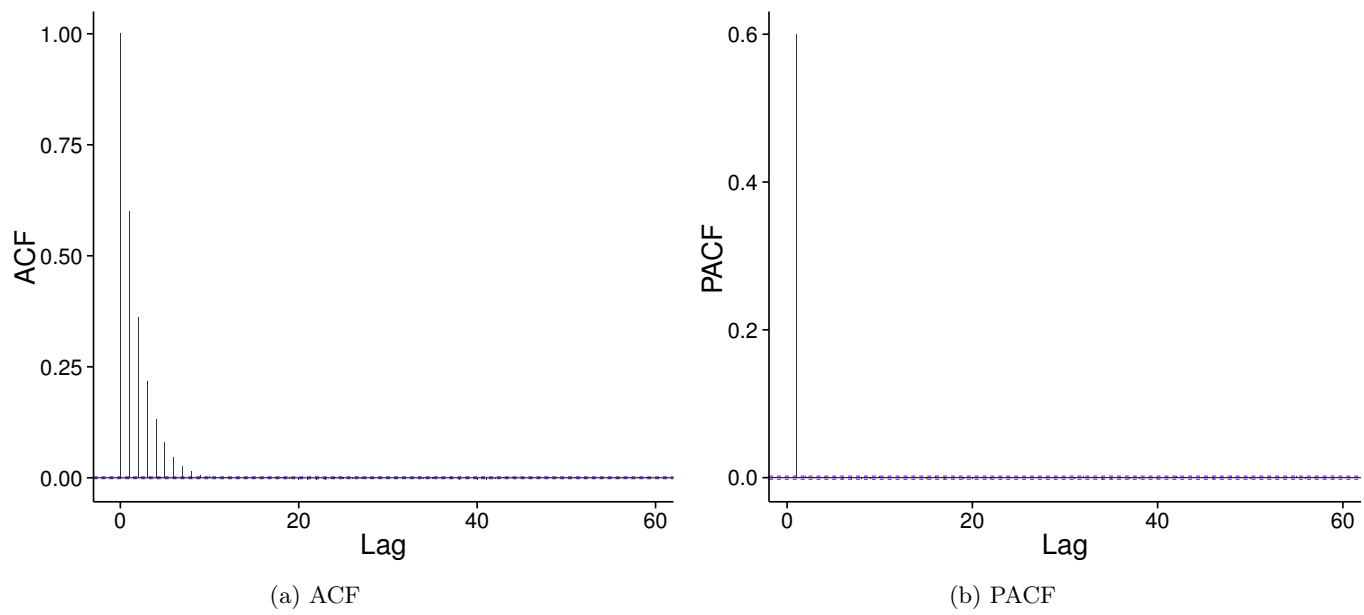


Figure 5.26: The ACF and PACF plot of the synthetic 100 year Gaussian X data set.

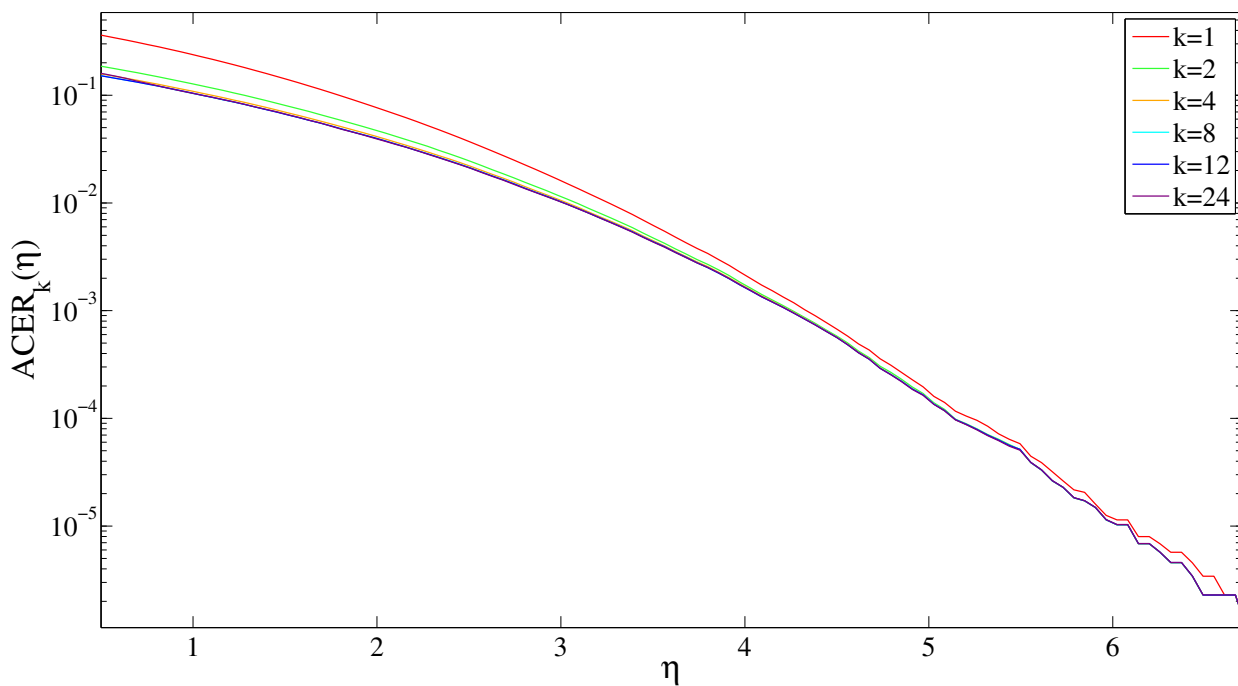


Figure 5.27: Comparison of the ACER estimates for $k = 1, 2, 4, 8, 12$ and 24 degrees of conditioning for the 100 year Gaussian Y data set.

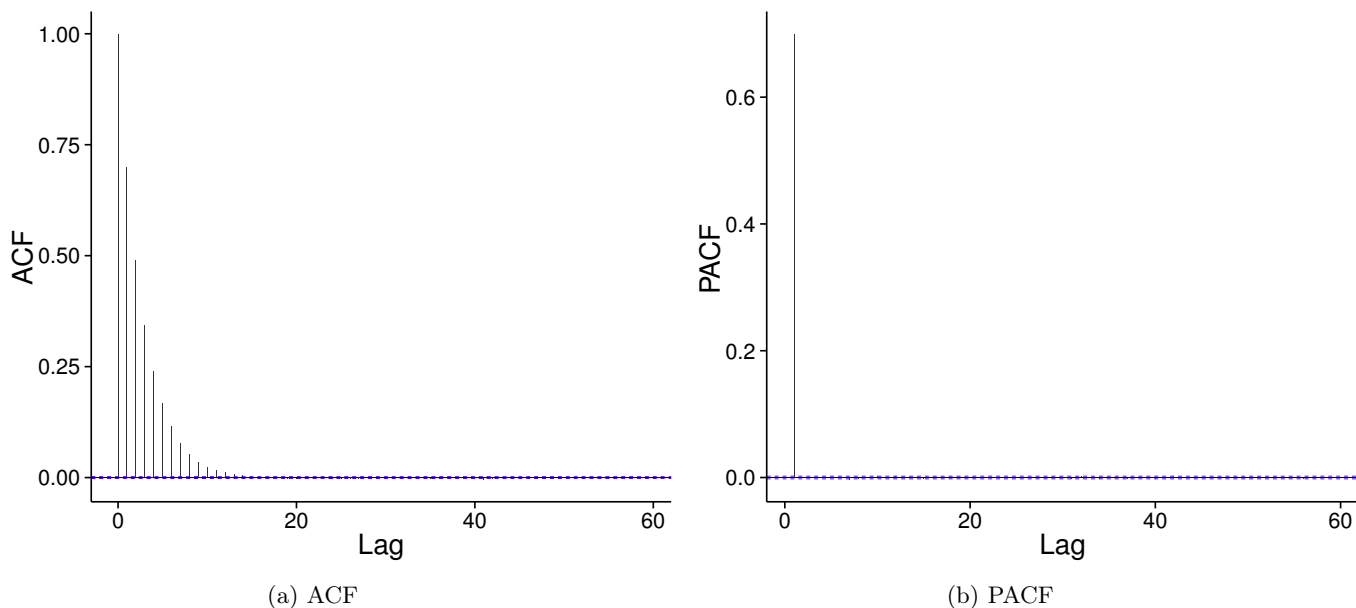


Figure 5.28: The ACF and PACF plot of the synthetic 100 year Gaussian Y data set.

We move ahead by plotting the univariate fitted marginals. These are seen in Figure 5.30. The figure shows a high degree of agreement between the two fitted copula models. Despite this, the figures clearly show a mismatch between the fitted ACER and Gumbel marginals in the far tail for both data sets. Further inspection reveals this difference to be $2.09 \cdot 10^{-07}$ and $1.84 \cdot 10^{-07}$, i.e. approximately the same error as the inequality found in the univariate fit for the 50 year synthetic data set.

We continue our analysis by finding the parameters for best fit between the empirically estimated bivariate ACER function and the four copula models. These parameters are presented in Table 5.7.

Table 5.7: Optimal parameters of the Gumbel-logistic (GL), Asymmetric logistic (AL), Negative logistic (NL) and Asymmetric negative logistic (ANL) fit with Gumbel and ACER marginals with their respective minimized mean square error (MSE) for the Gaussian 100 year data.

Marginal	Model	Parameters	MSE
Gumbel	GL	$r = 1$	0.0242
	AL	$r = 8.34, \phi = 0.06, \theta = 0.29$	0.0240
	NL	$r = 0.03$	0.0242
	ANL	$r = 0.03, \phi = 0.52, \theta = 0.50$	0.0242
ACER	GL	$r = 1.52$	0.0003
	AL	$r = 1.59, \phi = 1, \theta = 0.87$	0.0003
	NL	$r = 0.79$	0.0003
	ANL	$r = 0.86, \phi = 1, \theta = 0.88$	0.0003

It is evident from Table 5.7 that there is no reason favoring the asymmetric

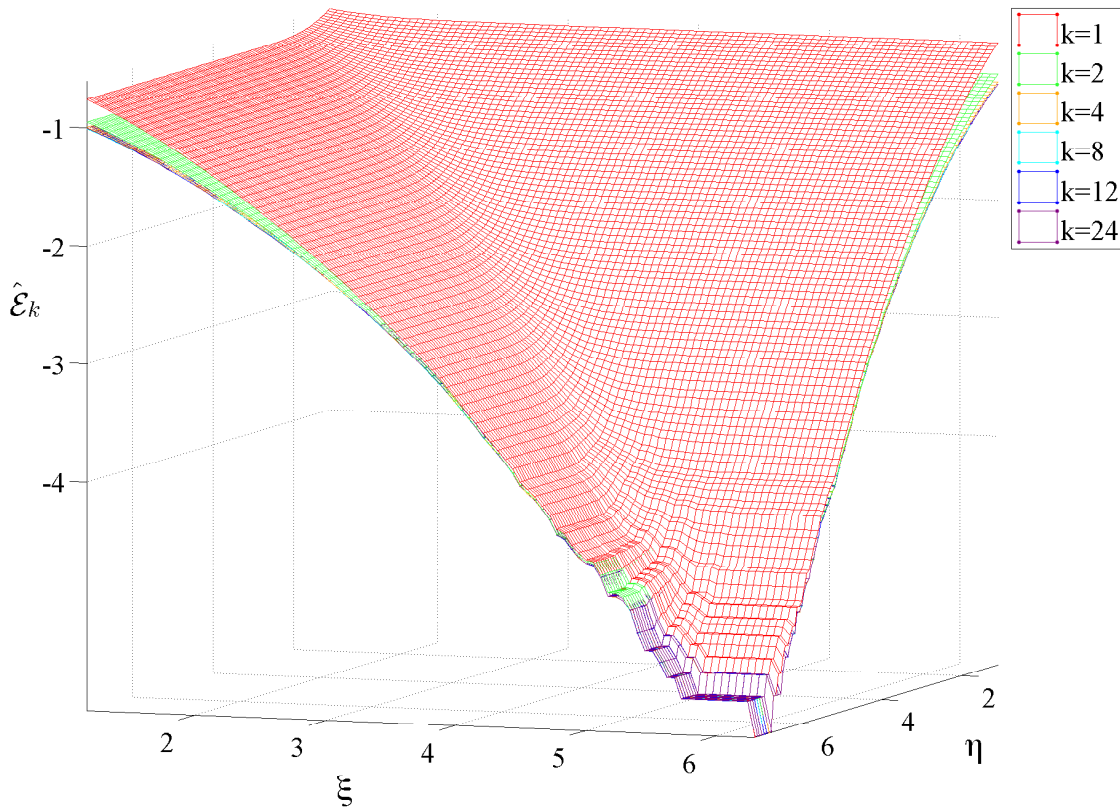
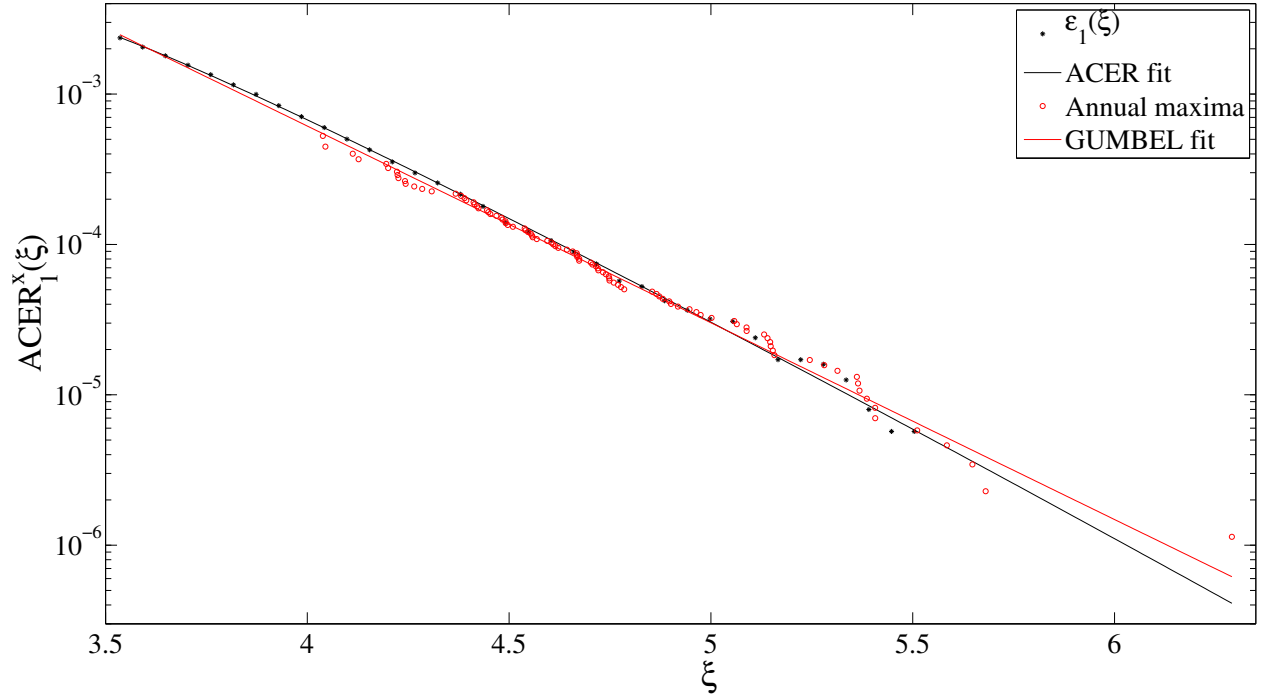


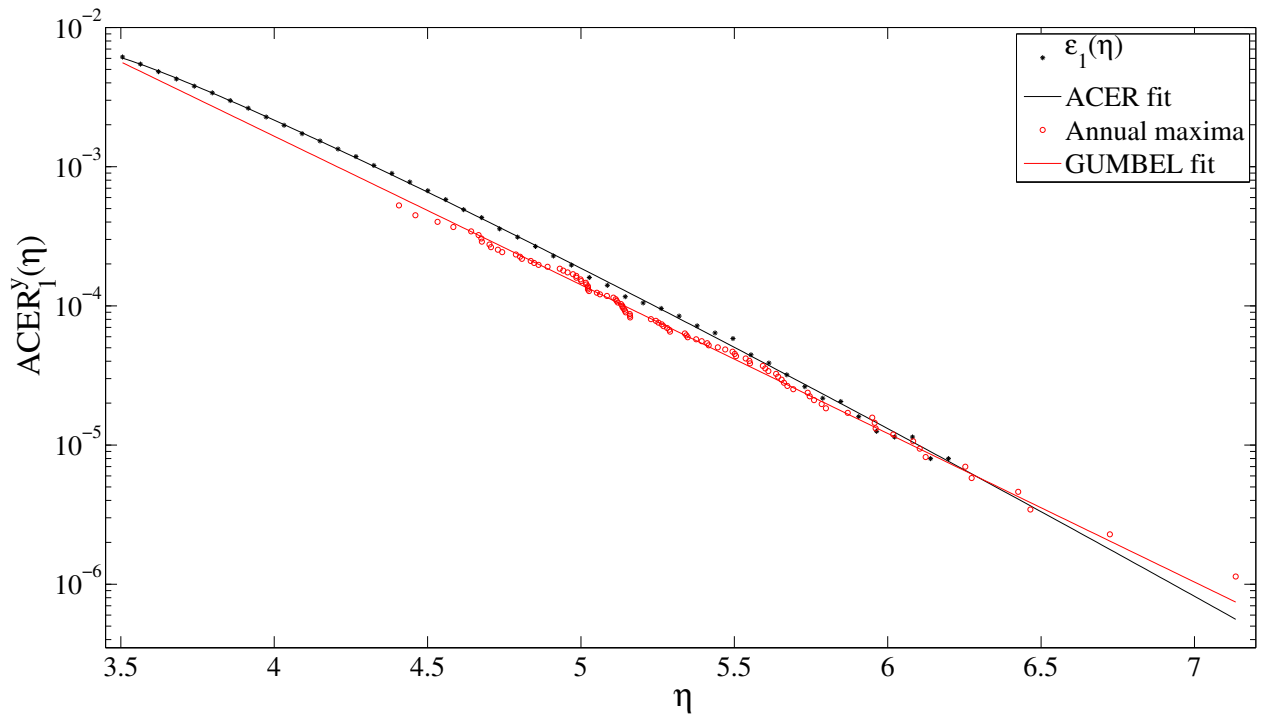
Figure 5.29: Comparison of the bivariate ACER surface estimates for $k = 1, 2, 4, 8, 12$ and 24 degrees of conditioning for the 100 year Gaussian X and Y data set, on a logarithmic scale.

above the non-asymmetric copula models as they yield the same minimized mean square error, when using both fitted Gumbel and ACER marginals. Additionally in the case using Gumbel marginals, these copula models obtain parameters that indicate independence. Using ACER marginals, we see that the dependence parameter stays approximately the same for the asymmetric and non-asymmetric cases and the ϕ and θ parameters are roughly equal to 1.

The corresponding contour plot of these optimal fitted analytical bivariate extreme value copulas is found in Figure 5.31 together with the empirically estimated bivariate ACER functions.



(a) The X data set.



(b) The Y data set.

Figure 5.30: Plot of the empirically estimated ACER functions, the fitted univariate ACER function, the annual maximum and the fitted Gumbel distribution for the synthetic 100 year Gaussian data set.

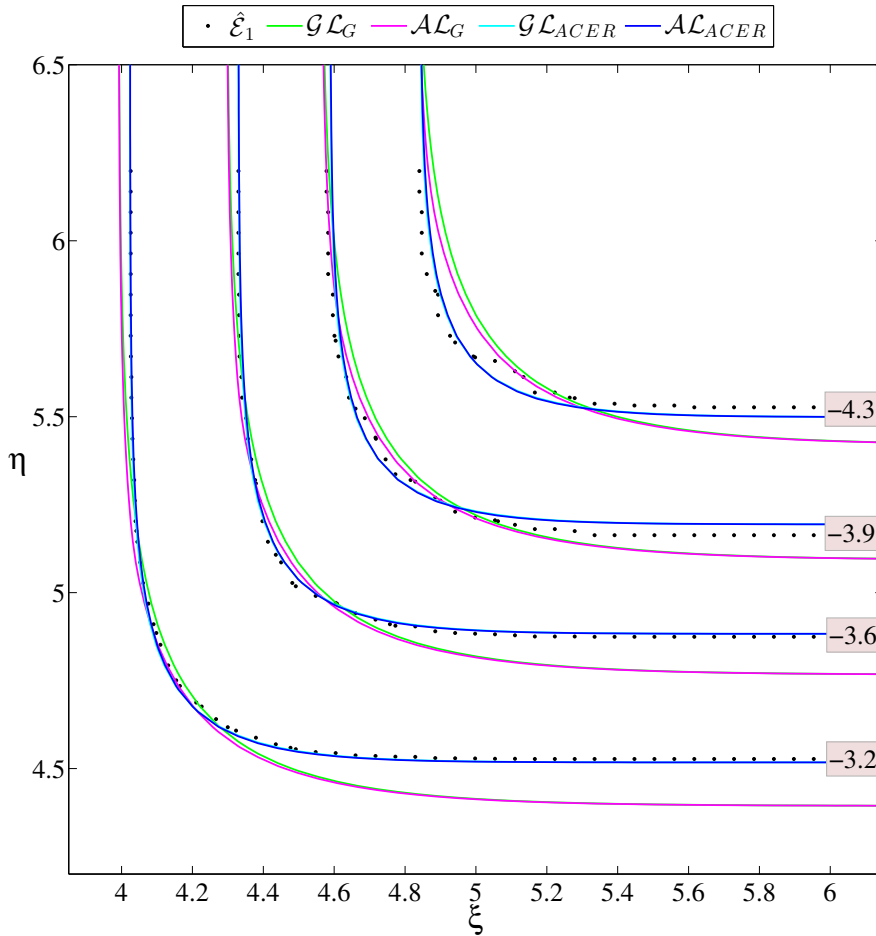


Figure 5.31: Contour plot of the empirically estimated bivariate ACER ($\hat{\mathcal{E}}_1$) surface, optimized Gumbel-logistic (\mathcal{GL}) and optimized Asymmetric logistic (\mathcal{AL}) surfaces using Gumbel and ACER marginals for the 100 year Gaussian data set. The red boxes indicate levels on a logarithmic scale.

Figure 5.31 shows high agreement between the empirically estimated bivariate ACER functions and the copula models with ACER marginals. Moreover, we see that the distribution of the Gumbel marginal copulas fit the sub-asymptotic distribution of the 100 year synthetic data better than previously observed. Despite this, it is obviously a mismatch between the distributions of the Gumbel marginal copulas in the Y dimension and the distributions of the observed time series. These differences do however seem to decrease as the return levels increase. The dependence structure of this copula approach also seem to be improved from previously, but its still not entirely equal to the observed values.

This result is also noticeable in the return value plot found in Figure 5.32. We gather the values representing the 10, 25, 50 and 100 year return period, and combine them into Table 5.8. The models shown in Figure 5.32 are chosen

based on the similarities and differences between the countour lines observed in Figure 5.31.

Table 5.8: Estimated 10, 25, 50 and 100 year return values for the Gumbel-logistic copula models with ACER and Gumbel marginals fitted based on the Gaussian 100 year synthetic data set.

Return period	GL_{Gumbel}		GL_{ACER}	
	X	Y	X	Y
10	5.31	6.00	5.28	6.03
25	5.62	6.39	5.57	6.38
50	5.85	6.68	5.78	6.63
100	6.08	6.96	5.99	6.88

Comparing the estimated return values using the copula models with their respective marginal distributions shows that both copula approaches yield very similar return values for all return periods. As the return period increases, the return value obtained by the ACER marginal copulas are slightly lower than those given by the Gumbel marginal copulas. However, this is expected by noticing the Gumbel and ACER lines in Figure 5.30. Despite this, the two copula approaches yield fairly consistent results, disagreeing the most in the 100 year return period with 0.08 and 0.09 for the X and Y data set, respectfully.

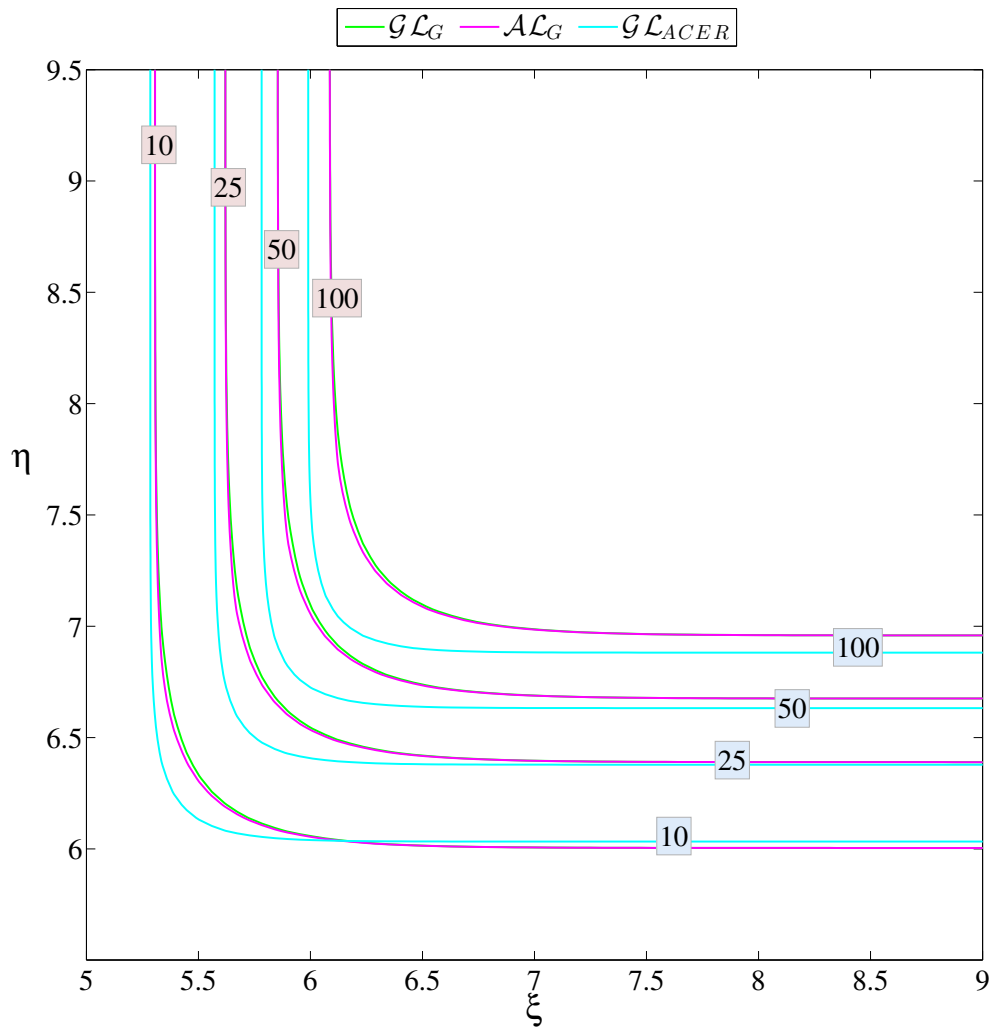


Figure 5.32: Contour plot of the return period levels for the optimized Gumbel-logistic (\mathcal{GL}) and Asymmetric logistic (\mathcal{AL}) surfaces with Gumbel and ACER marginals with respect to the 100 year Gaussian data. The red and blue boxes indicate return levels in years.

5.2 Wind Levels

Finally, we consider the wind levels obtained from the two lighthouses in the county Rogaland. Determining the appropriate ACER functions, $\hat{\varepsilon}_k(\xi)$ and $\hat{\varepsilon}_k(\eta)$, is done by looking at Figure 5.33 and 5.34. As we are dealing with a time series that are considered as non-stationary time series, the autocorrelation and partial autocorrelation function will not be of any help when determining the appropriate ACER function. We regard the incident $k = 24$, corresponding to conditioning the ACER function on wind levels recorded up to six days earlier, to be the final converged result. This is both supported by the ACER plots, as well as the knowledge that a storm rarely stays in the same place over a greater period.

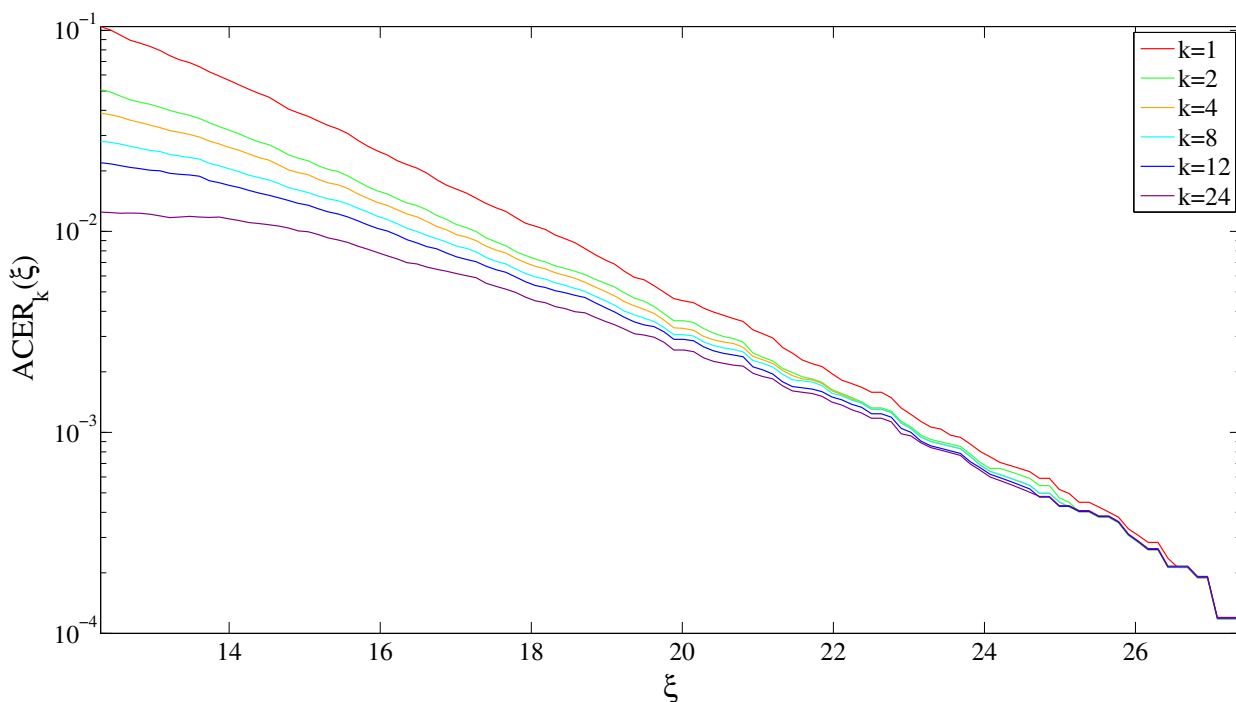


Figure 5.33: Comparison of the ACER estimates for $k = 1, 2, 4, 8, 12$ and 24 degrees of conditioning for the Obrestad-lighthouse data set.

By visual inspection of Figure 5.33 and 5.34, we see a significant temporary dependence between subsequent wind levels, but the cascade of ACER functions obviously converge in the tail. Therefore $\hat{\varepsilon}_1(\xi)$ and $\hat{\varepsilon}_1(\eta)$ are chosen to proceed with.

The corresponding estimated bivariate ACER surfaces $\hat{\mathcal{E}}_k(\xi, \eta)$ are observed in Figure 5.35. The converged ACER functions are plotted in a descending order, leading to overwriting of the surfaces corresponding to lower k -value. The cross-section of the surfaces at the high values of the wind level ξ gives the univariate ACER estimates for the measurements from Oberstad lighthouse while the cross section at a high value of the wind level η gives the univariate ACER function for the measurements from the Utsira lighthouse.

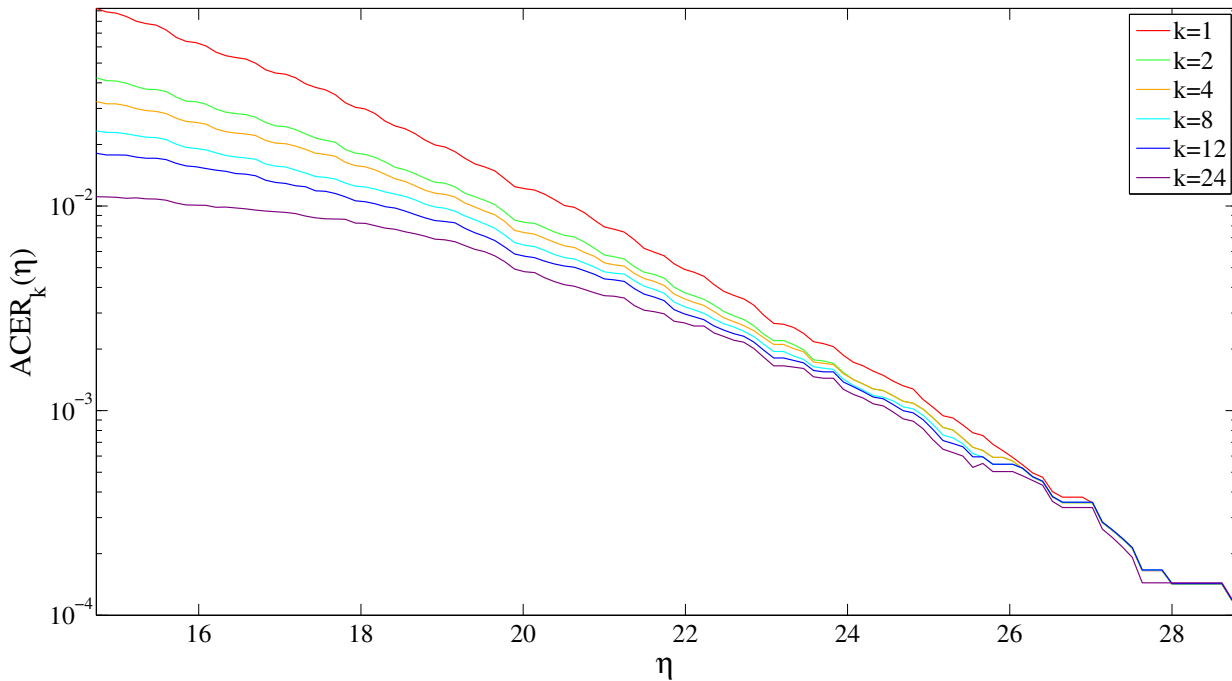


Figure 5.34: Comparison of the ACER estimates for $k = 1, 2, 4, 8, 12$ and 24 degrees of conditioning for the Utsira-lighthouse data set.

We proceed to check how well the fit of the univariate marginals are compared to the data at hand. In Figure 5.36, we plot the empirically estimated univariate ACER functions, the fitted univariate ACER line, the annual maximum of the data set and the fitted Gumbel distribution for both the Obrestad and Utsira data set. This figure reveals an overall high disagreement between the two fitted lines, which indicates a poor agreement when comparing the sub-asymptotic distributions. Further inspection reveals the difference in the far end of the tail to be $2.13 \cdot 10^{-5}$ and $1.21 \cdot 10^{-5}$ for the Obrestad and Utsira data set, respectively. These values are slightly less than the differences between the lines when evaluating the 10 year Gaussian data, implying that we may see the same behaviour when estimating the return values.

Moving forward, we estimate the parameters of optimal fit between the bivariate ACER model and the four copula approaches using different dependence models. The optimal estimates obtained are presented in Table 5.9. This table clearly shows that the complicated asymmetric copula models yield little benefit compared to the symmetric copula models for both marginal approaches. Furthermore, the optimal parameters of the copula models with Gumbel marginals show an optimal fit when assuming the data to be independent. Directing our focus to the estimated ϕ and θ parameters, we see that these are estimated to be 0. Inserting the parameters into Eq. (3.21) and (3.23), we obtain Eq. (3.20) and (3.22), respectively. I.e. we attain the copula models with Gumbel-logistic and Negative logistic dependence functions.

Using ACER marginals, we see that the ϕ and θ parameters of the asym-

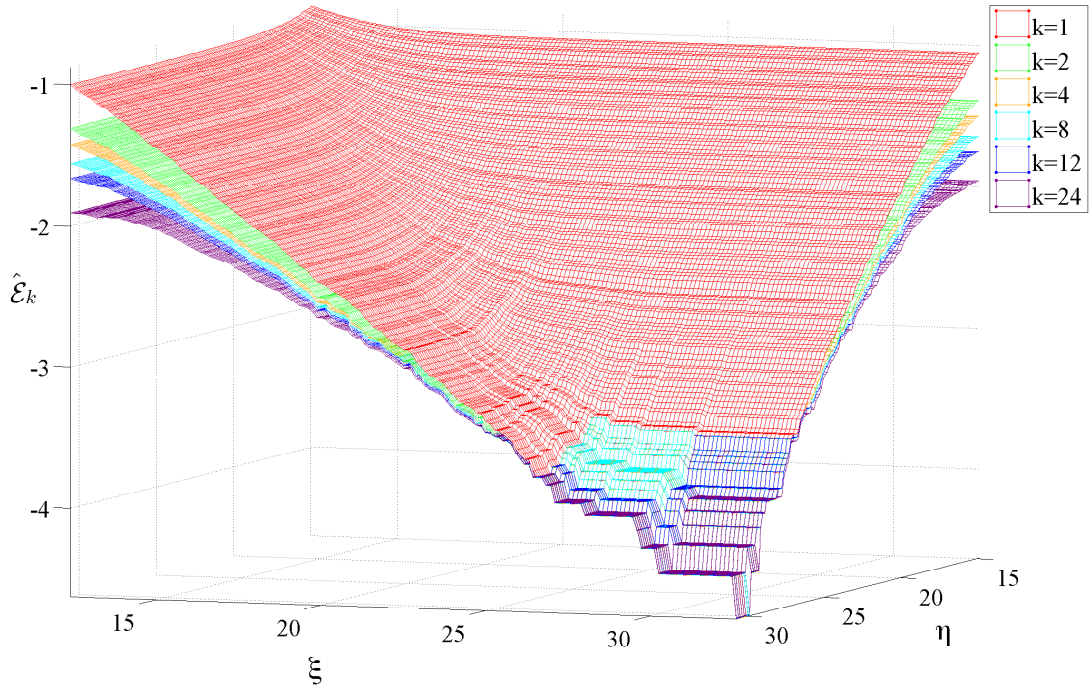


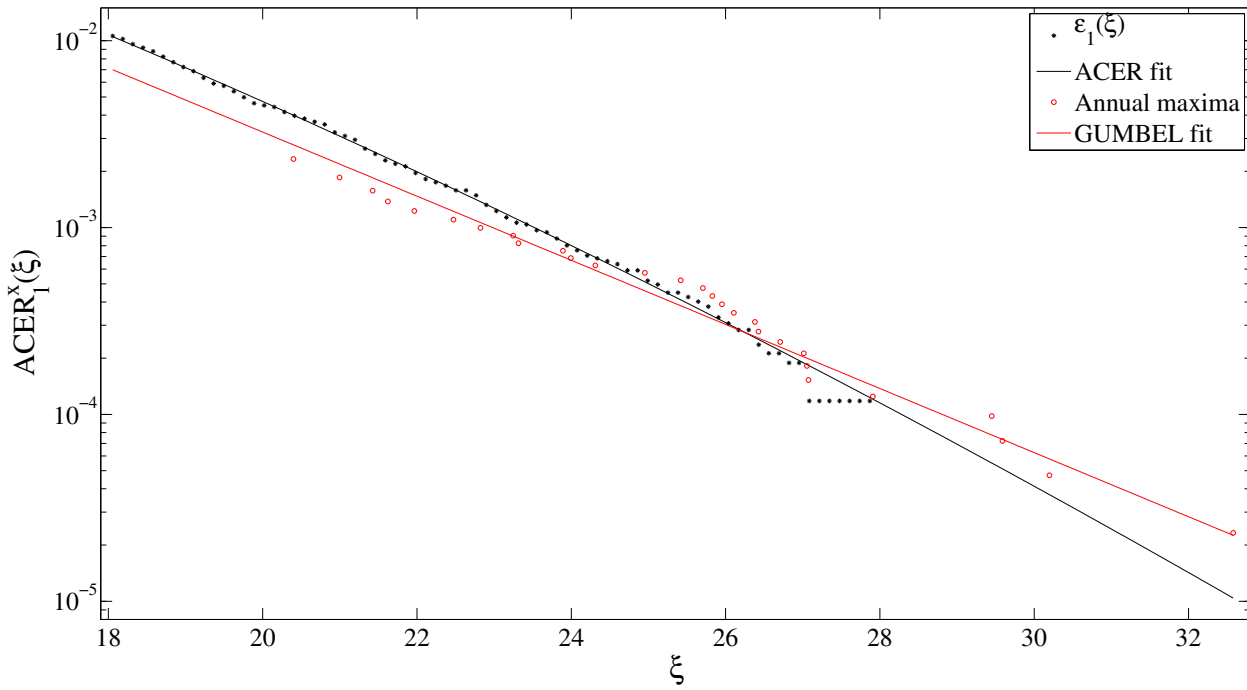
Figure 5.35: Comparison of the bivariate ACER surface estimates for $k = 1, 2, 4, 8, 12$ and 24 degrees of conditioning for the wind level data set, on a logarithmic scale.

metric models are close to 1. In addition, the dependence parameter r is fairly equal in both the asymmetric and non-asymmetric models, indicating resemblance between the two cases.

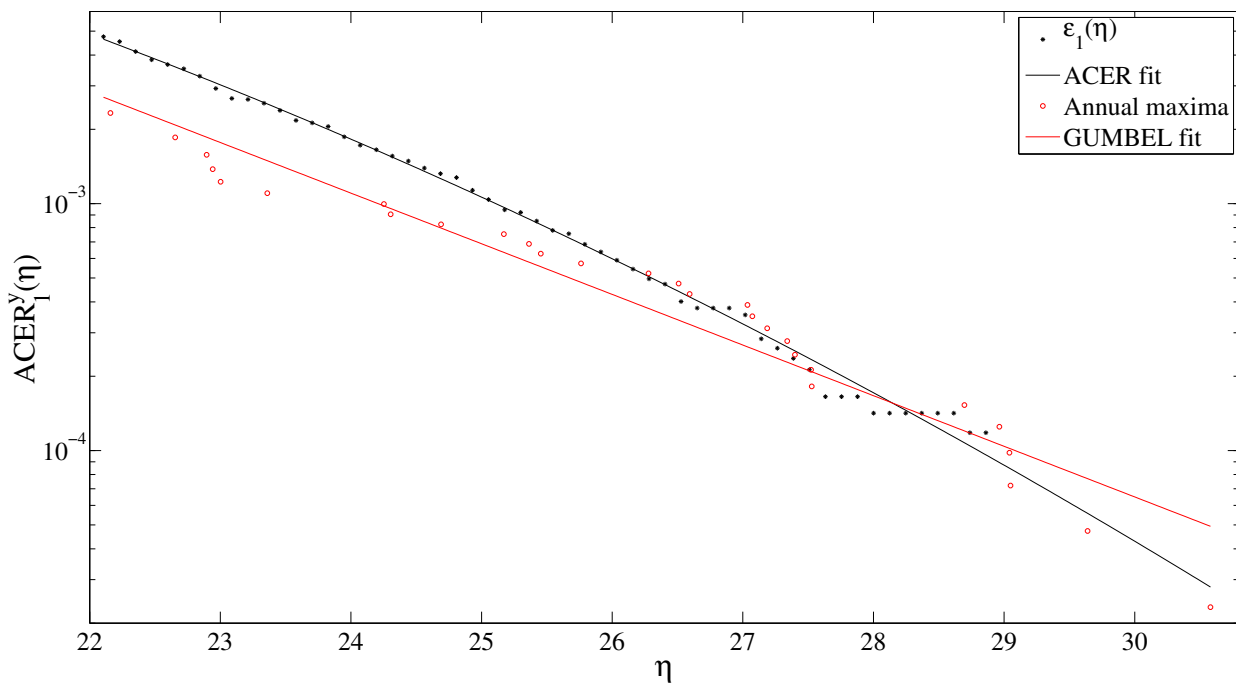
Table 5.9: Optimal parameters of the Gumbel-logistic (GL), Asymmetric logistic (AL), Negative logistic (NL) and Asymmetric negative logistic (ANL) fit with Gumbel and ACER marginals with their respective minimized mean square error (MSE) for the wind levels data set.

Marginal	Model	Parameters	MSE
Gumbel	GL	$r = 1$	0.1052
	AL	$r = 1, \phi = 0, \theta = 0$	0.1052
	NL	$r = 0.01$	0.1052
	ANL	$r = 0.01, \phi = 0, \theta = 0$	0.1052
ACER	GL	$r = 1.41$	0.0014
	AL	$r = 1.50, \phi = 0.78, \theta = 1$	0.0014
	NL	$r = 0.68$	0.0014
	ANL	$r = 0.78, \phi = 0.78, \theta = 1$	0.0014

Using these optimal estimated parameters, we plot the contour values of the empirically estimated bivariate ACER functions together with the contour lines of the copula models. These may be viewed in Figure 5.37.



(a) The Obrestad data set.



(b) The Utsira data set.

Figure 5.36: Plot of the empirically estimated ACER functions, the fitted univariate ACER function, the annual maximum and the fitted Gumbel distribution for the wind level data set.

As a result of the optimized parameters, the Gumbel-logistic and Asymmetric logistic copula models obtain the same values and hence the same contour line.

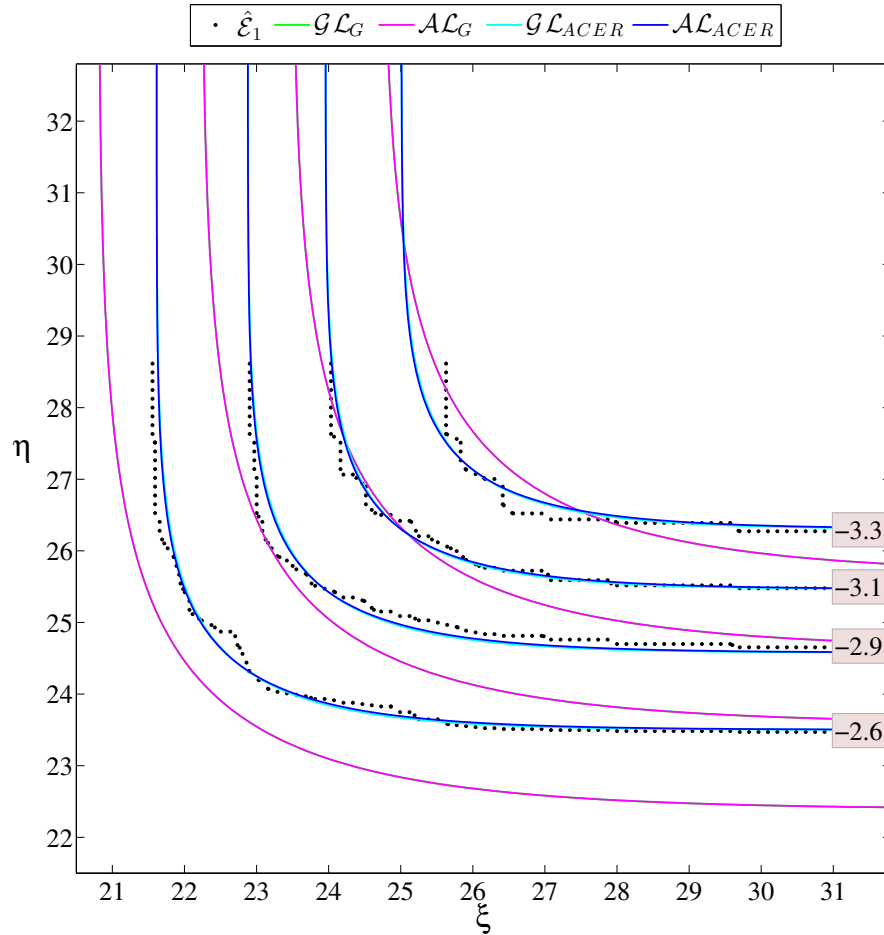


Figure 5.37: Contour plot of the empirically estimated bivariate ACER ($\hat{\mathcal{E}}_1$) surface, optimized Gumbel-logistic (\mathcal{GL}) and optimized Asymmetric logistic (\mathcal{AL}) surfaces using Gumbel and ACER marginals for the wind level data set. The red boxes indicate levels on a logarithmic scale.

Figure 5.37 shows a high equality between the empirically estimated bivariate ACER functions and the copula models with ACER marginals. We also see that the two different copula models using the ACER marginals yield the same values culminating in the same contour lines.

It is obvious that the contour lines of the Gumbel marginal copulas poorly match the contour points of the bivariate ACER. The Gumbel approach does not capture the sub-asymptotic distribution of the wind levels, and in addition we see that the dependence structure of the copula models also indicate a different dependence structure between the data than observed.

This mismatch is also observed in the return value plot found in Figure 5.38. Here we plot the Gumbel-logistic copula model with different marginal distributions. This is due to their simplicity and equality to the more complex asymmetric copula models.

We gather the estimated return values and place them in Table 5.10. From both Figure 5.38 and Table 5.10 we see a huge difference between the two copula approaches. The difference between the two copula models starts at around 0.7 and 0.5 for the Obrestad and Utsira locations. This discrepancy escalates to approximately 2.3 for both locations when the return value period reaches 100 years.

Table 5.10: Estimated 10, 25, 50 and 100 year return values for the Gumbel-logistic copula models with ACER and Gumbel marginals fitted based on the wind level data set. All values in [m/s].

Return period	\mathcal{GL}_{Gumbel}		\mathcal{GL}_{ACER}	
	Obrestad	Utsira	Obrestad	Utsira
10	29.64	29.78	28.92	29.27
25	32.04	31.79	30.74	30.58
50	33.82	33.28	32.06	31.51
100	35.59	34.77	33.33	32.39

Matching this case to the synthetic data sets, we see a clear resemblance between this real world data set and the 10 year synthetic data set. The differences between the univariate marginal fits are approximately the same and the difference in return values show the same tendency.

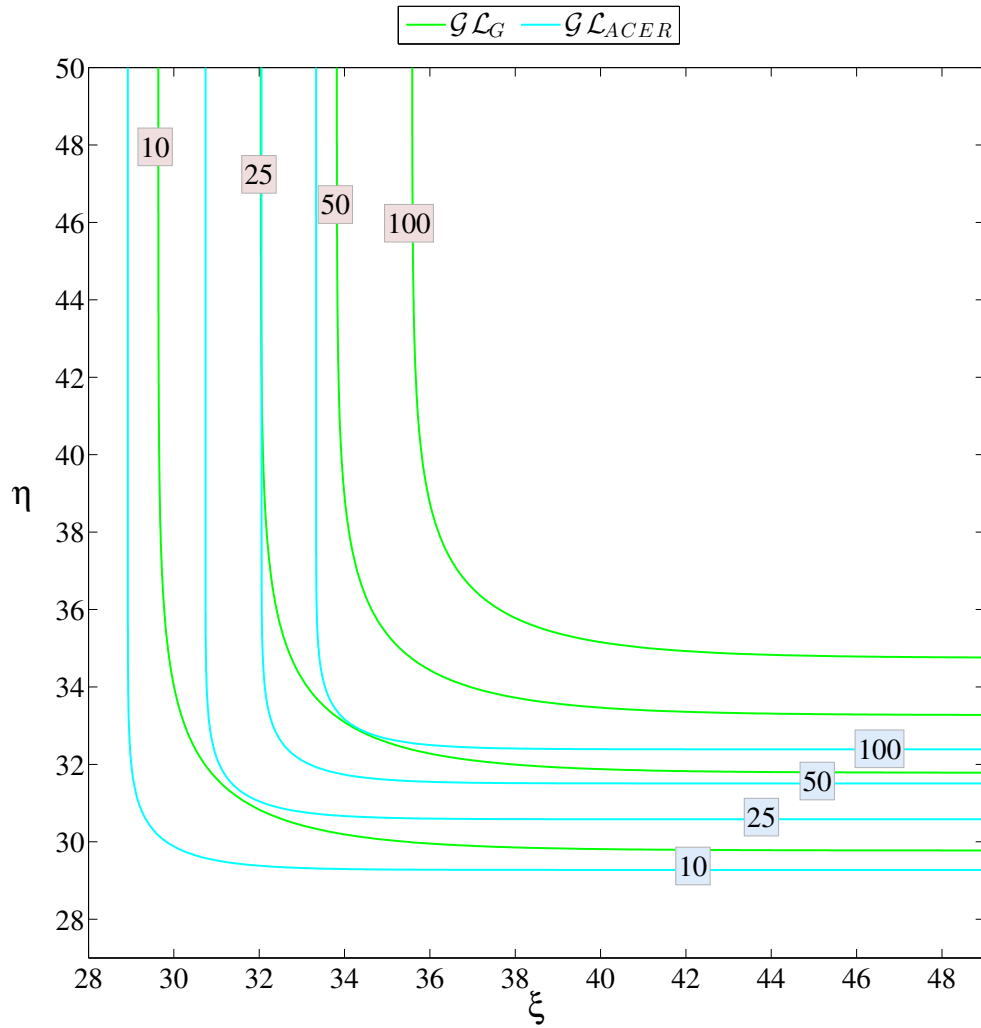


Figure 5.38: Contour plot of the return period levels for the optimized Gumbel-logistic (\mathcal{GL}) surface with Gumbel and ACER marginals with respect to the wind level data. The red and blue boxes indicate return levels in years.

Conclusion

In this report, a description of the bivariate ACER method has been given using a cascade of conditioning approximations that converge to the exact extreme value distribution, with the latent statistical uncertainty, of the data analyzed. It is obvious from the theory that the empirically estimated bivariate ACER method does not provide enough information to estimate high quantiles in the joint distribution, and the behaviour of the bivariate ACER function as a continuous function of two variables can not be decided using the data.

As a result of this, a sub-asymptotic functional form of the ACER surface have been approximated using a copula representation of the bivariate extreme value distribution with marginal extreme value distributions based on the fitted univariate ACER function. In comparison to this procedure, a traditional copula approach using Gumbel marginals has also been done. These Gumbel marginals have been fitted using maximum likelihood estimation with the data sets annual maximum values. To further test the different copula approaches we introduced four dependence functions, namely the Gumbel-logistic, Asymmetric logistic, Negative logistic and Asymmetric negative logistic.

As we are dealing with extreme value statistics of limited time series, the best way to judge a fitted extreme value method is to check how it fits the sub-asymptotic distribution of the evaluated time series.

The analysis of the stationary synthetic time series in [Chapter 5](#) shows that there is a high level of agreement between the distribution of the empirically estimated bivariate ACER methods and the copula representations with univariate ACER marginals in all dimensions. The copula approaches with ACER marginals also captures a high degree of the dependence structure in the evaluated time series.

Analysis further show that there are discrepancies between the bivariate ACER method and the Gumbel marginal copulas. These consists of the Gumbel marginal copula approaches lack to match the sub-asymptotic distribution of the data, and their inability to capture the dependence structures of the time series. These disagreements are greatest when we are evaluating short time series. For longer time series, these differences decrease.

Analysis of the unstationary real world time series consisting of wind levels yield the same results. Despite consisting of 29 years, there are great inequalities between the distributions of the two marginal copula approaches. Again the copula approaches with ACER marginals provides the best fit to the sub-asymptotic distribution of the time series, while the Gumbel approach display a limited fit.

This leads to the conclusion that the copula approach using the novel univariate ACER method as marginal distributions will be a great improvement to the traditional approach using Gumbel marginals, when data are limited. Specifically, the adaptation of the univariate ACER method to the ACER functions is not as vulnerable to limited time series as fitting a Gumbel distribution using the traditional extreme value theory approach of blocking. Being able to make use of more data, the ACER marginal copula approach is not limited to the maximum likelihood approach which yields parameters with great uncertainty when few data points are available.

Furthermore, choosing which one of the four optimized dependence functions to continue with, was made insignificant as all four models with identical marginal distribution gave an approximately similar fit and return values. I.e. there was no reason to pick the more complicated Asymmetric logistic and Asymmetric negative logistic above the Gumbel-logistic or the Negative logistic dependence function.

Bibliography

- [1] S. Coles. *An Introduction to Statistical Modeling of Extreme Values*. Springer Series in Statistics, Springer, 2001.
- [2] N. T. Kottegoda G. Salvadori, C.D. Michele and R. Rosso. *Extremes In Nature An Approach Using Copulas*. 2007.
- [3] J. Galambos. Order statistics of samples from multivariate distributions. *Journal of the American Statistical Association*, vol. 70, pages 674–680, 1975.
- [4] E. J. Gumbel. Bivariate logistic distributions. *Journal of the American Statistical Association* 56(294), pages 335–349, 1961.
- [5] Norwegian Meteorological Institute. Available from <http://www.met.no/English/>.
- [6] H. Joe. Families of min-stable multivariate exponential and multivariate extreme value distributions, 1990.
- [7] H. Joe. Multivariate extreme-value distributions with applications to environmental data. *The Canadian Journal of Statistics*, vol. 1, pages 47–64, 1994.
- [8] O. Karpa. ACER user guide. Available from <http://folk.ntnu.no/karpa/ACER/>.
- [9] A. Naess. On the long-term statistics of extremes. *Applied Ocean Research*, vol. 6, no. 4, pages 227–228, 1984.
- [10] A. Naess. A note on the bivariate acer method. Working paper no. N1-2011, 2011.
- [11] A. Naess and O. Gaidai. Estimation of extreme values from sampled time series. *Structural Safety* 31, pages 325–334, 2009.
- [12] A. Naess O. Gaidai and O. Karpa. Estimation of extreme values by the average conditional exceedance rate method. *Journal of Probability and Statistics*, pages 1208–1217, 2013.
- [13] J. Pickands. Multivariate extreme value distributions. *Bulletin of the International Statistical Institute* 49s, pages 859–878, 1981.

- [14] J. A. Tawn. Bivariate extreme value theory: Models and estimation. *Biometrika* 75(3), pages 397–415, 1988.
- [15] W. W. S. Wei. *Time Series Analysis - Univariate and Multivariate Methods*. Pearson - Addison-Wesley, 2006.

Appendix

In this appendix we first show how synthetic data are generated using time series, followed by the R code produced to create the synthetic data. Furthermore, the optimization of parameters and copula representation are presented in MATLAB code.

A.1 Generation of Synthetic Time Series

Theory

As we wish to simulate two time series, we want control of certain aspects and properties of these. Using Vector Autoregressive models (VAR) as discussed in [15], we start with the model

$$\begin{aligned} X_t &= \alpha X_{t-1} + a_{1t}, \\ Y_t &= \beta Y_{t-1} + a_{2t}, \end{aligned} \tag{A.1}$$

where a_{1t} and a_{2t} are white noise, i.e. Gaussian distributed with 0 mean and standard deviation equal to 1.

To create these two time series with a given correlation, we need to fix the correlation between the white noise vectors. This is done by generating a_{1t} and a_{2t} from the multivariate normal distribution with a given correlation coefficient, ρ . Furthermore, the two time series are generated with a given burn in period of 10% of the process' length, and the correlated white noise is inserted into each process.

R Code

```
1 library(MASS)
  library(stats)
3
4 # ----- #
5 # -- User specified values -- #
6 # ----- #
7 days = 365
  years = 10
9 n = 24*days*years # Amount of generated data
  BurnIn = 0.1*n # Burn in value
11 rho = 0.90 # Correlation factor
  alpha = 0.6
13 beta = 0.7
15 set.seed(1) # For reproducibility
17 # ----- #
18 # - Generating Gaussian data - #
19 # ----- #
20 # Evaluates Eq. (A.1) in the rapport.
21 eps = mvrnorm(n+BurnIn, mu=c(0,0), Sigma=cbind(c(1, rho), c(rho, 1)))
23 X_norm = arima.sim(list(ar=alpha), n, innov=eps[BurnIn+1:n, 1],
25 start.innov=eps[1:BurnIn, 1])
27 Y_norm = arima.sim(list(ar=beta), n, innov=eps[BurnIn+1:n, 2],
 start.innov=eps[1:BurnIn, 2])
```

Listing A.1: Gaussian synthetic time series.

A.2 MATLAB Code

Below, the edited MATLAB code are found. Note that it is only the scripts that have been changed from the original code written by Oleh Karpa that are being displayed in this appendix. In addition, the optimization scripts used for the Negative logistic and the Asymmetric negative logistic dependence function are virtually the same as the Gumbel-logistic and Asymmetric logistic, and therefore only the two previously mentioned are displayed. All MATLAB code are being displayed in the Dropbox folder accessible from <http://goo.gl/v55Qfo>.

```

1 function [ Logistic_marg ] = ...
2     Logistic_Gumbel_marg(marginal_X, marginal_Y, N, k, yrs , r)
3 % Description:
4 % Calculates Eq. (3.20) in the project.
5 % Inputs:
6 % - marginal_X, marginal_Y: Vectors containg the univariate
7 %     Gumbel distributions.
8 % - r: Estimated optimal value for the dependence parameter.
9 constant = (yrs/(N-k+1));
10 for j = 1: numel(marginal_Y)
11     for i = 1: numel(marginal_X)
12         Logistic_marg(j, i) = constant.*(((marginal_X(i)).^(r) ...
13             +(marginal_Y(j)).^(r)).^(1/r));
14     end
15 end
16 end

```

Listing A.2: The Gumbel-logistic dependence function with Gumbel marginals.

```

1 function [ Asymmetric_Logistic_marg ] = ...
2     Asymmetric_Logistic_Gumbel_marg(marginal_X, marginal_Y, N, k, yrs , r ,
3     phi , theta)
4 % Description:
5 % Calculates Eq. (3.21) in the project.
6 % Inputs:
7 % - marginal_X, marginal_Y: Vectors containg the univariate
8 %     Gumbel distributions.
9 % - r, phi, theta: Estimated optimal value of the parameters.
10 constant = (yrs/(N-k+1));
11 for j = 1: numel(marginal_Y)
12     for i = 1: numel(marginal_X)
13         Asymmetric_Logistic_marg(j, i) = ...
14         constant.*((1-phi)*marginal_X(i)+(1-theta)*marginal_Y(j)+ ...
15         ((phi*marginal_X(i)).^(r)+(theta*marginal_Y(j)).^(r)).^(1/r))
16     ;
17     end
18 end
19 end

```

Listing A.3: The Asymmetric logistic dependence function with Gumbel marginals.

```

1 function [ Logistic_marg ] = ...
2     Logistic_ACER_marg(marginal_X, marginal_Y, r)
3 % Description:
4 % Calculates Eq. (3.26) in the project.
5 % Inputs:

```

```

6 % - marginal_X, marginal_Y: Vectors containg the univariate
%                               ACER distributions.
8 % - r: Estimated optimal value for the dependence parameter.
for j = 1:numel(marginal_Y)
10     for i = 1:numel(marginal_X)
12         Logistic_marg(j,i) = (((marginal_X(i)).^(r)...
                               +(marginal_Y(j)).^(r)).^(1/r));
14     end
16 end

```

Listing A.4: The Gumbel-logistic dependence function with ACER marginals.

```

function [ Asymmetric_Logistic_marg] = ...
2   Asymmetric_Logistic_ACER_marg(marginal_X,marginal_Y,r,phi,theta)
% Description:
4 % Calculates Eq. (3.27) in the project.
% Innputs:
6 % - marginal_X, marginal_Y: Vectors containg the univariate
%                               ACER distributions.
8 % - r, phi,theta: Estimated optimal value of the parameters.
for j = 1:numel(marginal_Y)
10     for i = 1:numel(marginal_X)
12         Asymmetric_Logistic_marg(j,i) = ...
            ((1-phi)*marginal_X(i) + (1-theta)*marginal_Y(j) + ...
            ((phi*marginal_X(i)).^(r) + (theta*marginal_Y(j)).^(r))
            .^(1/r));
14     end
16 end
end

```

Listing A.5: The Asymmetric logistic dependence function with ACER marginals.

```

1 function [fin_sol, fmin, pos, sol, W] = ...
   Optim_Bivar_Logistic_Gumbel_marg(biACER, CI,marginal_X,marginal_Y
   ,N,k,yrs,ro)
3
% Description:
5 % Optimizes the r parameters of Eq. (3.20) in the
% rapport by minimizing the mean square error function seen in
7 % Eq. (3.30) under the constraints described in Eq. (3.33).
% Innputs:
9 % - biACER: Values of the bivariate ACER estimates.
% - CI: Confidence interval of the biACER.
11 % - marginal_X, marginal_X: Vectors containg the marginal Gumbel
%                               distributions.
13 % Output:
% - fin_sol: Vector of final optimized parameters.
15 % - fmin: Minimum F-statistic using the optimized parameters.
% - sol: A matrix containing solutions on each row, using
   different
17 %           optimizing methods.
% - pos: The row-number of the sol-matrix where the optimal
   parameters
19 %           giving the minimum F-statistic is given.
% - W: The normalized weights, calculated in Eq. (3.31).
21
23 CI_plus = biACER + CI;

```

```

CI_minus = biACER - CI;
25
W = (log(CI_plus)-log(CI_minus)).^(-2);
27
pos_index = W>0;
real_index = imag(W)~=0;
29
if ~isempty(pos_index)
    W = abs(W);
31
elseif ~isempty(real_index)
    W = abs(W);
33
end
35
% Normalizing weights to have sum(w)=1
W = W/sum(sum(W));
37
clear pos_index real_index condition;

39
% 1) Global 3 param LOG-level constraint optimization
F_test = @(x)sum(...
41
    sum(...
    W.*(log(biACER) - ...
43
    log(Logistic_Gumbel_marg(marginal_X,marginal_Y,...
    N,k,yrs,x(1)+x(2))) ).^2 )); %x = [r]
45
sol = 100*ones(3,3);
47
warning off all;

51
F1 = F_test;

53
nlnineq = @(x) [];
nlneq = @(x) [];
55
nonlinfcn = @(x) deal(nlnineq(x),nlneq(x));

57
optst_logGlobal = optimset('Display','off',...
    'Algorithm','interior-point',...
59
    'MaxFunEvals',10000,'MaxIter',10000,...
    'TolX',1e-12,'TolFun',1e-12);

61
[sol(1,1:2),~] = fmincon(F1,[1/sqrt(1-ro) 1/sqrt(1-ro)],...
63
    [],[],[],[],...
    [0.5 0.5],... % Lower constraints
65
    [Inf Inf],... % Upper constraints
    nonlinfcn,optst_logGlobal);
67
sol(1,3) = F_test(sol(1,1:2));
if any(imag(sum(sol(1,:))))
69
    sol(1,:) = 100*ones(1,3);
end
71
clear F1 optst_logGlobal nlnineq nlneq nonlinfcn;

73
% 2) Global 3 param LOG-level Least Squares constraint
% optimization
75
F2 = @(x) sqrt(...
77
    sum(...
    W.*(log(biACER) - ...
79
    log(Logistic_Gumbel_marg(marginal_X,marginal_Y,...
    N,k,yrs,x(1)+x(2))) ).^2 )); %x = [r]
81
optst_log_all = optimset('Display','off',...
83
    'Algorithm','trust-region-reflective',...
    'MaxFunEvals',10000,'MaxIter',10000,...
85
    'TolX',1e-12,'TolFun',1e-12);

```

```

87 [sol(2,1:2),~] = lsqnonlin(F2,[1/sqrt(1-ro) 1/sqrt(1-ro)],...
      [0.5 0.5],... % Lower constraints
      [Inf Inf],... % Upper constraints
89      optst_log_all);
sol(2,3) = F_test(sol(2,1:2));
91 if any(imag(sum(sol(2,:))))
      sol(2,:) = 100*ones(1,3);
93 end
clear F2 optst_log_all;
95
[fmin, pos] = min(sol(:,3));
97 fin_sol = sol(pos,1:2);
99
end

```

Listing A.6: Optimization function for the Gumbel-logistic dependence function with Gumbel marginals.

```

function [fin_sol, fmin, pos, sol, W] = ...
2 Optim_Bivar_Asymetric_Logistic_Gumbel_marg(biACER, CI, marginal_X,
      marginal_Y, N, k, yrs, ro)
% Description:
4 % Optimizes the r, fi and teta parameters of Eq. (3.21) in the
% rapport by minimizing the mean square error function seen in
6 % Eq. (3.35) under the constraints described in Eq. (3.36).
% Innputs:
8 % - biACER: Values of the bivariate ACER estimates.
% - CI: Confidence interval of the biACER.
10 % - marginal_X, marginal_Y: Vectors containg the marginal
%      Gumbel distributions.
12 % Output:
% - fin_sol: Vector of final optimized parameters.
14 % - fmin: Minimum F-statistic using the optimized parameters.
% - sol: A matrix containing solutions on each row, using
      different
16 %      optimizing methods.
% - pos: The row-number of the sol-matrix where the optimal
      parameters
18 %      giving the minimum F-statistic is given.
% - W: The normalized weights, calculated in Eq. (3.31).
20
CI_plus = biACER + CI;
22 CI_minus = biACER - CI;
24 W = (log(CI_plus)-log(CI_minus)).^(-2);
26 pos_index = W>0;
real_index = imag(W)~=0;
28 if ~isempty(pos_index)
      W = abs(W);
30 elseif ~isempty(real_index)
      W = abs(W);
32 end
% Normalizing weights to have sum(w)=1
34 W = W/sum(sum(W));
clear pos_index real_index condition;
36
% 1) Global 3 param LOG-level constraint optimization
38 F_test = @(x)sum(...
      sum(...
40      W.*( log(biACER) - ...

```

```

42         log(Asymmetric_Logistic_Gumbel_marg(marginal_X,...
43           marginal_Y,N,k,yrs,x(1),x(2),x(3))) ).^2));
44         % x = [r fi teta]
45
46     sol = 100*ones(3,4);
47
48     warning off all;
49
50     F1 = F_test;
51
52     nlnineq = @(x) [];
53     nlneq = @(x) [];
54     nonlinfcn = @(x) deal(nlnineq(x),nlneq(x));
55
56     optst_logGlobal = optimset('Display','off',...
57       'Algorithm','interior-point',...
58       'MaxFunEvals',10000,'MaxIter',10000,...
59       'TolX',1e-12,'TolFun',1e-12);
60     [sol(1,1:3),~] = fmincon(F1,[1/sqrt(1-ro) 0.5 0.5],[[],[],[],[]],...
61       [1 0 0],... % Lower constraints
62       [Inf 1 1],... % Upper constraints
63       nonlinfcn,optst_logGlobal);
64     if any(imag(sum(sol(1,:))))
65         sol(1,:) = 100*ones(1,4);
66     end
67     sol(1,4) = F_test(sol(1,1:3));
68     clear F1 optst_logGlobal nlnineq nlneq nonlinfcn;
69
70     % 2) Global 3 param LOG-level Least Squares constraint
71     optimization
72
73     F2 = @(x) sqrt(sum(W.*( ...
74       log(biACER) - ...
75       log(Asymmetric_Logistic_Gumbel_marg(marginal_X,...
76         marginal_Y, N,k,yrs,x(1),x(2),x(3))) ).^2));
77     % x = [r fi teta]
78
79     optst_log_all = optimset('Display','off',...
80       'Algorithm','trust-region-reflective',...
81       'MaxFunEvals',10000,'MaxIter',10000,...
82       'TolX',1e-12,'TolFun',1e-12);
83     [sol(2,1:3),~] = lsqnonlin(F2,[1/sqrt(1-ro) 0.5 0.5],...
84       [1 0 0],... % Lower constraints
85       [Inf 1 1],... % Upper constraints
86       optst_log_all);
87     if any(imag(sum(sol(2,:))))
88         sol(2,:) = 100*ones(1,4);
89     end
90     sol(2,4) = F_test(sol(2,1:3));
91     clear F2 optst_log_all;
92
93     [fmin, pos] = min(sol(:,4));
94     fin_sol = sol(pos,1:3);
95
96 end

```

Listing A.7: Optimization function for the Asymmetric logistic dependence function with Gumbel marginals.

```

236 % ----- %
238 % ----- TRADITIONAL EV ----- %
239 % ----- %
240
242 % ----- Univariate fit ----- %
dataX = max(X); % Extract the maximum yearly value
244 dataY = max(Y); % for both time series.
246 % Parameters for Gumbel:
parmhat_X = evfit(-dataX); % mu sigma
248 parmhat_Y = evfit(-dataY); % mu sigma
250 % Calculates the cumulative distribution of the observed maxima
sorted_data_X = sort(dataX);
252 sorted_data_Y = sort(dataY);
F_x = [];
254 F_y = [];
for i=1:numel(dataX)
256     F_x(i) = -(yrs_X/(Npoints-k_choise+1))*log(i/(numel(dataX)+1));
        F_y(i) = -(yrs_Y/(Npoints-k_choise+1))*log(i/(numel(dataY)+1));
258 end
260 x_vals_X = linspace(min(min(blXtmp),min(dataX))-eps,...
                    max(max(blXtmp),max(dataX))+eps,N_X);
262 x_vals_Y = linspace(min(min(blYtmp),min(dataY))-eps,...
                    max(max(blYtmp),max(dataY))+eps,N_Y);
264
Gumbel_fit_X = yrs_X*gumb_uni(x_vals_X,-parmhat_X(1),...
266     parmhat_X(2))./(Npoints-k_choise+1);
Gumbel_fit_Y = yrs_Y*gumb_uni(x_vals_Y,-parmhat_Y(1),...
268     parmhat_Y(2))./(Npoints-k_choise+1);
270 acer_fit_Xtmp_k = epsilon(x_vals_X, fin_sol_X);
acer_fit_Ytmp_k = epsilon(x_vals_Y, fin_sol_Y);
272
274 % Univariate plot
figure
276 clf
semilogy(blXtmp, acerXtmp, '*k','MarkerSize',4)
278 hold on
semilogy(x_vals_X, acer_fit_Xtmp_k, 'k')
280 hold on
semilogy(sorted_data_X, F_x, 'or','MarkerSize',4)
282 hold on
semilogy(x_vals_X, Gumbel_fit_X, 'r')
284 xlabel('\xi')
ylabel('ACER^x_1(\xi)')
286 legend('\epsilon_1(\xi)', 'ACER fit', 'Annual maxima', 'GUMBEL fit')
editplot33;
288
figure
290 clf
semilogy(blYtmp, acerYtmp, '*k','MarkerSize',4)
292 hold on
semilogy(x_vals_Y, acer_fit_Ytmp_k, 'k')
294 hold on
semilogy(sorted_data_Y, F_y, 'or','MarkerSize',4)
296 hold on
semilogy(x_vals_Y, Gumbel_fit_Y, 'r')

```

```

298 xlabel('\eta')
    ylabel('ACER^y_1(\eta)')
300 legend('\epsilon_1(\eta)', 'ACER fit', 'Annual maxima', 'GUMBEL fit')
    editplot33;
302
    % Refit the marginal distributions
304 Gumbel_fit_X = gumb_uni(bl_X, -parmhat_X(1), parmhat_X(2));
    Gumbel_fit_Y = gumb_uni(bl_Y, -parmhat_Y(1), parmhat_Y(2));
306
    acer_fit_X = epsilon(bl_X, fin_sol_X);
308 acer_fit_Y = epsilon(bl_Y, fin_sol_Y);
310
312
314 % ----- Dependence functions ----- %
    % Here we find the optimal parameter(s) of the dependence
316 % functions under their respective constraints, using Gumbel
    % and ACER marginals. They are then being fitted with the
318 % parameters.
320 % Gumbel-Logistic dependence function
    [fin_sol_g_l, ~, ~, sol_g_l, ~] = ...
322     Optim_Bivar_Logistic_Gumbel_marg(ACER_hat_mean, CI_BI, ...
        Gumbel_fit_X, Gumbel_fit_Y, Npoints, k_choise, yrs_X, ro);
324
    [fin_sol_a_l, ~, ~, sol_a_l, ~] = ...
326     Optim_Bivar_Logistic_ACER_marg(ACER_hat_mean, CI_BI, ...
        acer_fit_X, acer_fit_Y, ro);
328
330 % Asymmetric Logistic dependence function
    [fin_sol_g_al, ~, ~, sol_g_al, ~] = ...
332     Optim_Bivar_Asymetric_Logistic_Gumbel_marg(ACER_hat_mean, ...
        CI_BI, Gumbel_fit_X, Gumbel_fit_Y, Npoints, k_choise, yrs_X, ro);
334
336 [fin_sol_a_al, ~, ~, sol_a_al, ~] = ...
    Optim_Bivar_Asymetric_Logistic_ACER_marg(ACER_hat_mean, ...
338     CI_BI, acer_fit_X, acer_fit_Y, ro);
340 % Negative Logistic dependence function
    [fin_sol_g_nl, ~, ~, sol_g_nl, ~] = ...
342     Optim_Bivar_Negative_Logistic_Gumbel_marg(ACER_hat_mean, ...
        CI_BI, Gumbel_fit_X, Gumbel_fit_Y, Npoints, k_choise, yrs_X);
344
    [fin_sol_a_nl, ~, ~, sol_a_nl, ~] = ...
346     Optim_Bivar_Negative_Logistic_ACER_marg(ACER_hat_mean, ...
        CI_BI, acer_fit_X, acer_fit_Y);
348
    % Asymmetric Negative Logistic dependence function
350 [fin_sol_g_anl, ~, ~, sol_g_anl, ~] = ...
    Optim_Bivar_Asymetric_Negative_Logistic_Gumbel_marg(...
352     ACER_hat_mean, CI_BI, Gumbel_fit_X, Gumbel_fit_Y, ...
        Npoints, k_choise, yrs_X);
354
356 [fin_sol_a_anl, ~, ~, sol_a_anl, ~] = ...
    Optim_Bivar_Asymetric_Negative_Logistic_ACER_marg(ACER_hat_mean
    , ...
358     CI_BI, acer_fit_X, acer_fit_Y);

```

```

360 % Copula models are being calculated with their respective
    % parameter values.
362
    % Gumbel-Logistic dependence function
364 Logistic_Gumbel_fit = ...
        Logistic_Gumbel_marg(Gumbel_fit_X, Gumbel_fit_Y, Npoints, ...
366         k_choise, yrs_X, fin_sol_g_l(1)+fin_sol_g_l(2));
368 Logistic_ACER_fit = ...
        Logistic_ACER_marg(acer_fit_X, acer_fit_Y, ...
370         fin_sol_a_l(1)+fin_sol_a_l(2));
372 % Asymmetric Logistic dependence function
    Asymmetric_Logistic_Gumbel_fit = ...
374 Asymmetric_Logistic_Gumbel_marg(Gumbel_fit_X, Gumbel_fit_Y, ...
        Npoints, k_choise, yrs_X, fin_sol_g_al(1), fin_sol_g_al(2), ...
376         fin_sol_g_al(3));
378 Asymmetric_Logistic_ACER_fit = ...
        Asymmetric_Logistic_ACER_marg(acer_fit_X, acer_fit_Y, ...
380         fin_sol_a_al(1), fin_sol_a_al(2), fin_sol_a_al(3));
382 % Negative Logistic dependence function
    Negative_Logistic_Gumbel_fit = ...
384 Negative_Logistic_Gumbel_marg(Gumbel_fit_X, Gumbel_fit_Y, ...
        Npoints, k_choise, yrs_X, fin_sol_g_nl(1)+fin_sol_g_nl(2));
386
388 Negative_Logistic_ACER_fit = ...
        Negative_Logistic_ACER_marg(acer_fit_X, acer_fit_Y, ...
390         fin_sol_a_nl(1)+fin_sol_a_nl(2));
392 % Asymmetric Negative Logistic dependence function
    Asymmetric_Negative_Logistic_Gumbel_fit = ...
394 Asymmetric_Negative_Logistic_Gumbel_marg(Gumbel_fit_X, ...
        Gumbel_fit_Y, Npoints, k_choise, yrs_X, fin_sol_g_anl(1), ...
396         fin_sol_g_anl(2), fin_sol_g_anl(3));
398 Asymmetric_Negative_Logistic_ACER_fit = ...
        Asymmetric_Negative_Logistic_ACER_marg(acer_fit_X, ...
400         acer_fit_Y, fin_sol_a_anl(1), fin_sol_a_anl(2), fin_sol_a_anl(3));
402 % Contour fit
    % Here we make optimal scales for the contour plot.
404 % The optimal models are then being fitted by running
    % the marginals for the computed interval.
406 m1 = max(max(log10(ACER_hat_mean)));
    m2 = max(max(log10(Logistic_Gumbel_fit)));
408 m3 = max(max(log10(Asymmetric_Logistic_Gumbel_fit)));
    m4 = max(max(log10(Negative_Logistic_Gumbel_fit)));
410 m5 = max(max(log10(Asymmetric_Negative_Logistic_Gumbel_fit)));
    m6 = max(max(log10(Logistic_ACER_fit)));
412 m7 = max(max(log10(Asymmetric_Logistic_ACER_fit)));
    m8 = max(max(log10(Negative_Logistic_ACER_fit)));
414 m9 = max(max(log10(Asymmetric_Negative_Logistic_ACER_fit)));
    a = (min([m1, m2, m3, m4, m5, m6, m7, m8, m9]));
416
    clear m1 m2 m3 m4
418 m1 = min(min(log10(ACER_hat_mean)));
    m2 = min(min(log10(Logistic_Gumbel_fit)));
420 m3 = min(min(log10(Asymmetric_Logistic_Gumbel_fit)));

```

```

m4 = min(min(log10(Negative_Logistic_Gumbel_fit)));
422 m5 = min(min(log10(Asymmetric_Negative_Logistic_Gumbel_fit)));
m6 = min(min(log10(Logistic_ACER_fit)));
424 m7 = min(min(log10(Asymmetric_Logistic_ACER_fit)));
m8 = min(min(log10(Negative_Logistic_ACER_fit)));
426 m9 = min(min(log10(Asymmetric_Negative_Logistic_ACER_fit)));
b = (max([m1, m2, m3, m4, m5]))+0.1;
428
clear m1 m2 m3
430 v1 = linspace(a, (b+a)/2, 8);
v2 = linspace((b+a)/2, b, 5);
432 v = [v1, v2(2:end)];
clear a b v1 v2
434
stepX = bar_lev_X(2)-bar_lev_X(1);
436 blx = [bar_lev_X(1:end-1)-0.5, (bar_lev_X(end)-0.5):stepX:...
        bar_lev_X(ceil(numel(bar_lev_X)/2)) + bar_lev_X(end)];
438 clear stepX
stepY = bar_lev_Y(2)-bar_lev_Y(1);
440 bly = [bar_lev_Y(1:end-1), bar_lev_Y(end):stepY:...
        bar_lev_Y(ceil(numel(bar_lev_Y)/2)) + bar_lev_Y(end)];
442 clear stepY
444
446 acer_fit_X = epsilon(blx, fin_sol_X);
acer_fit_Y = epsilon(bly, fin_sol_Y);
448 Gumbel_fit_X = gumb_uni(blx, -parmhat_X(1), parmhat_X(2));
Gumbel_fit_Y = gumb_uni(bly, -parmhat_Y(1), parmhat_Y(2));
450
452 % Refitting:
% Gumbel-Logistic dependence function
454 Logistic_Gumbel_fit = ...
    Logistic_Gumbel_marg(Gumbel_fit_X, Gumbel_fit_Y, Npoints, ...
456     k_choise, yrs_X, fin_sol_g_l(1)+fin_sol_g_l(2));
458 Logistic_ACER_fit = Logistic_ACER_marg(acer_fit_X, acer_fit_Y, ...
    fin_sol_a_l(1)+fin_sol_a_l(2));
460
% Asymmetric Logistic dependence function
462 Asymmetric_Logistic_Gumbel_fit = ...
    Asymmetric_Logistic_Gumbel_marg(...
464     Gumbel_fit_X, Gumbel_fit_Y, Npoints, k_choise, yrs_X, ...
    fin_sol_g_al(1), fin_sol_g_al(2), fin_sol_g_al(3));
466
Asymmetric_Logistic_ACER_fit = ...
468     Asymmetric_Logistic_ACER_marg(acer_fit_X, acer_fit_Y, ...
    fin_sol_a_al(1), fin_sol_a_al(2), fin_sol_a_al(3));
470
% Negative Logistic dependence function
472 Negative_Logistic_Gumbel_fit = ...
    Negative_Logistic_Gumbel_marg(Gumbel_fit_X, Gumbel_fit_Y, ...
474     Npoints, k_choise, yrs_X, fin_sol_g_nl(1)+fin_sol_g_nl(2));
476
Negative_Logistic_ACER_fit = ...
    Negative_Logistic_ACER_marg(acer_fit_X, acer_fit_Y, ...
478     fin_sol_a_nl(1)+fin_sol_a_nl(2));
480
% Asymmetric Negative Logistic dependence function
Asymmetric_Negative_Logistic_Gumbel_fit = ...
482     Asymmetric_Negative_Logistic_Gumbel_marg(Gumbel_fit_X, ...

```

```

484     Gumbel_fit_Y, Npoints, k_choise, yrs_X, fin_sol_g_anl(1), ...
        fin_sol_g_anl(2), fin_sol_g_anl(3));

486 Asymmetric_Negative_Logistic_ACER_fit = ...
    Asymmetric_Negative_Logistic_ACER_marg(acer_fit_X, ...
488     acer_fit_Y, fin_sol_a_anl(1), fin_sol_a_anl(2), fin_sol_a_anl(3));

490

492 % Contour plot
493 % We plot the optimal bivariate ACER, HR, ANL and NL methods.
494 % We further add a text-box with the levels on a logarithmic
495 % scale and a legend.
496 C = [v(5), v(7), v(8), v(9)];

498 figure;
499 clf
500 for ii = 1:numel(C)
501     CtableACER{ii} = contourc(bar_lev_X, bar_lev_Y, ...
502         log10(ACER_hat_mean), [C(ii) C(ii)]);
503     CtableACER{ii}(:, CtableACER{ii}(1,:) == C(ii)) = [];
504     if ~isempty(CtableACER{ii})
505         plot(CtableACER{ii}(1,:), CtableACER{ii}(2,:), '.', ...
506             'Color', 'k', 'LineWidth', 2, 'Markersize', 10)
507     end

508     hold on

509     CtableL_G_fit{ii} = contourc(blx, bly, ...
510         log10(Logistic_Gumbel_fit), [C(ii) C(ii)]);
511     CtableL_G_fit{ii}(:, CtableL_G_fit{ii}(1,:) == C(ii)) = [];
512     if ~isempty(CtableL_G_fit{ii})
513         plot(CtableL_G_fit{ii}(1,:), CtableL_G_fit{ii}(2,:), '- ', ...
514             'Color', [0 1 0], 'LineWidth', 1.5)
515     end

516     hold on

517     CtableAL_G_fit{ii} = contourc(blx, bly, ...
518         log10(Asymmetric_Logistic_Gumbel_fit), [C(ii) C(ii)]);
519     CtableAL_G_fit{ii}(:, CtableAL_G_fit{ii}(1,:) == C(ii)) = [];
520     if ~isempty(CtableAL_G_fit{ii})
521         plot(CtableAL_G_fit{ii}(1,:), CtableAL_G_fit{ii}(2,:), ...
522             '- ', 'Color', [1 0 1], 'LineWidth', 1.5)
523     end

524     hold on

525     CtableL_A_fit{ii} = contourc(blx, bly, ...
526         log10(Logistic_ACER_fit), [C(ii) C(ii)]);
527     CtableL_A_fit{ii}(:, CtableL_A_fit{ii}(1,:) == C(ii)) = [];
528     if ~isempty(CtableL_A_fit{ii})
529         plot(CtableL_A_fit{ii}(1,:), CtableL_A_fit{ii}(2,:), '- ', ...
530             'Color', [0 1 1], 'LineWidth', 1.5)
531     end

532     hold on

533     CtableAL_A_fit{ii} = contourc(blx, bly, ...
534         log10(Asymmetric_Logistic_ACER_fit), [C(ii) C(ii)]);
535     CtableAL_A_fit{ii}(:, CtableAL_A_fit{ii}(1,:) == C(ii)) = [];
536     if ~isempty(CtableAL_A_fit{ii})
537         plot(CtableAL_A_fit{ii}(1,:), CtableAL_A_fit{ii}(2,:), ...
538             '- ', 'Color', [0 0 1], 'LineWidth', 1.5)
539     end

540 end

```

```

end
546 xlim ([min(min(CtableACER{1}))-1 bar_lev_X(end)+1])
548 ylim ([min(min(CtableACER{1}))-1 max(max(CtableACER{1}))+1])

550 for ii = 1:numel(C)
552     text(max(CtableACER{ii}(1,:)),min(CtableACER{ii}(2,:)),...
554         horzcat(num2str(C(ii),'%10.2g')),...
556         'HorizontalAlignment','Right','FontSize',22,'FontName',...
558         'Times New Roman','BackgroundColor',[0.94 0.87 0.87],...
560         'Edgecolor',[.7 .7 .7]);
562 end

564 legenda = legend(...
566     horzcat(['$\hat{\mathcal{E}}_{\{ \text{num2str(k_choise) }\}}$'],...
568     horzcat(['$\mathcal{GL}_{\{G\}}$'],...
570     horzcat(['$\mathcal{AL}_{\{G\}}$'],...
572     horzcat(['$\mathcal{GL}_{\{ACER\}}$'],...
574     horzcat(['$\mathcal{AL}_{\{ACER\}}$'],...
576     'Location',[0.525 0.9596 0.01 0.01],'Orientation','horizontal');
578 set(legenda,'Interpreter','LaTeX')
580 xlabel('\xi','FontSize',26)
582 ylabel('\eta','Rotation',0,'FontSize',26)
584 editplot33

586 clear ii precision X_mesh Y_mesh CtableACER CtableACER_real...
588     CtableAL_fit CtableGL_fit CtableGL_hat CtableGL_MOM

590 % Return contour level plot
592 % Here we plot a contour plot of the GL and AL method using
594 % Gumbel and ACER marginals. We further add a text-box with
596 % the levels yearly scale and a legend.

598 stepX = bar_lev_X(2)-bar_lev_X(1);
600 blx = [bar_lev_X(1:end-1), bar_lev_X(end):stepX:...
602     bar_lev_X(ceil(numel(bar_lev_X)/2)) + bar_lev_X(end)];
604 clear stepX
606 stepY = bar_lev_Y(2)-bar_lev_Y(1);
608 bly = [bar_lev_Y(1:end-1), bar_lev_Y(end):stepY:...
610     bar_lev_Y(ceil(numel(bar_lev_Y)/2)) + bar_lev_Y(end)];
612 clear stepY

614 acer_fit_X = epsilon(blx, fin_sol_X);
616 acer_fit_Y = epsilon(bly, fin_sol_Y);
618 Gumbel_fit_X = gumb_uni(blx,-parmhat_X(1),parmhat_X(2));
620 Gumbel_fit_Y = gumb_uni(bly,-parmhat_Y(1),parmhat_Y(2));

622 % Refitting:
624 % Gumbel-Logistic dependence function
626 Logistic_Gumbel_fit = ...
628     Logistic_Gumbel_marg(Gumbel_fit_X, Gumbel_fit_Y,...
630     Npoints, k_choise, yrs_X, fin_sol_g_l(1)+fin_sol_g_l(2));

632 Logistic_ACER_fit = ...
634     Logistic_ACER_marg(acer_fit_X, acer_fit_Y,...
636     fin_sol_a_l(1)+fin_sol_a_l(2));

638 % Asymmetric Logistic dependence function
640 Asymmetric_Logistic_Gumbel_fit = ...
642     Asymmetric_Logistic_Gumbel_marg(Gumbel_fit_X,Gumbel_fit_Y,...

```

```

608     Npoints, k_choise, yrs_X, fin_sol_g_al(1), fin_sol_g_al(2), ...
        fin_sol_g_al(3));

610     Asymmetric_Logistic_ACER_fit = ...
        Asymmetric_Logistic_ACER_marg(acer_fit_X, acer_fit_Y, ...
612         fin_sol_a_al(1), fin_sol_a_al(2), fin_sol_a_al(3));

614     % Negative Logistic dependence function
        Negative_Logistic_Gumbel_fit = ...
616         Negative_Logistic_Gumbel_marg(Gumbel_fit_X, Gumbel_fit_Y, ...
            Npoints, k_choise, yrs_X, fin_sol_g_nl(1)+fin_sol_g_nl(2));
618

        Negative_Logistic_ACER_fit = ...
620         Negative_Logistic_ACER_marg(acer_fit_X, acer_fit_Y, ...
            fin_sol_a_nl(1)+fin_sol_a_nl(2));
622

        % Asymmetric Negative Logistic dependence function
624         Asymmetric_Negative_Logistic_Gumbel_fit = ...
            Asymmetric_Negative_Logistic_Gumbel_marg(Gumbel_fit_X, ...
626             Gumbel_fit_Y, Npoints, k_choise, yrs_X, fin_sol_g_anl(1), ...
                fin_sol_g_anl(2), fin_sol_g_anl(3));
628

        Asymmetric_Negative_Logistic_ACER_fit = ...
630         Asymmetric_Negative_Logistic_ACER_marg(acer_fit_X, ...
            acer_fit_Y, fin_sol_a_anl(1), fin_sol_a_anl(2), fin_sol_a_anl(3));
632

634     figure;
        clf
636     for ii = 1:numel(pr)
        CtableL_G_fit{ii} = contourc(blx, bly, Logistic_Gumbel_fit, ...
638         [level(ii) level(ii)]);
        CtableL_G_fit{ii}(:, CtableL_G_fit{ii}(1,:)) == level(ii) = [];
640         if ~isempty(CtableL_G_fit{ii})
            plot(CtableL_G_fit{ii}(1,:), CtableL_G_fit{ii}(2,:), '- ', ...
642             'Color', [0 1 0], 'LineWidth', 1.5)
            end
644         hold on

        CtableAL_G_fit{ii} = contourc(blx, bly, ...
646         Asymmetric_Logistic_Gumbel_fit, [level(ii) level(ii)]);
        CtableAL_G_fit{ii}(:, CtableAL_G_fit{ii}(1,:)) == level(ii) = [];
648         if ~isempty(CtableAL_G_fit{ii})
            plot(CtableAL_G_fit{ii}(1,:), CtableAL_G_fit{ii}(2,:), ...
650             '- ', 'Color', [1 0 1], 'LineWidth', 1.5)
            end
652         hold on

        CtableL_A_fit{ii} = contourc(blx, bly, Logistic_ACER_fit, ...
656         [level(ii) level(ii)]);
        CtableL_A_fit{ii}(:, CtableL_A_fit{ii}(1,:)) == level(ii) = [];
658         if ~isempty(CtableL_A_fit{ii})
            plot(CtableL_A_fit{ii}(1,:), CtableL_A_fit{ii}(2,:), '- ', ...
660             'Color', [0 1 1], 'LineWidth', 1.5)
            end
662         hold on

        CtableAL_A_fit{ii} = contourc(blx, bly, ...
664         Asymmetric_Logistic_ACER_fit, [level(ii) level(ii)]);
        CtableAL_A_fit{ii}(:, CtableAL_A_fit{ii}(1,:)) == level(ii) = [];
666         if ~isempty(CtableAL_A_fit{ii})
            plot(CtableAL_A_fit{ii}(1,:), CtableAL_A_fit{ii}(2,:), ...
668

```

```

        '-', 'Color', [0 0 1], 'LineWidth', 1.5)
670     end
671 end
672 for ii = 1: numel(pr)
673     sizeL_G_fit = size(CtableL_G_fit{ii});
674     sizeL_A_fit = size(CtableL_A_fit{ii});
675     min_size_fit = min(sizeL_G_fit(2), sizeL_A_fit(2));
676     x_upper(ii) = find(abs(CtableL_G_fit{ii}(2,1:min_size_fit) - ...
677         CtableL_A_fit{ii}(2,1:min_size_fit)) >= 0.001, 1, 'last');
678     x_upper(ii) = CtableL_G_fit{ii}(1, x_upper(ii));
679     x_lower(ii) = find(abs(CtableL_G_fit{ii}(1,1:min_size_fit) - ...
680         CtableL_A_fit{ii}(1,1:min_size_fit)) >= 0.001, 1, 'first');
681     x_lower(ii) = CtableL_A_fit{ii}(1, x_lower(ii));
682
683     y_upper(ii) = find(abs(CtableL_G_fit{ii}(1,1:min_size_fit) - ...
684         CtableL_A_fit{ii}(1,1:min_size_fit)) >= 0.001, 1, 'first');
685     y_upper(ii) = CtableL_G_fit{ii}(2, y_upper(ii));
686     y_lower(ii) = find(abs(CtableL_G_fit{ii}(2,1:min_size_fit) - ...
687         CtableL_A_fit{ii}(2,1:min_size_fit)) >= 0.001, 1, 'last');
688     y_lower(ii) = CtableL_G_fit{ii}(2, y_lower(ii));
689     text(x_upper(ii) - 1.1, y_lower(ii), ...
690         horzcat(num2str(1/(1-exp(-level(ii)*...
691             (Npoints-k_choise+1)/yrs_X)), '%10.4g')) , ...
692         'HorizontalAlignment', 'Right', 'FontSize', 22, ...
693         'FontName', 'Times New Roman', ...
694         'BackgroundColor', [0.87 0.92 0.98], 'Edgecolor', [.7 .7 .7]);
695     text(x_lower(ii), y_upper(ii) - 1.1, ...
696         horzcat(num2str(1/(1-exp(-level(ii) * ...
697             (Npoints-k_choise+1) / yrs_X)), '%10.4g')) , ...
698         'HorizontalAlignment', 'Right', 'FontSize', 22, 'FontName', ...
699         'Times New Roman', 'BackgroundColor', [0.94 0.87 0.87], ...
700         'Edgecolor', [.7 .7 .7]);
701 end
702
703
704
705 legenda = legend( ...
706     horzcat(['$\mathcal{G}$', 'GL_{G}$']) , ...
707     horzcat(['$\mathcal{A}$', 'AL_{G}$']) , ...
708     horzcat(['$\mathcal{G}$', 'GL_{ACER}$']) , ...
709     horzcat(['$\mathcal{A}$', 'AL_{ACER}$']) , ...
710     'Location', [0.525 0.9596 0.01 0.01], 'Orientation', 'horizontal');
711 set(legenda, 'Interpreter', 'LaTeX')
712 xlabel('\xi')
713 ylabel('\eta', 'Rotation', 0)
714 editplot33
clear ii precision

```

Listing A.8: The part of the BiMAIN.m file that have been edited.